

# **Capacitive-Resistive Bioelectrical Signal Measurement Method for Wearable Systems**

Alexsandr Igorevitch Ianov

Submitted to the Graduate School of Systems and Information  
Engineering in Partial Fulfillment of the Requirements for the Ph.D.  
Degree of Engineering at the University of Tsukuba

March 2015

# Abstract

Bioelectrical signals have become an important source of information about the human body and are commonly used in modern hospitals and healthcare facilities during diagnosis, treatment including surgery and recovery by monitoring of patients. Bioelectrical measurement through resistive coupling is traditionally used in such case, but the limitations and effort required to record a satisfactory signal are a big obstacle in the adoption of bioelectrical measurements in daily life. On the other hand, capacitive coupling bioelectrical sensors achieve capacitive coupling between the electrode lead and the user's skin, thereby removing the need for skin preparation and electromechanical contact with the skin, a core property which potentially facilitates high usability and wearability. Though many different models of capacitive coupling bioelectrical sensors have been developed, they all only focus on internal noise sources whereas noise from motion artefacts or nearby electrical appliances has been so far ignored. Because of that, bioelectrical measurements either have less than ideal accuracy or can only be recorded in very limited and artificially controlled environments with some types of bioelectrical signals recording are yet to be reported.

The purpose of this research is to bring the signal robustness expected from traditionally used contact type resistive electrodes and to the potentially more comfortable and practical non contact type capacitive electrodes by reducing the dependency of the bioelectrical information on the contact state between the sensor and the user's skin, approaching this problem from both a internal and external level perspective as well as from system level perspective and developing a hybrid sensor capable of both resistive and capacitive ECG, EMG, EOG and EEG bioelectrical signal measurements.

Development of a novel electric circuit model based on both resistive and capacitive measurement principles as well as all the associated internal noise factors, namely internal thermoelectrical noise, current drift and saturating noise recovery. We extend the sensor model for external noise noise monitoring, namely external electromagnetic noises and motion artifacts and developing a built in dual differential input noise cancelling method. We design and develop a sensor module satisfying the conditions of the developed models introduced. After that, we verify noise and response system properties as well as resistive and capacitive ECG, EOG, EMG and EEG measurements. Because there is no commercial capacitive bioelectrical sensing system, we compare our sensor against traditional wet resistive wet electrodes and obtain similar results. Finally we develop a novel wearable high spatial and temporal resolution and self contained system for EEG measurements in order to minimise noise and demonstrate the full advantages of high wearability and usability that our developed sensors provide. We hope to contribute bringing bioelectrical measurement based prevention and treatment methods that rely on bioelectrical signals in to daily life.

# Contents

Abstract .....	I
Contents.....	II
List of Figures .....	V
1 Introduction .....	1
1.1 The importance and applications of wearable bioelectrical measurement .....	1
1.2 Bioelectricity principles .....	3
1.3 Resistive bioelectrical measurement .....	5
1.4 Capacitive bioelectrical measurement.....	6
1.5 Internal and external noise counter measures and system level optimisations towards a hybrid approach for bioelectrical measurement .....	7
1.6 The purpose of this research .....	8
1.7 The structure of this paper.....	8
2 Wearable hybrid resistive-capacitive design.....	10
2.1 Hybrid resistive and capacitive bioelectrical measurement introduction and requirements .....	10
2.2 Optimal input impedance and minimal thermo-electrical noise .....	10
2.2.1 Equivalent circuit model .....	10
2.2.2 Optimal parameter setting .....	12
2.3 Noise from optimal input design and counter measurements .....	13
2.3.1 Input current leakage and voltage drift .....	13
2.3.2 High impedance bootstrapping method.....	15
2.4 Dual input based noise cancelling for hybrid resistive-capacitive sensing method .....	17
2.5 Hardware design .....	19
2.5.1 Developed sensor unit.....	19
2.5.2 Data recording unit.....	19
2.6 Noise and parameter evaluation.....	21

2.6.1	Frequency response.....	21
2.6.2	Electromagnetic noise spectrum .....	23
2.6.3	Output drift.....	25
2.6.4	Motion artifacts and input saturation recovery measurements.....	26
2.6.5	Noise cancelling evaluation measurement.....	27
2.7	Discussion .....	29
2.8	Conclusion.....	29
3	Bioelectrical signal measurement using developed hybrid electrode .....	30
3.1	Introduction.....	30
3.2	Bioelectrical signal measurement, evaluation methods and results.....	31
3.2.1	Electrocardiogram measurement .....	31
3.2.2	Upper body electromyogram measurement.....	32
3.2.3	Lower body electromyogram measurement.....	36
3.2.4	Electrooculogram measurement .....	37
3.2.5	Electroencephalogram measurement .....	39
3.3	Bioelectrical signal measurement analysis.....	40
3.3.1	Electrocardiogram measurement .....	40
3.3.2	Upper body electromyogram measurement.....	40
3.3.3	Lower body electromyogram measurement.....	40
3.3.4	Electrooculogram measurement .....	41
3.3.5	Electroencephalogram measurement .....	41
3.4	Discussion .....	41
3.5	Conclusion.....	42
4	Wearable high resolution high speed hybrid resistive-capacitive bioelectrical sensing system.....	43
4.1	Realising the full potential hybrid resistive capacitive measurement system ...	43

4.2 Fully integrated electroencephalogram measurement system .....	45
4.2.1 Small package hybrid electrodes .....	45
4.2.2 Headgear mechanism .....	45
4.2.3 Built in electronics .....	50
4.3 Parallel bioelectrical signal processing using wearable graphical processing unit .....	52
4.4 EEG measurement experiments .....	55
4.4.1 Basic EEG measurement benchmark using the developed wearable EEG monitoring system and small size hybrid electrodes .....	55
4.4.2 Full scalp beta wave EEG measurement .....	56
4.5 Discussion .....	58
4.6 Conclusion .....	60
5 Discussion.....	61
5.1 Academic and practical advantages of the hybrid bioelectrical measurement model, noise cancelling methods and parallel processing methods .....	61
5.2 An engineering approach to prevention and treatment of major health issues. 62	
5.3 Further applications and expansions for the techniques developed in this research .....	63
6 Conclusion .....	64
7 Future works .....	65
Acknowledgements.....	66
Bibliography .....	67
Related Papers .....	72

# List of Figures

Figure 1 - Bioelectrical signals and example of wearable applications	2
Figure 2 - Ion channels and generation of bioelectrical signals	4
Figure 3 - The structure of this research	9
Figure 4 - Basic hybrid capacitive-resistive sensor model	12
Figure 5 - Capacitor being charged by input bias from a real op-amp	14
Figure 6 - resistor based input bias current leakage	15
Figure 7 - Example of back to back diode circuit	17
Figure 8 - Redesigned circuit model with bootstrapped feedback circuit	17
Figure 9 -Redesigned circuit model with dual input noise cancelling circuit	18
Figure 10 - Noise cancelling lead implementation and recording system	20
Figure 11 - Developed sensor	21
Figure 12 - Frequency response measurement setup	22
Figure 13 - Frequency response for the developed sensor	22
Figure 14 - Noise spectrum measurement setup	23
Figure 15 - Noise spectrum of the developed electrode	24
Figure 16 - ECG measured without the bootstrapping feedback circuit	25
Figure 17 - ECG measured with the bootstrapping feedback circuit	25
Figure 18 - Recovery time without bootstrapping feedback circuit	26
Figure 19 - Recovery time with bootstrapping feedback circuit	27
Figure 20 - Noise cancelling Experiment setup	27
Figure 21 - measured data when the human arm was in rest when the robotic arm was not moving(right is zoomed up)	28
Figure 22 - Robot arm was moving without noise cancelling on the bioelectrical sensor(right is zoomed up)	28
Figure 23 - Robot arm was moving with noise cancelling on the bioelectrical sensor(right is zoomed up)	28
Figure 24 - Electrode placement for ECG measurement	31
Figure 25 - Measured ECG data in which we can verify the existence of all component wave forms	31
Figure 26 - Positioning of the sensor for EMG measurements	32
Figure 27 - Electrode positioning of the simultaneous dynamic EMG measurement with wet electrodes and hybrid electrodes in capacitive mode	33

Figure 28 - simultaneous dynamic EMG measurement with wet electrodes and hybrid electrodes in capacitive mode	33
Figure 29 - Capacitively coupled EMG measurement under multiple loads	34
Figure 30 - Robot control using Capacitively coupled EMG	35
Figure 31 - Capacitive coupled EMG from the quadriceps measured during walking	36
Figure 32 - Positioning of the sensors for EOG measurements	37
Figure 33 - Blinking results and correlation factor with traditional electrodes	38
Figure 34 - EOG(Eyeball muscular activity) measurements and correlation factor with traditional electrodes	38
Figure 35 - Positioning of the sensors for EEG measurements	39
Figure 35 - EEG measurement results with correlation coefficients	39
Figure 36 - Developed small package hybrid electrodes	45
Figure 37 - custom electrode placement method	46
Figure 38 - Headgear frame	47
Figure 39 - Electrode grid configured	48
Figure 40 - complete wearable Electrode grid with user	49
Figure 41. ADC board diagram	50
Figure 42 - Developed ADc board	51
Figure 43 - Developed GUI	52
Figure 44 - Developed wearable CUDA EEG data processing algorithm	53
Figure 45 - $\mu$ -band measurements as EEG response to motor stimulus	56
Figure 46 - Task design for beta wave measurement	57
Figure 47 - During the beta wave measurement experiment	57
Figure 48 - Sample data showing beta wave during relaxation and calculation	57
Figure 49 - Example of expanding the wearable internal and external noise cancelling techniques in to non wearable/handheld bioelectrical measurement devices	62
Figure 50 - Expanding the developed noise cancelling and parallel processing methods into other types of biosignals as well as application development for treatment and prevention of cardio, muscular and neural disorders.	65

# 1 Introduction

## 1.1 The importance and applications of wearable bioelectrical measurement

Since the first studies on the use of electrical signals derived from cardiac activity in 1872 by Alexander Muirhead for medical purposes[1], bioelectricity amplification and recording electronic instrumentation technology has been continuously researched. Thanks to those advancements, through the last century, bioelectrical signals have become an important source of information about the human body and are commonly used in modern hospitals and healthcare facilities, during diagnosis, treatment including surgery and recovery monitoring of patients. Bioelectrical signals are either measured by themselves or in conjunction with other types of biosignals, such as blood pressure[2,3] or body movement[4,5], using devices ranging from large desktop computers to smartphone sized handheld and wearable devices, as shown in Fig.1.

In particular, wearable and stand-alone implementations of these technologies are increasingly more relevant in a wide selection of academic and engineering fields, ranging from medicine and rehabilitation to sports and entertainment. Wearable implementations of bioelectrical sensing technologies are easier to integrate in the daily life activities and contribute to the prevention and treatment of cardio-vascular and neurological disorders as well as support and augmentation of motion and man-machine interfaces[6,7].

Based on signal source location, source nature, frequency and amplitude bioelectrical signals can be classified in many types. In this study we focus on the four types below:

1) Electrocardiogram(ECG): ECG is a category of bioelectrical signals originated from the heart activity, in particular electrical signals originated as a byproduct of the sequential contraction of cardiac muscles and are recorded by placing sensors over skin. In the order of  $10\mu\text{V}$  up to  $1\text{mV}$ , wearable ECG measurements done by a Holter Monitor for long periods of time are frequently used to diagnose cardiac diseases or measure cardiac stress[8,9] under physical exercises[10,11] are classical applications.

2) Electromyogram(EMG): EMG signals are generated by skeletal striated muscular contracting simultaneously when generating torque, are in the order of  $10\mu\text{V}$  up to  $100\mu\text{V}$  and are measured over the skin surface. Wearable measurements are used to interface with exoskeletons such as the HAL robot suit[12,13,14], prosthetic limbs[16,17] as well as evaluation of biomechanical performance in sports[18,19].

3) Electrooculogram(EOG): EOG signals are a variation of EMG signals generated by the muscles actuating eye movement. Due to the spontaneous and quick characteristics of eye movements, EOG signals usually have pulse-like characteristics granting those signals their

own category for practical application reasons. Wearable EOG signals are commonly used as an input in man-machine interfaces for fully-disabled patients. Applications in the prediction and interpretation of human emotions through face expressions[20,21] and in entertainment and virtual reality have also been proposed[22,23].

4) Electroencephalogram(EEG): EEG signals are bioelectrical signals measured on the scalp of the user. Compared to the other types, EEG signals are very weak signals in the order of  $0.1\mu\text{V}$  up to  $10\mu\text{V}$  generated by the collective neural activity inside the brain. Wearable EEG signals are used in the psychology and psychiatric fields, such as diagnosis of sleep disorders[24,25] and epilepsy[26]. Applications in the as as man-machine interfaces and in entertainment have also been proposed[27].

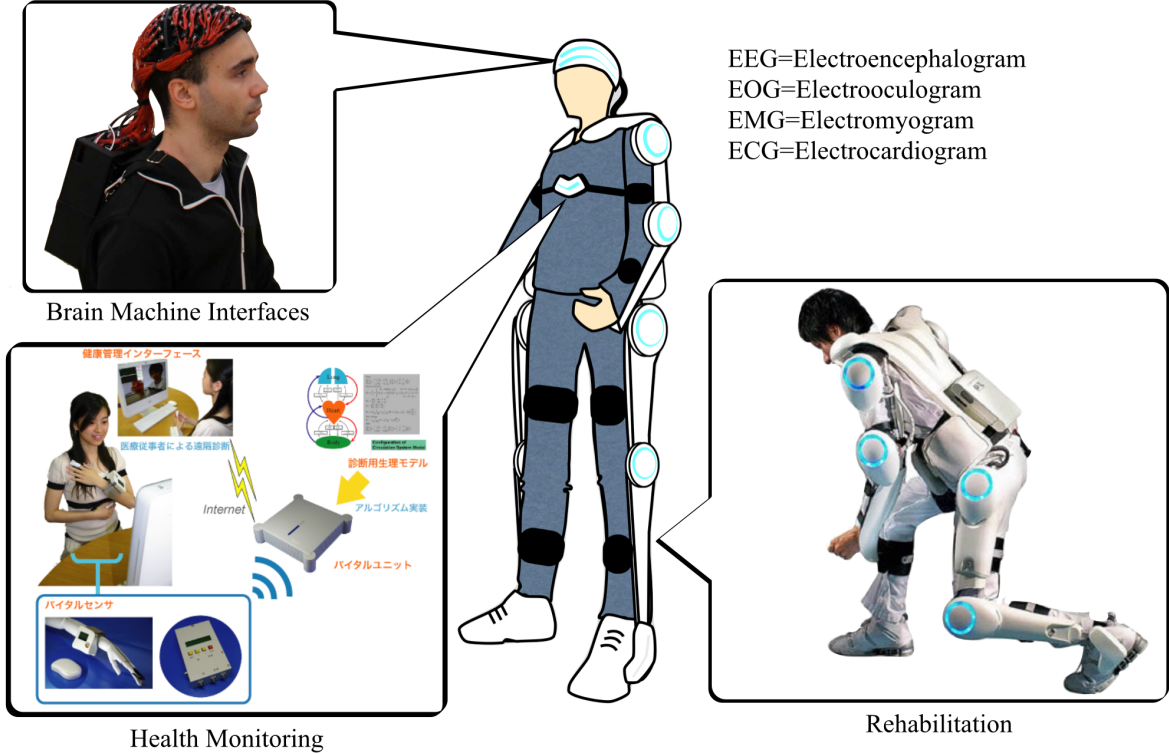


**FIGURE 1 - BIOELECTRICAL SIGNALS AND EXAMPLE OF WEARABLE APPLICATIONS**

## 1.2 Bioelectricity principles

Bioelectrical signals are originated at cellular level as the resulting sum from the electrical potential caused by various biochemical reactions and the ionic displacements associated to them[28]. The most relevant and useful bioelectrical potentials used in this research are originated from the inhibition and excitation of neural and muscular cellular tissue[29]. For the purposes of this research, bioelectrical signals can be categorised in two major different types based on function: resting potentials and action potentials.

Resting potentials are the default electrical potential in living cells at rest. The difference of concentration of potassium( $K^+$ ) and sodium( $Na^+$ ) ions in the intracellular and extracellular mediums creates a resting potential of  $-70 \pm 20mV$  across the cellular membrane[30]. The difference in the ionic concentration between intra and extracellular mediums is a direct result of the resting selective permeability of the cellular membrane, which favours  $K^+$  ions in the intracellular fluid. The concentration of  $K^+$  and  $Na^+$  relative to the concentration of chloride ion( $Cl^-$ ) regulates the equilibrium at rest[31].

Action potentials are the response of the cell towards external stimuli. They are a short pulse that travels through the cell membrane when the stimuli successfully disturbs the resting potential beyond a threshold. When an action potential occurs, the electrical potential across the cellular membrane is reversed, until it peaks. As shown in Figure 2, when activation happens voltage-gated ion channels become temporary permeable to their respective ions, allowing sodium to flow into the cell and potassium to flow out of the cell, increasing the electrical potential on a limited region of the membrane. The peak voltage can trigger the reaction on neighbouring regions of the membrane creating a cascade effect. After the voltage-gated ion channels become inactivated and later deactivated,  $Na^+/K^+$ -ATPase, also known as the sodium-potassium pump, actively brings the membrane to its original resting state through the consumption of energy in form of adenosine triphosphate(ATP).

At cellular levels, single action potential can be recorded by directly placing microelectrodes inside and around the cell and measuring the short-lasting rises and falls of electrical potential on the cell. However, at macroscopic levels, many brain and muscle related phenomena occur by having a large number of cells manifesting active potential simultaneously. When such phenomena occurs, the total sum of electrical potential can be strong enough to allow the propagation of electrical signals through multiple layers of biological tissue and, eventually, skin.

## Cell Membrane Potential

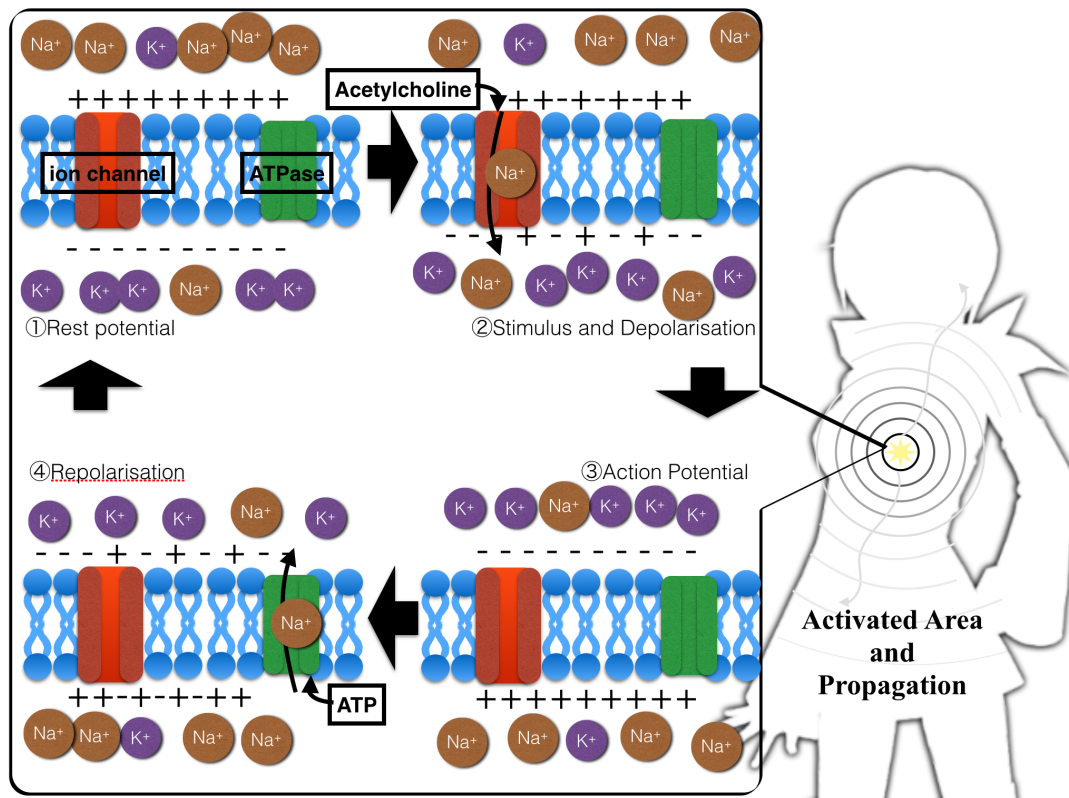
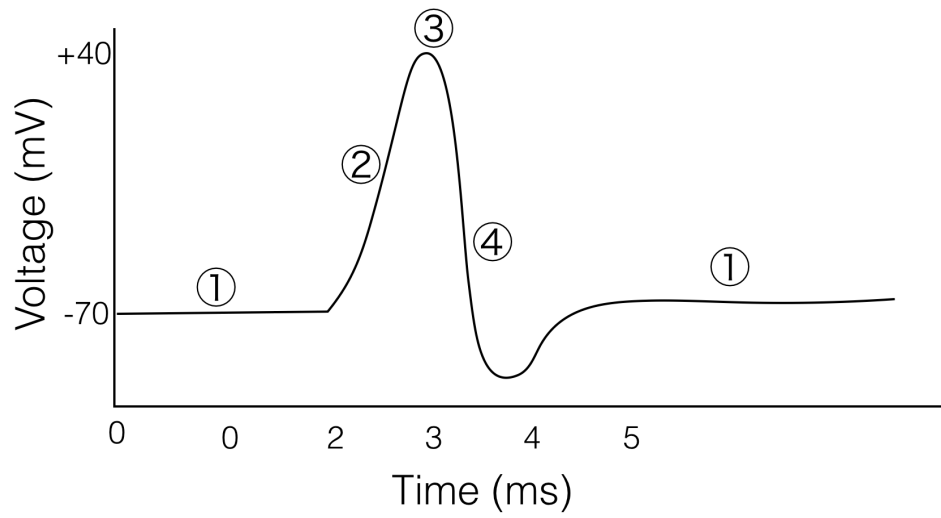


**FIGURE 2 - ION CHANNELS AND GENERATION OF BIOELECTRICAL SIGNALS**

## 1.3 Resistive bioelectrical measurement

Bioelectrical signals over the user's skin are measured by establishing electrical coupling between the skin and a recording device. Electrical coupling can be realised in two different ways: resistive coupling and capacitive coupling. In this subsection we focus on resistive coupling which consists in creating and maintaining electrical coupling through direct mechanical contact between the skin and a conductor attached to the recording device input. Multiple types of electrode based sensors are used for this type of measurement.

Wet resistive electrodes such as the Vitrode (Nihonkohden, Japan) or the electrodes used in the G.Tec electrode cap (G.Tec Medical Engineering GMBH, Austria) are used widely to perform these measurements. However, the use of wet electrodes has major drawbacks such as the requirement for skin preparation and the use of conductive or adhesive gels[32,33]. As a solution to those problems, dry resistive electrodes have been developed to increase sensor performance and usability[34,35]. Dry electrodes involve an active resistive contact with the user's skin, which eliminates the need to use a gel and the problems associated with its use. Skin preparations such as body hair removal and cleaning may be required because constant electromechanical skin contact remains a requirement[35]. Furthermore the lack of adhesive gels make dry electrodes difficult to use over clothing. Also, in extreme cases, patients with exposed wounds, such as high degree burns, or allergies may not be capable of attaching neither wet nor dry electrodes directly to their bodies.

While resistive coupling based bioelectrical measurement is traditionally used on medical facilities as well as research and sports, the limitations and effort required to record a satisfactory signal are a big obstacle in the adoption of bioelectrical measurements in daily life, and the spread of novel technologies that could help in the prevention and treatment of cardio, muscular or neural disorders.

## 1.4 Capacitive bioelectrical measurement

By contrast, in order to solve problems associated with the various types of resistive coupling bioelectrical sensors, non contact electrodes have been proposed. Non contact electrodes rely on capacitive coupling between the electrode sensing lead and user's skin. Capacitive coupling bioelectrical sensors achieve capacitive coupling between the electrode lead and the user's skin, thereby removing the need for skin preparation and electromechanical contact with the skin, a core property which potentially facilitates high usability and wearability.

However, ultra-high input impedances ( $10^{16}\sim 10^{18}\Omega$ ) are required by the design[36,37]. The ultra-high impedance input is highly susceptible to any electrostatic noise that originates from the surroundings. Therefore, robust shielding, isolation, and current leakage prevention techniques are required to reduce the noise. Furthermore, complex low noise bootstrapping techniques are required to avoid drift due to the bias current from the input. These disadvantages indicate that capacitive electrodes are considerably larger, noisier, and more expensive than conventional electrodes[37].

Furthermore, though many different models of capacitive coupling bioelectrical sensors have been developed, they all only focus on internal noise sources, whereas noise from motion artefacts or nearby electrical appliances has been so far ignored. Because of that many reported capacitive coupled bioelectrical signals such as EEG or ECG[38,39,40,41], either have less than ideal accuracy or can only be recorded in very limited and artificially controlled environments, while some types of bioelectrical signals, such as capacitively coupled upper and lower body EMG signals during motion in realistic application scenarios are yet to be reported.

Moreover, because capacitive bioelectrical measurement techniques rely on different physical phenomena, a system level engineering approach that takes into consideration the strengths and weaknesses of bioelectrical measurements through capacitive coupling is an important step in towards the practical realisation of these technologies.

## **1.5 Internal and external noise counter measures and system level optimisations towards a hybrid approach for bioelectrical measurement**

Daily life bioelectrical monitoring requires a sensor that gives the potentially high usability of capacitive coupling electrodes while retaining the high sensor performance of conventional electrodes. A hybrid sensor capable of such function could be achieved by simultaneously being capable of both resistive and capacitive coupling methods, thus minimising the dependency of the bioelectrical information on the user skin-electrode interface. In order to achieve that, we must approach this problem from 3 different points of view: development of a hybrid resistive and capacitive sensing model and internal sensor noise, external noise counter-measures and system level design.

Previous studies only considered human body-electrode coupling in their designs, which maximised the input impedance. We also propose the use of noise source coupling in the sensor model. This model allows us to optimise the electrode impedance so that it is sufficiently high to record bioelectrical signals but low enough to reject external electrical noise. Moreover, internal noise originated from input current leaks and shielding must also be assessed and appropriately processed.

Furthermore, in order to solve the problems from previous bioelectrical measurement through capacitive coupling technologies, noise from real life situations such as motion artifacts or near high-power devices such as electrical motors must also be assessed and countered. By extending the developed hybrid resistive-capacitive bioelectrical measurement model by actively measuring noise and cancelling it from the sensor output. This new model would allow the development of a novel dual input noise cancelling electrode design, one for noise and one for bioelectrical signals, at different input impedance settings which are locally processed using analog circuits, resulting in a cleaner signal output.

Finally, developing wearable systems that are built around the advantage of having high wearability and usability provided by capacitive coupling, but that are still strong against disadvantages such as higher environmental electrostatic noise sensitivity is the final step in taking full advantage of the hybrid resistive-capacitive bioelectrical measurement methods. In particular, self-contained wearable system capable of multichannel, high spatial and temporal resolution recordings using parallel analog and digital processing techniques could improve the signal and information quality recorded from the developed sensor while also demonstrating its usefulness and opening the path for further improvements and applications, in particular for EEG measurements where high wearability, low noise, high spatial and temporal resolution are desirable qualities.

## **1.6 The purpose of this research**

The purpose of this research is to bring the signal robustness expected from traditionally used contact type resistive electrodes and to the potentially more comfortable and practical non contact type capacitive electrodes by reducing the dependency of the bioelectrical information on the contact state between the sensor and the user's skin, by approaching this problem from both a internal and external level perspective as well as from system level perspective and developing a hybrid sensor capable of both resistive and capacitive ECG, EMG, EOG and EEG bioelectrical signal measurements. In order to realise the above, the following objectives must be achieved:

(1) Development of a novel electric circuit model based on both resistive and capacitive measurement principles as well as all the associated internal noise factors, namely internal thermo electrical noise, current drift and saturating noise recovery.

(2) Extend the sensor model for external noise noise monitoring, namely external electromagnetic noises and motion artifacts and developing a dual differential input noise cancelling method that can be built in on each sensor.

(3) Designing and developing a sensor module satisfying the conditions of the developed models introduced in (1) and (2). After that, verify noise and response system properties as well as resistive and capacitive ECG, EOG, EMG and EEG measurements.

(4) Develop a novel wearable high spatial and temporal resolution and self contained system for EEG measurements in order to minimise noise and demonstrate the full advantages of high wearability and usability that our developed sensors provide.

## **1.7 The structure of this paper**

Figure 3 shows objectives while illustrating the overall structure of this paper.

In this chapter we discussed the basic principles behind bioelectricity as well as the latest advances and different approaches in the development of bioelectric signal measurement techniques.

In Chapter 2 we develop the sensing model by focusing on both internal and external noise sources as well as designing and constructing the sensor module and basic measurement hardware. We also measure internal noise levels, noise cancelling capabilities and compare to previous researches.

Chapter 3 is focused on actually using the developed hybrid sensor to measure ECG, world first upper limb and lower limb capacitive coupled EMG, EOG and EEG signals and

compare to previous researches on capacitive coupling bioelectrical signal sensor as well as traditional methods and standards.

Chapter 4 goes in to the development of system level improvements to take full advantage of our developed hybrid sensor. In this chapter we develop a novel wearable high spatial and temporal resolution and self contained system for EEG. In order to do so we develop parallel digital processing algorithms build around the limitations of a original wearable GPGPU based data processing device. Furthermore, we measure noise characteristics, multichannel EEG measurements and analyse the impact that our novel wearable parallel processing and hybrid bioelectrical sensing methods had on the data.

Chapter 5 discusses the impact of our research on both resistive and capacitive bioelectrical measurement methods, how it our developed sensors can help in the treatment and prevention of cardio, mucular and neural disorders and how the our wearable parallel processing technologies can be extended beyond bioelectricity measurements.

Finally in Chapter 6 we present the summary and conclusion to this paper.

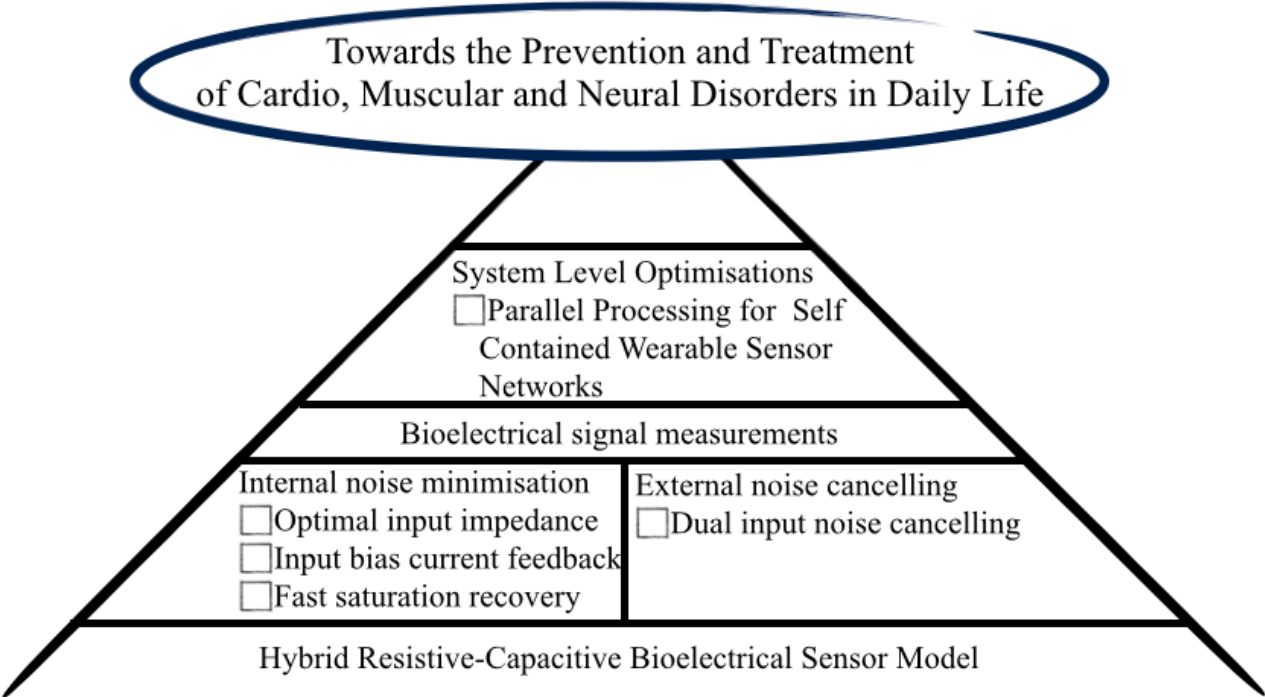


**FIGURE 3 - THE STRUCTURE OF THIS RESEARCH**

## **2 Wearable hybrid resistive-capacitive design**

### **2.1 Hybrid resistive and capacitive bioelectrical measurement introduction and requirements**

Non contact electrodes that are capable of achieving capacitive coupling between the electrode lead and the user's skin, thereby removing the need for skin preparation and electromechanical contact with the skin facilitating high usability, have been proposed. However previous researches only focused on internal noise sources and minimalistic sensor models, thus only reporting results from limited bioelectrical measurements done under very specific and controlled conditions[38,40].

In this chapter we designed a novel sensor circuit model based on the consideration of the electronic components imperfections and the user skin-sensor interface, which also accounted for the internal thermoelectrical noise sources and input bias current. The model contains the basic hybrid measurement principle derived from both resistive contact sensors and capacitive coupling sensors. On top of this we create a bias current feedback circuit that eliminates current leakage and the increasing output voltage offset caused by it. Finally we expand the circuit model into a dual input system for dual input environmental noise cancelling.

Using this model, we developed an optimal original hybrid electrode that was capable of resistive contact and capacitive coupling sensing with an input impedance of  $1\text{ T}\Omega$ , which is about  $10^4\sim 10^6$  times smaller than that proposed in other studies[36], immune to internal current leakage and quick to recover from input saturating disturbances while also being capable of providing noise cancelling capabilities to external noise sources from electrical motor equipped robots and motion artifacts.

### **2.2 Optimal input impedance and minimal thermo-electrical noise**

#### **2.2.1 Equivalent circuit model**

We designed our hybrid resistive capacitive electrode such that it could function as a resistive contact electrode if electromechanical contact with the skin was not possible. Thus, the electrode collected bioelectrical signals via capacitive coupling if electromechanical contact was not possible. Capacitive sensing measures bioelectrical signals using the AC coupling between the electrode lead and the skin. Figure 4 shows the equivalent circuit for our proposed electrode containing a human body, the electrode-skin signal collection interface,

the electrode circuit, and noise sources. The total electrical current in the electrode input is given by equation (1) as the sum of the currents from the noise sources and the current from the bioelectrical signal, i.e.,

$$\frac{V_I}{R_c} = \frac{(V_B - V_I)}{Z_B} + \frac{(V_N - V_I)}{Z_N} \quad (1)$$

where  $V_B$  is the bioelectrical signal voltage,  $V_I$  is the electrode input voltage,  $V_N$  is the total noise source voltage on the electrode board,  $Z_B$  is the skin-electrode interface impedance,  $R_c$  is the electrode input impedance, and  $Z_N$  is the noise input impedance on the electrode board. We can assume that the values for  $Z_B$ , and  $Z_N$  are very large; therefore, we can simplify equation (1) as

$$V_I = R_c Z_N \frac{V_B}{Z_B Z_N + R_c Z_B + R_c Z_N} + R_c Z_B \frac{V_N}{Z_B Z_N + R_c Z_B + R_c Z_N} \quad (2)$$

where  $Z_B$  is represented as

$$Z_B = (R_B^{-1} + C_B 2\pi f)^{-1} \quad (3)$$

where  $C_B$  is the capacitance,  $R_B$  is the resistance between the electrode and the skin, and  $f$  is the signal frequency.

From equation (2) and (3), we can infer that the collected signal is highly dependent on the impedance of the electrode-skin interface and the total input impedance of the circuit, while the input impedance of the electrode should be considerably higher than the impedance at the electrode-skin interface. When our electrode is in the resistive contact mode,  $C_B \rightarrow 0$  so  $Z_B$  is highly dependent on  $R_B$ . When our electrode is in the capacitive coupling mode, however,  $R_B \rightarrow \infty$  so  $Z_B$  is highly dependent on  $C_B$ . From equation (3), we may assume the presence of noise sources in the surroundings that are connected via capacitive coupling to the input of the circuit. The impedance between the noise source and the electrode input is usually much higher than the impedance of the electrode-skin interface. Therefore, signals from the electrostatic noise sources may be amplified as well as or better than the bioelectrical signals if the electrode input impedance is excessively high. The effects of noise on the ultra-high impedance input may be strong if the electrode makes recordings using capacitive coupling sensing because  $Z_B$  is already very high. Therefore, the input impedance should be set to a minimal value, which is sufficiently high to allow bioelectrical signals to be recorded.

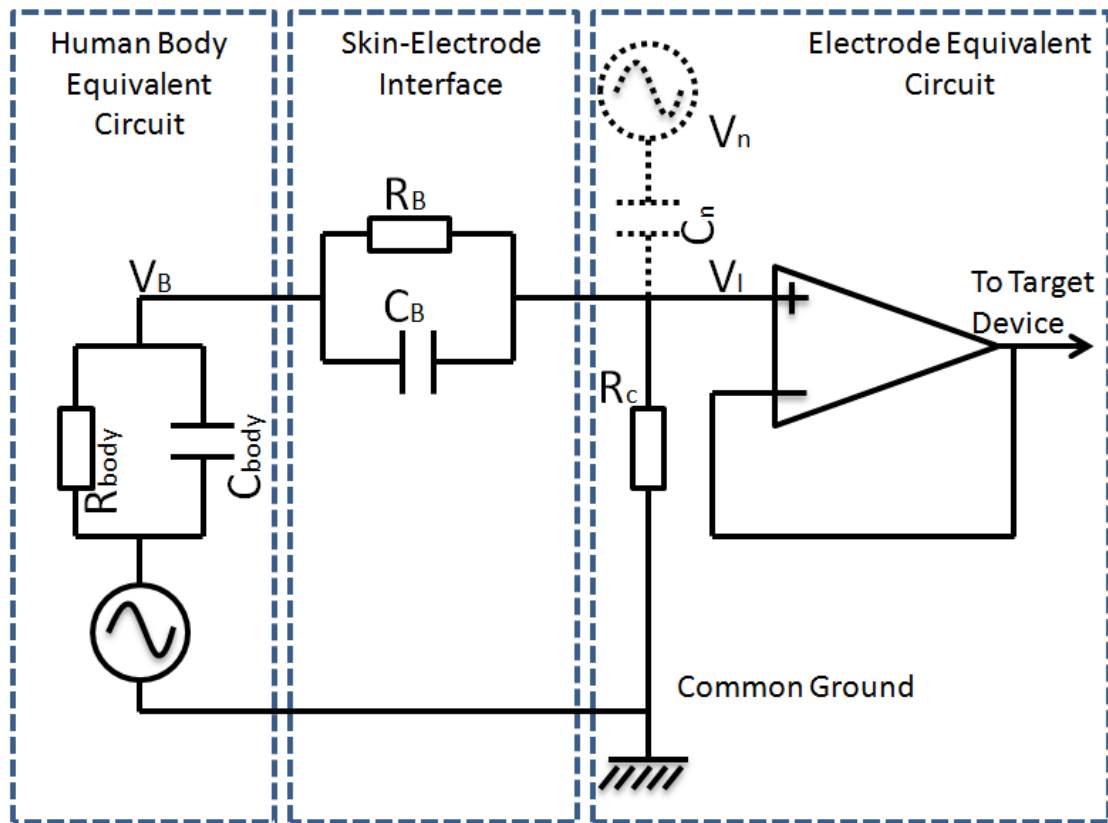


FIGURE 4 - BASIC HYBRID CAPACITIVE-RESISTIVE SENSOR MODEL

### 2.2.2 Optimal parameter setting

To measure the bioelectrical signals used by medical applications, our electrode needed to measure signals with frequencies ranging from 3 Hz to 100 Hz[42,43]. The capacitive coupling mode requires a higher impedance than the resistive contact mode; therefore, the minimal circuit input impedance requirement is the input impedance used for the capacitive coupling measurements.

The capacitance of the skin-electrode interface in the capacitive coupling mode is given as

$$C_B = \epsilon_r \epsilon_0 \frac{A}{d} \quad (4)$$

where  $\epsilon_0$  is the dielectric constant in vacuum,  $\epsilon_r$  is the relative dielectric constant to the material,  $A$  is the electrode lead area nearest to the skin, and  $d$  is the distance between the skin and the electrode lead. As discussed in the previous section, we do not need to calculate the noise signal components in equation (2) because setting the input impedance at a minimal

value also allows us to perform noise signal minimization. Given that  $R_{sei} \rightarrow \infty$  in the capacitive coupling mode and by inserting combining equations (2), (3), and (4), we define the circuit input impedance as follows (5).

$$R_c = \frac{V_{IN}}{V_{BES}} \cdot \frac{d}{\epsilon_r \epsilon_0 A 2\pi f} \quad (5)$$

In the capacitive mode and based on the equivalent circuit described in Figure 4, our electrode is a first-order high-pass filter with a theoretical cut-off frequency that is derived as follows:

$$F_{cut-off} = \frac{1}{2\pi R C_B} \quad (6)$$

where  $C_B$  can be calculated from equation (4), and  $R$  is the input impedance of the operational amplifier used in the electrode design.

## 2.3 Noise from optimal input design and counter measurements

### 2.3.1 Input current leakage and voltage drift

As shown in Figure 5, in capacitive coupling mode, bioelectrical sensors have only the equivalent of a capacitor connected to the input of the preamplifier circuit. Given that on a realistic operational amplifier there will be input bias current caused by the current leakage from semiconductor imperfections, there will be accumulation of charge over time on the input lead. Therefore the output voltage of such system can be expressed as

$$V_{out} = A_{opa} C_B \int i_{Bias} dt \quad (7)$$

where  $A_{opa}$  is the operational amplifier amplification factor,  $t$  is the charging time, which is the operational time of the system,  $i_{Bias}$  is the input bias current.

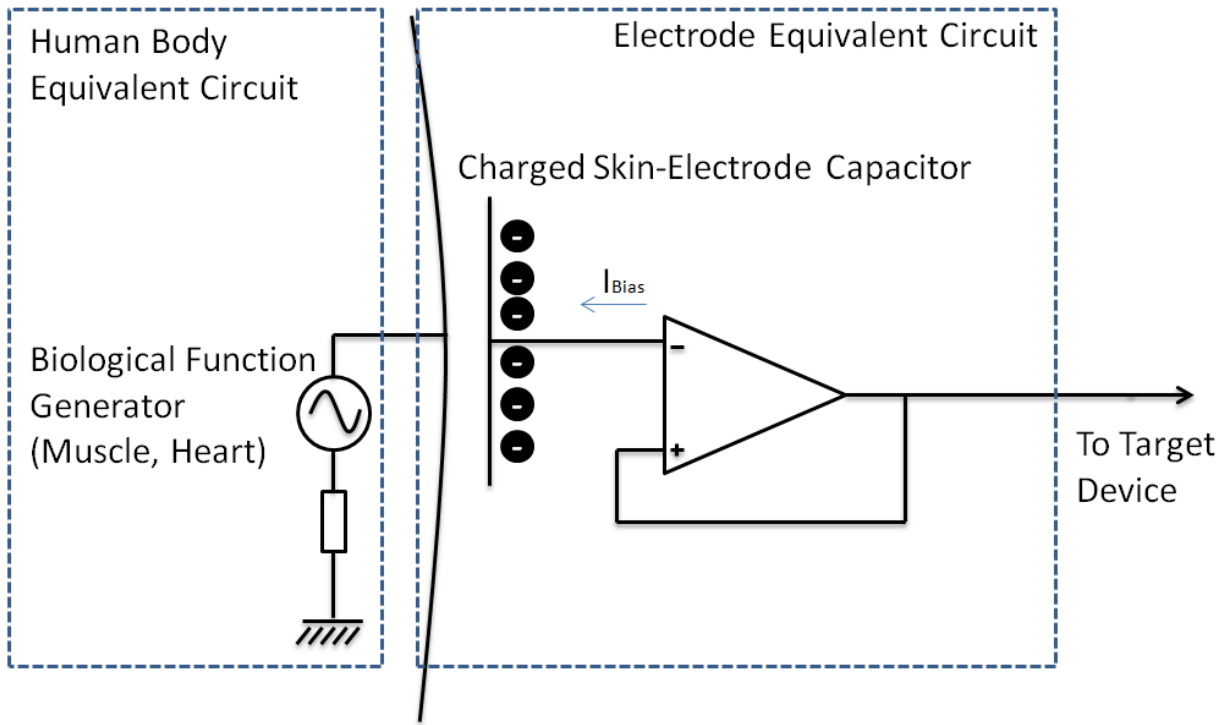


**FIGURE 5 - CAPACITOR BEING CHARGED BY INPUT BIAS FROM A REAL OP-AMP**

The output voltage will start drifting as soon as the sensor is turned on and depending on the amplification factor as well as the type of operational amplifier used on the preamplifier circuit, it will eventually saturate the output at varying speeds. Furthermore, strong motion artefacts and body electrostatic discharges may also cause the input to saturate. Having a circuit to return the circuit to its original state as quickly as possible is an important requirement for future signal processing[44].

The obvious way to restrict the effects of bias current on the input is to add a resistor between the input and reference voltage, as shown in Figure 6. However given that resistors have their thermoelectrical noise defined by the Johnson-Nyquist noise equation as

$$V_{noise} = \sqrt{4k_B T Z} \quad (8)$$

where  $V_{noise}$  is the thermoelectrical noise,  $k_B$  is the Boltzmann constant,  $T$  is the temperature in Kelvin and  $Z$  is the impedance of the passive component. By adding a resistor to the input lead of the hybrid sensor, the input impedance will be close to the total resistance of the operational input impedance and resistor in parallel. Therefore a very high value resistor must be attached to the input lead, adding up to several mV of thermoelectrical noise to the input, far surpassing the amplitude of the target bioelectrical signals.

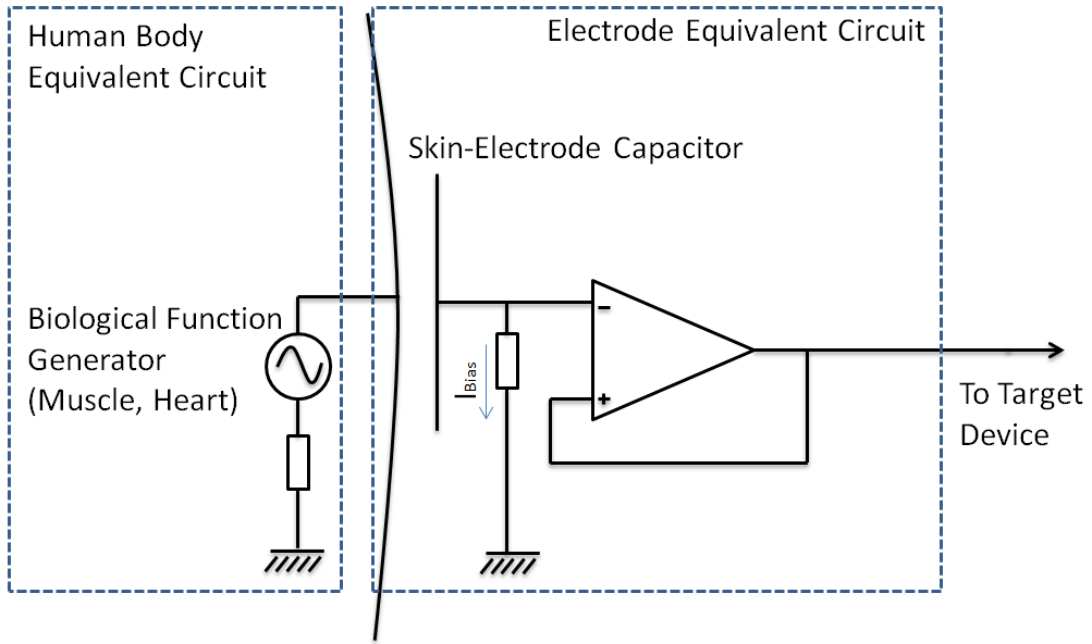


**FIGURE 6 - RESISTOR BASED INPUT BIAS CURRENT LEAKAGE**

Another approach consists in adding discharge transistors between the input lead and reference voltage, as it's been proposed in previous researches[39,40]. Unlike resistors, and similar to the operational amplifier inputs each transistor has unique high impedance values when not activated. However, in order to discharge the input lead, those transistors must be discharged. Discharge can happen in multiple fashion, depending on the adopted method, but they can introduce consistent pulse like noise from the discharge operation, gate/base current leakage noise, data distortion from temporary lower impedance and oscillation from the charging/discharging cycle. This is a major obstacle for high frequency bioelectrical signals, in particular EMG signals.

### 2.3.2 High impedance bootstrapping method

Given that input bias current based voltage drift is a relatively slow signal, if we can implement a low impedance low pass filter circuit to the input circuit without changing the high impedance input for higher frequency bioelectrical signals, then we could limit the range of the bias current base voltage drift. Therefore we define the input bias current as

$$(9) \quad i_{Bias} = i_{in}(f_{Bias})$$

where  $f_{Bias}$  is the frequency of the input bias current,  $i_{in}(f_{Bias})$  is the current component in this frequency, and  $i_{Bias}$  is the input bias current.

In this research we propose a new frequency dependant bootstrapped current leakage limiting circuit based on back to back diodes. Back to back diodes are a common circuit technique shown in Figure 7 that limits the voltage between a certain range from a given reference voltage, based on their drop voltage. Therefore when the accumulated voltage at the input lead goes above or bellow the back to back diode threshold, the input impedance at the input lead drops while the accumulated charge flows out. The problem with a passive back to back diode circuit is that during the discharge, electrical signals of all frequency will be lost. In this research we propose a solution to this problem by, instead of using a static reference voltage we use a dynamic reference based on a high pass filter feedback circuit which is defined as

$$f_{Bias} = \frac{1}{2\pi R_D C_D} \quad (10)$$

where  $C_D$  and  $R_D$  are the passive components responsible for the anti-drift high pass filter in the feedback bootstrap circuit.  $V_{out}=V_{in}$  as it is the non amplified preamplifier circuit, which is being used as simply a impedance converter. The updated model with our bootstrapped feedback circuit is shown in Figure 8.

With this feedback circuit, signals with frequency above  $f_{bias}$  will have still have a high input impedance because there is no differential of potential between the input bias and reference voltage, small thermoelectrical noise as there are no passive components and small switching noise as there is no constant switching of active components. On the other hand, signals with lower frequencies will slowly and continuously being discharged as those signals with those frequencies were filtered out by the high pass filter in the bootstrap feedback circuit. This relationship between the the input bias frequency and the feedback current  $i_D$  is given as

$$\begin{aligned} f_{in} > f_{Bias} &\Rightarrow V_D(f_{in}) \cong V_{out} = V_{in} \Rightarrow i_D \rightarrow 0 \\ f_{in} < f_{Bias} &\Rightarrow V_D(f_{in}) \rightarrow V_{REF} \Rightarrow i_D \rightarrow i_{Bias} \end{aligned} \quad (11)$$

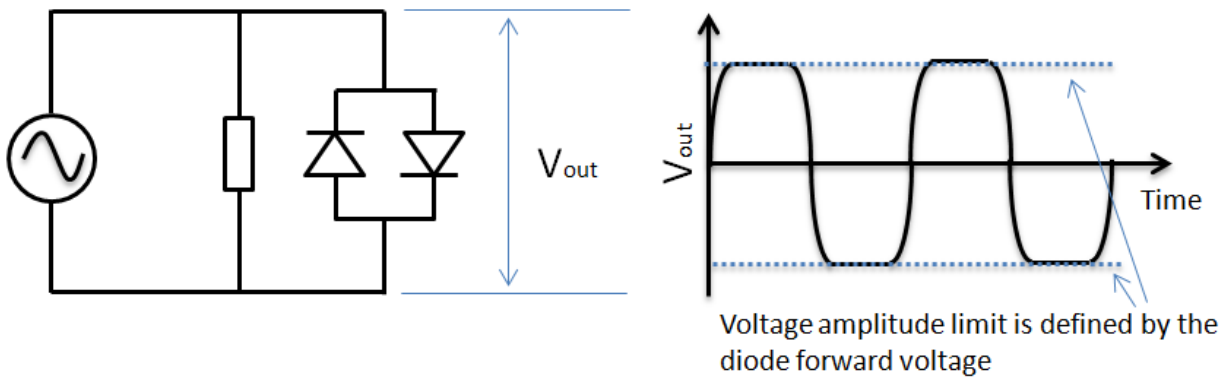


FIGURE 7 - EXAMPLE OF BACK TO BACK DIODE CIRCUIT

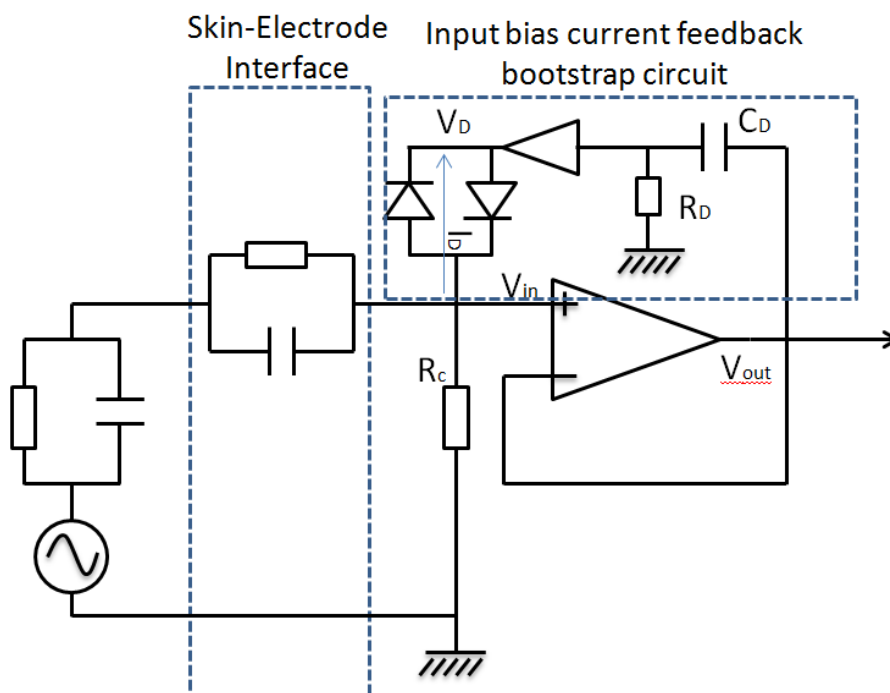


FIGURE 8 - REDESIGNED CIRCUIT MODEL WITH BOOTSTRAPPED FEEDBACK CIRCUIT

## 2.4 Dual input based noise cancelling for hybrid resistive-capacitive sensing method

So far we focused only on internal noise sources such as thermoelectrical noise and input bias current. Noise from real life situations such as motion artifacts or near high-power devices such as electrical motors are still a issue. In this study, by focusing on extending our

hybrid resistive-capacitive bioelectrical measurement model by actively measuring noise and cancelling it from the sensor output. This new model allow us to develop a new electrode design with two inputs, one for noise and one for bioelectrical signals, at different input impedance settings which are locally processed using analog circuits, resulting in a cleaner signal output.

This new model for our hybrid electrodes contains two built in sensing leads, one for the bioelectrical signals and one for the noise signals. The sensor output is given as the difference of potential of both sensing leads as

$$V_{out} = V_{in} - V_{in\_N} \tag{12}$$

where  $V_{out}$  is the sensor output,  $V_{in}$  is the bioelectrical signal with noise and  $V_{in\_N}$  is only non white noise such as motion artifacts or pulses from nearby electrical devices. Figure 9 shows the equivalent circuit when the electrodes are in use.

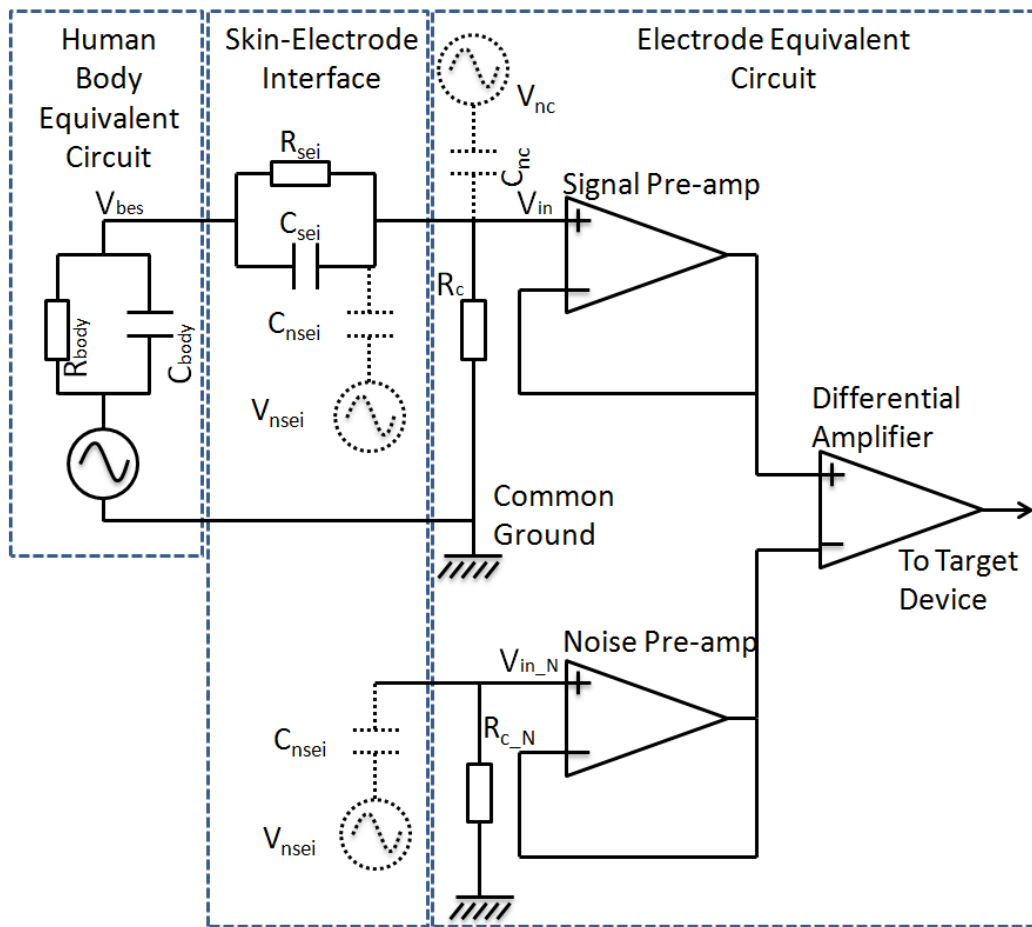


FIGURE 9 -REDESIGNED CIRCUIT MODEL WITH DUAL INPUT NOISE CANCELLING CIRCUIT

## **2.5 Hardware design**

### **2.5.1 Developed sensor unit**

Based on the proposed model above and assuming a maximum 3 mm distance between the electrode and the scalp, a circular electrode lead with 38 mm diameter and signal input impedance of  $1\text{ T}\Omega$  was developed. Furthermore, in similar fashion the noise electrode lead is designed so that only coupling with environment noise sources is significant. Under these conditions a 1 mm thick ring shaped electrode lead with outer radius of 40 mm is designed. Input impedance  $R_{c\_N}$  is also reduced to  $1\text{ M}\Omega$ , so that only noise signals with frequency above the myoelectrical frequency spectrum are measured. In resistive contact mode the area of the leads has little effect on the input impedance and low input impedance contact are enough to measure bioelectrical signal.

Because of that the noise sensing lead is electrically isolated using a thin layer of PCB resist coating. Without the coating, in resistive contact mode, very similar bioelectrical signals would be collected by both the bioelectrical and noise sensing leads, cancelling each other during the differential preamplifier stage at the electrode. As our built in noise sensing electrode lead can only filter out signals with higher frequency than myoelectrical signals, effectively acting as a very high order Low Pass Filter, a High Pass Filter circuit is also implemented using traditional circuits in order to eliminate undesirable offset voltages that can appear due to the difference in potential between both electrode sensing leads. Furthermore, back-to-back diodes are also attached to the leads in order to reduce the effects from input bias current.

In order to further increase sensor robustness, shielding attached to the noise cancelling lead was implemented as shown in Figure 12 by making use of inner layers of a multi layer printed circuit board, in which the electronic components as well as most of the circuit pattern is located in the component layer and the sensing leads in the solder layer. The assembled electrode is shown in Figure 11.

### **2.5.2 Data recording unit**

The developed electrode data recording and evaluation system also shown in Figure 10 included three stages. In the first stage, a second instrumentation amplifier receives analog signals from two electrodes and outputs the amplified difference between them. The second stage is responsible for conditioning the signal for the AD converter. The final stage involved a 16-bit AD converter connected via an SPI channel to a microcontroller. Signal sampling was performed at 1 kHz. Data was transferred from the controller to a laptop computer via a Bluetooth connection. This system is compatible with the hybrid electrodes and the commercially available Vitrode electrodes for simultaneous comparative recordings. The common ground was connected to a clean exposed body area of the user via a stainless steel

plate. Each sensor was connected to the system using a 1 meter long cable. Noise frequency spectrum measurement experiments were performed for both resistive and capacitive modes using this system by placing two electrodes face to face on differential input.

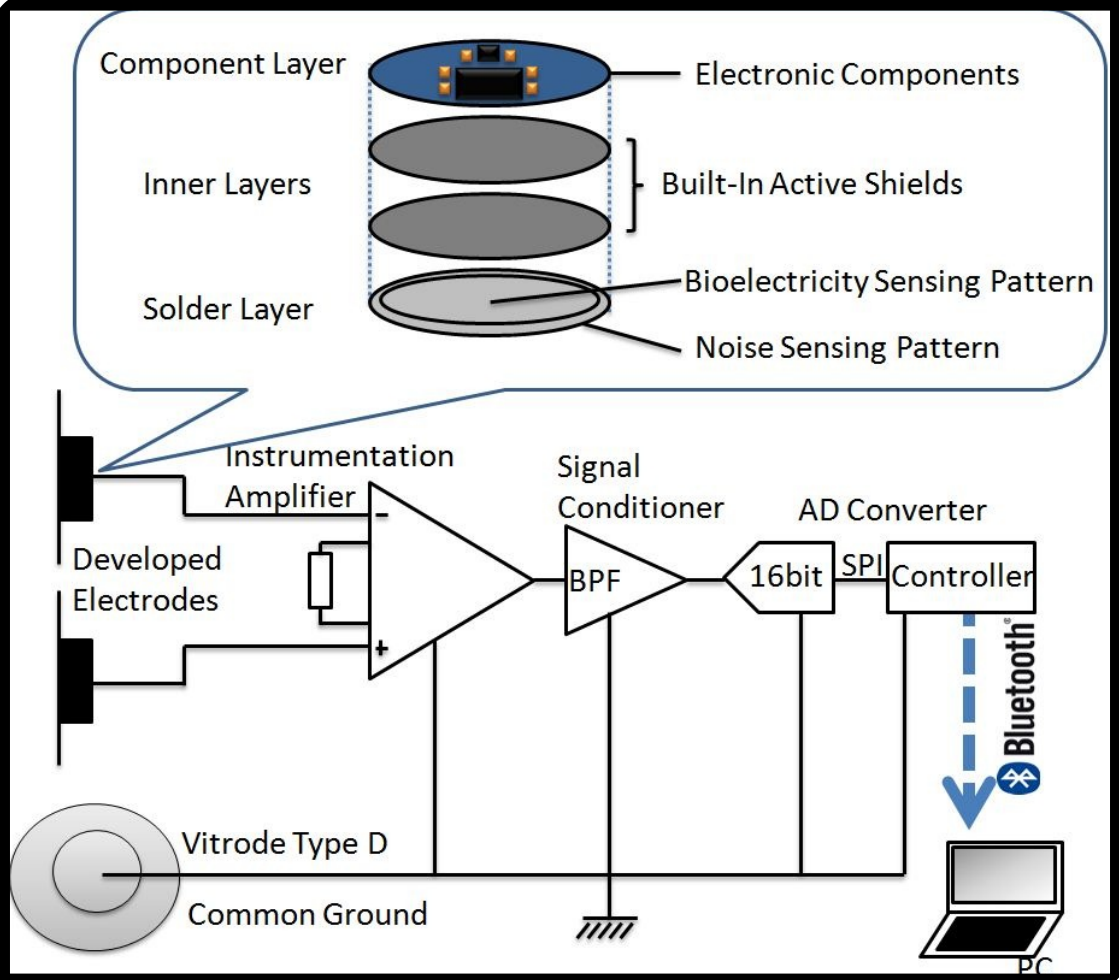
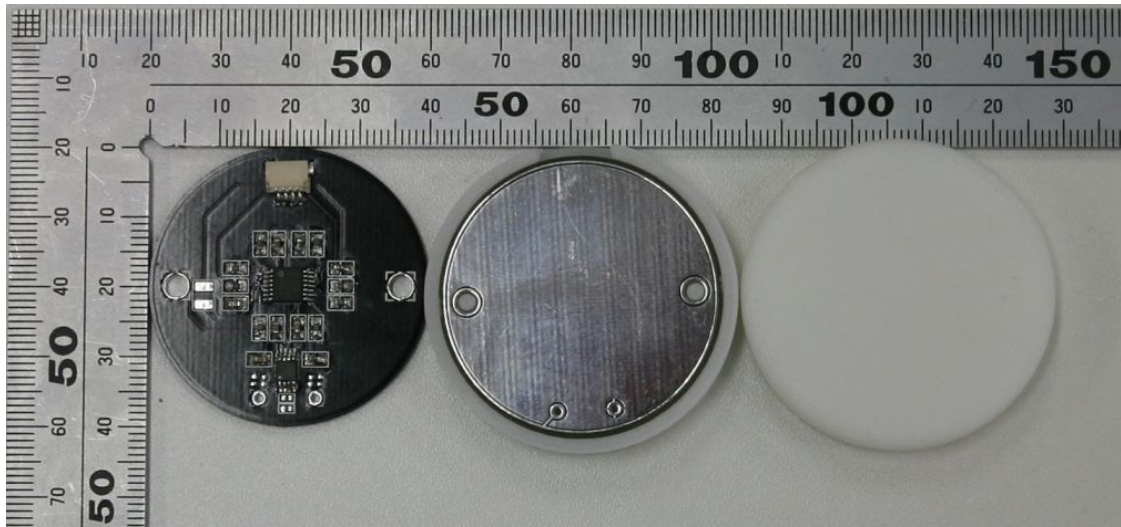


FIGURE 10 - NOISE CANCELLING LEAD IMPLEMENTATION AND RECORDING SYSTEM



**FIGURE 11 - DEVELOPED SENSOR**

## **2.6 Noise and parameter evaluation**

### **2.6.1 Frequency response**

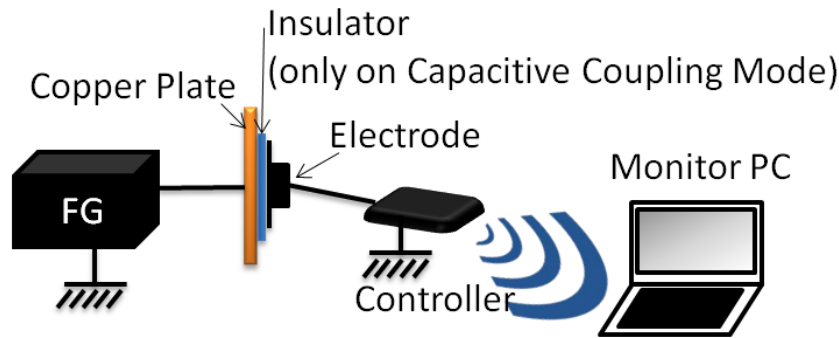
In this experiment, we measured the frequency responses of our electrodes in the resistive contact mode and the capacitive coupling mode. The experimental setups are shown in Figure 12. The electrode made direct contact with a metal signal plate attached to a function generator (WF1946B, NF Corporation, Japan) when measuring the resistive contact mode signals. To determine the capacitive mode responses, the electrode and the metal signal plate were separated by a 1 mm thick insulating rubber layer. The filters used in the data collection system shown in Figure 11 were bypassed in this experiment to facilitate direct measurements of the electrode frequency responses.

Figure 15 shows the results for the Vitrode and the hybrid electrode in the resistive mode and capacitive mode, as well as the theoretical frequency responses of the electrode in the capacitive mode. The results show that the frequency response of our electrode in the resistive mode was identical to that of Vitrode F. As both electrodes directly connect the substrate to the amplifier, there was no phase or gain change in the target frequency band.

Our results showed that the experimental cutoff frequency of 2.7 Hz was close to the theoretical cutoff frequency of 2.3 Hz. The results also showed that the hybrid electrode and the model behaved in a very similar manner to a first-order high-pass filter, as predicted by

our model. The difference in the cutoff frequency was attributed to the assumptions of our model, which only considered the ideal electronic components of the system. When developing the electrode, we added new resistive and capacitive features on the basis of the high-impedance input bias current escape path circuit described in Section 3.1 and the printed circuit board pattern and materials. The resultant input impedance was a combination of the amplifier input impedance and the impedance from the new elements. The difference in the input impedance created a difference in the cutoff frequency.

Our model was not a perfect representation of the entire system; however, 2.7 Hz was very close to the target cutoff frequency and it was an adequate value for applications in the 3–100 Hz band, which are discussed in this paper.



**FIGURE 12 - FREQUENCY RESPONSE MEASUREMENT SETUP**

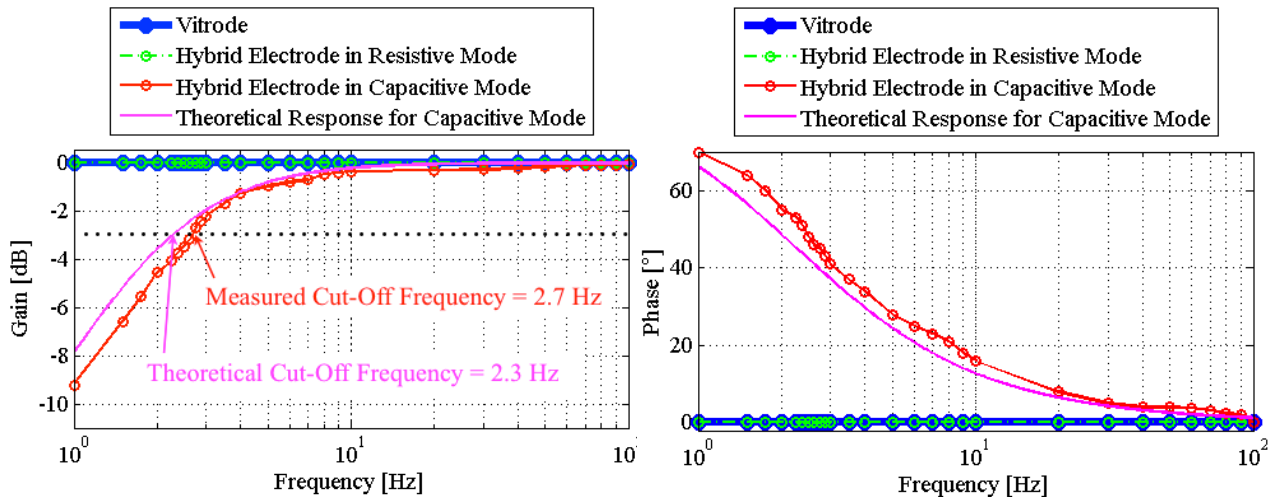


**FIGURE 13 - FREQUENCY RESPONSE FOR THE DEVELOPED SENSOR**

## 2.6.2 Electromagnetic noise spectrum

The noise levels attributable to the electronic sources of the electrode were measured by connecting the inputs of two electrodes. Resistive contact mode measurements were performed by directly shorting the inputs of the two electrodes. Capacitive coupling mode measurements were performed by placing the inputs face to face, separated by only a 3 mm thick insulating vinyl layer. The experiment setup is shown in Figure 14. The noise spectrum of the Vitrode F wet Ag/AgCl electrodes was also measured in a manner similar to that used for our electrodes in the resistive mode.

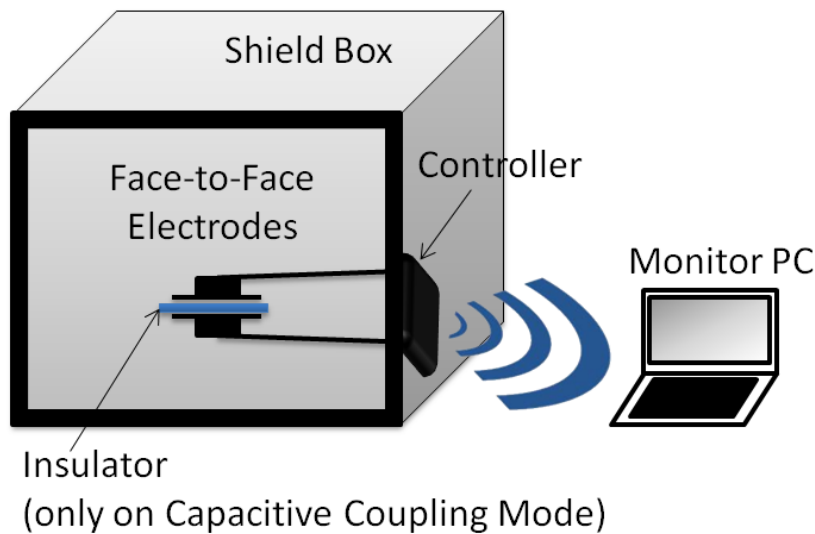


**FIGURE 14 - NOISE SPECTRUM MEASUREMENT SETUP**

The noise spectrum obtained is shown in Figure 15. The Vitrode and the hybrid electrode in the resistive mode had very similar noise spectrum characteristics in the 10-100 Hz band because they were both resistive contact-type electrodes and they were electrically coupled better with the substrate than the environment. In the 1-10 Hz band, however, our hybrid electrodes had about  $1 \mu\text{V}/\text{Hz}^{1/2}$  less noise than the Vitrode because our electrode was an active, pre-amplified type of electrode whereas the Vitrode was a passive electrode.

Because the Vitrode F is a passive electrode, it was more susceptible to displacement currents due to chemical degradation of the Ag/AgCl gel and electrostatic effects in the 1m long cable that connected the electrode lead to the amplifier and the measurement system.

However, the hybrid electrode in the capacitive mode was about 0.3 and  $1 \mu\text{V}/\text{Hz}^{1/2}$  noisier than the other two cases. According to the model shown in Figure 11 and equations (2) and (3), the relative value of the impedance value was lower in the capacitive mode when coupling the environmental noise sources ( $Z_{nc}$  and  $Z_{nsei}$ ) compared with the impedance of the coupling with the signal source ( $Z_{sei}$ ) in the resistive contact mode. This condition allowed the electrode to couple the environment noise sources better. However, our new optimal impedance electrode design indicated that the noise levels were at least two times smaller than

the weakest bioelectrical signals considered in this study and 4-6  $\mu\text{V}/\text{Hz}^{1/2}$  smaller than the capacitive coupling electrodes proposed in other studies[40,41].

This low noise characteristic in the resistive and capacitive modes was comparable to that of conventional electrodes, and it showed that our electrode was a viable sensor for detecting ECG, EMG, EEG and EOG signals.

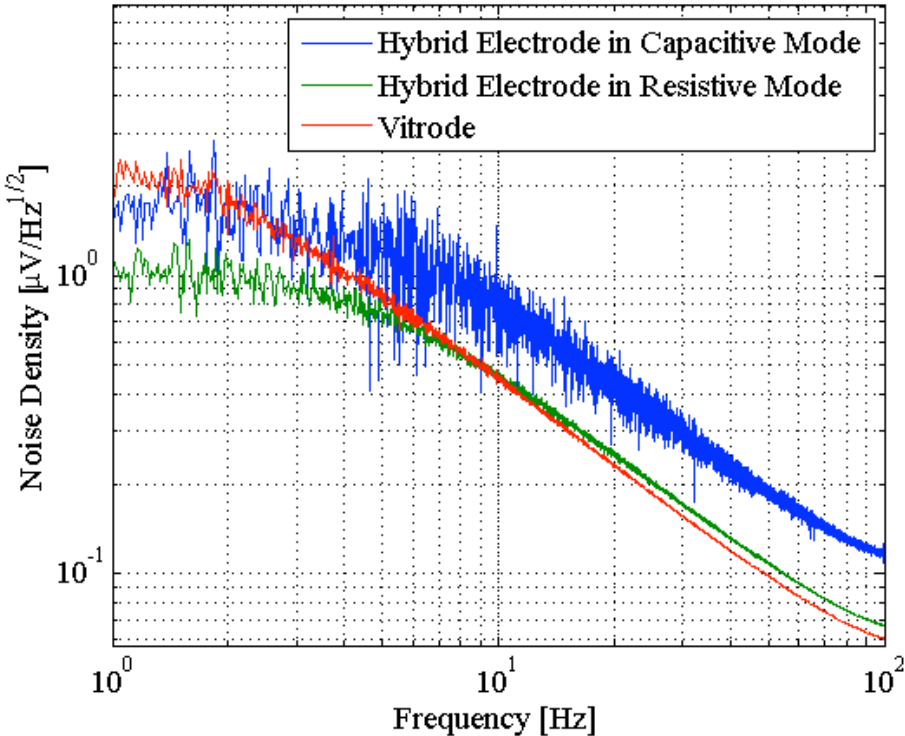
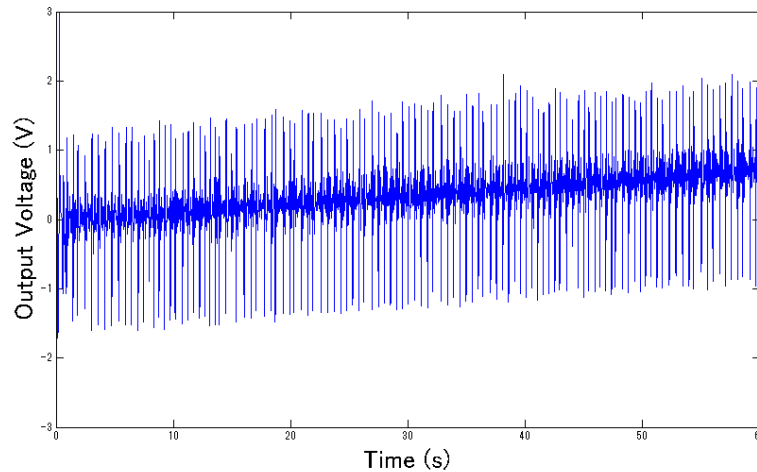


FIGURE 15 - NOISE SPECTRUM OF THE DEVELOPED ELECTRODE

### 2.6.3 Output drift

Output drift was measured by attaching the developed hybrid electrodes in capacitive mode with a 3mm thick vinyl tape isolating over the sensing lead to a participant's chest with and without the feedback bootstrapping circuit. Figure 16 shows the ECG data collected over the period of 60 seconds without the bootstrapping circuit and Figure 17 shows the ECG data collected over the same amount of time with the bootstrapping circuit being implemented.

The sensor from Figure 17 shows no drift and potential to keep measuring the ECG signal for an indefinite amount of time, whereas the sensor Figure 18 clearly shows an output drift of 0.64V/min, indicating that it would start losing bioelectrical waveform information in another 2 minutes and be completely saturated in less than 10 minutes.



**FIGURE 16 - ECG MEASURED WITHOUT THE BOOTSTRAPPING FEEDBACK CIRCUIT**

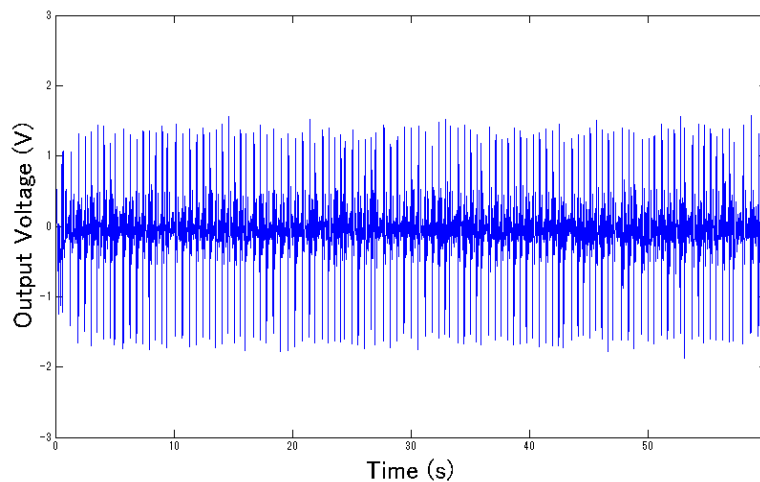


**FIGURE 17 - ECG MEASURED WITH THE BOOTSTRAPPING FEEDBACK CIRCUIT**

### 2.6.4 Motion artifacts and input saturation recovery measurements

Similarly to the previous experiment, input saturation recovery was measured by attaching the developed hybrid electrodes in capacitive mode with a 3mm thick vinyl tape isolating over the sensing lead to a participant’s chest with and without the feedback bootstrapping circuit. Saturating perturbation was introduced during the ECG measurements as a motion artefact by momentarily removing the sensors from the top of the participant’s chest. Figure 18 shows the ECG data collected over the period of 10 seconds and perturbation at the 3.1 second mark without the bootstrapping circuit and Figure 19 shows the ECG data collected over the same amount of time and perturbation at the 3.7 second with the bootstrapping circuit being implemented.

The sensor without the feedback circuit from Figure 18 takes over a second to recover from the saturating perturbation while the sensor with the feedback bootstrapping circuit on Figure 19 takes only half a second to recovery. This experiment was repeated 10 times, with the bootstrap-less sensor having a recovery time of  $1.3\pm 0.2$  seconds of recovery whereas the bootstrapped sensor having a recovery time of  $0.5\pm 0.1$  seconds.

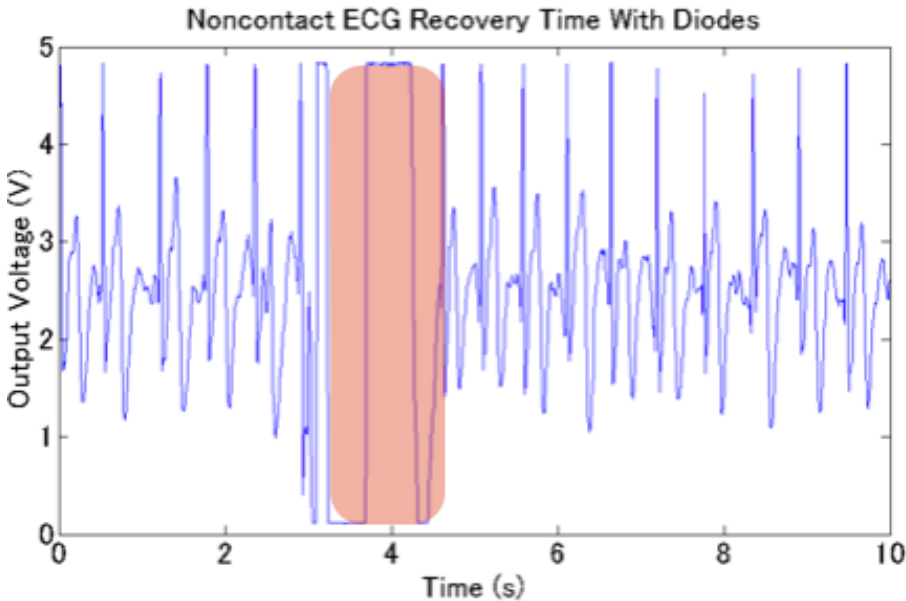
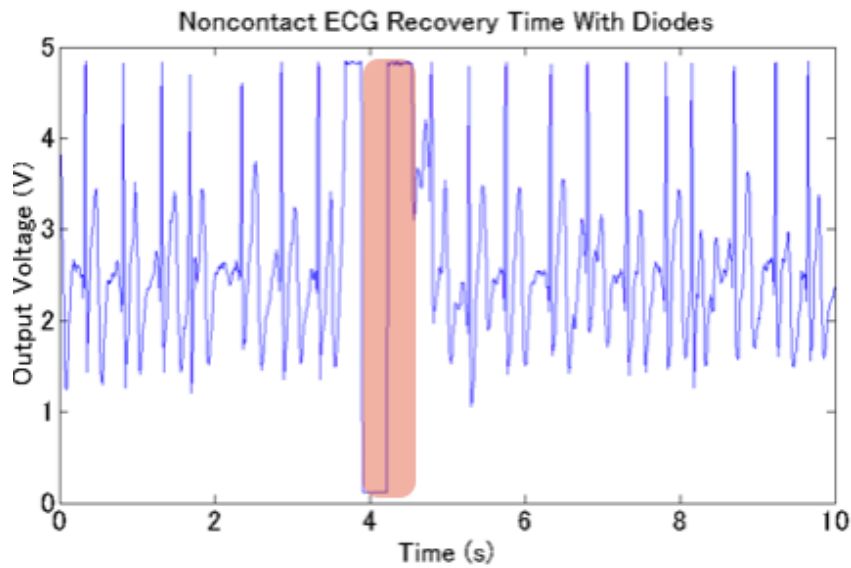


FIGURE 18 - RECOVERY TIME WITHOUT BOOTSTRAPPING FEEDBACK CIRCUIT



**FIGURE 19 - RECOVERY TIME WITH BOOTSTRAPPING FEEDBACK CIRCUIT**

### **2.6.5 Noise cancelling evaluation measurement**

Noise cancelling effect was evaluated by attaching sensors with and without the noise cancelling sensor to the participant's arm when the arm was in contact with a moving robotic arm (Kinova Jaco, Canada) moving performing a repetitive movement at approximately 2.4Hz, as shown in Figure 20. Figure 21 shows the measured data when the human arm was in rest when the robotic arm was not moving; Figure 22 when the robot arm was moving without noise cancelling on the bioelectrical sensor and Figure 23 when the robot arm was moving with noise cancelling. The sensor recording without noise cancelling registered an average amplitude of  $0.11 \pm 0.09V$  whereas the sensor with noise cancelling registered an amplitude of only  $0.02 \pm 0.01V$  and a noise reduction of 15.4 dB.

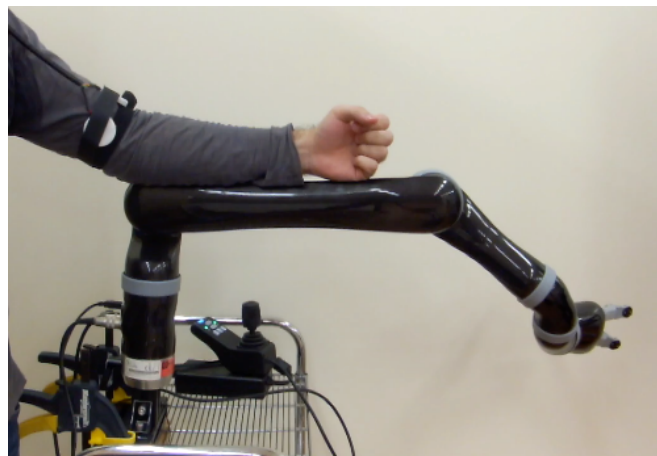


**FIGURE 20 - NOISE CANCELLING EXPERIMENT SETUP**

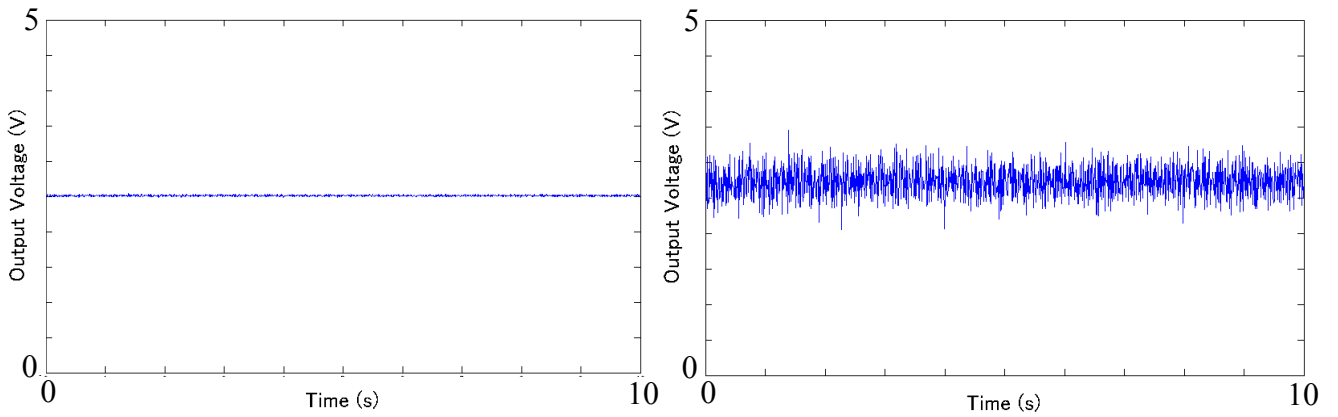


**FIGURE 21 - MEASURED DATA WHEN THE HUMAN ARM WAS IN REST WHEN THE ROBOTIC ARM WAS NOT MOVING(RIGHT IS ZOOMED UP)**

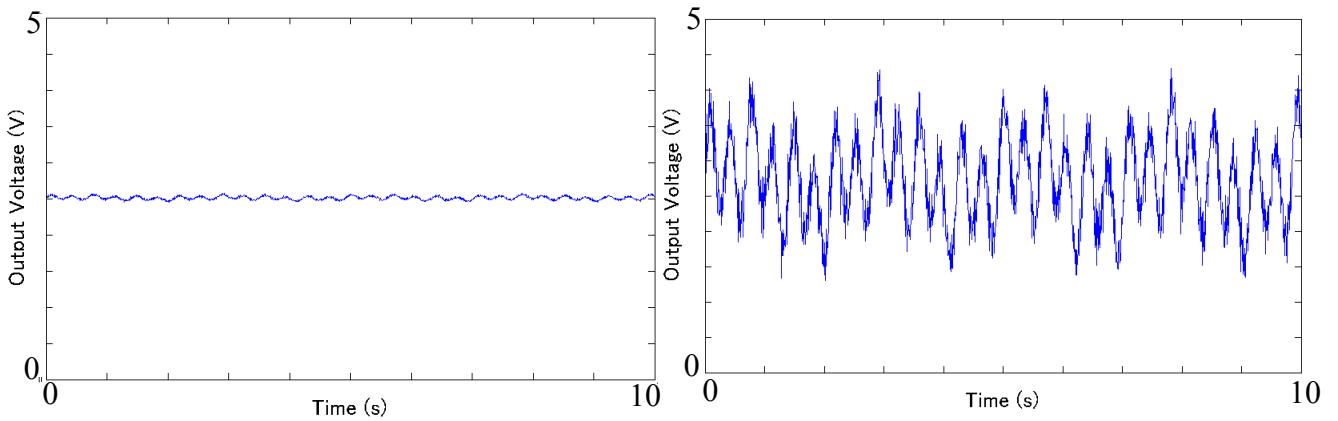


**FIGURE 22 - ROBOT ARM WAS MOVING WITHOUT NOISE CANCELLING ON THE BIOELECTRICAL SENSOR(RIGHT IS ZOOMED UP)**

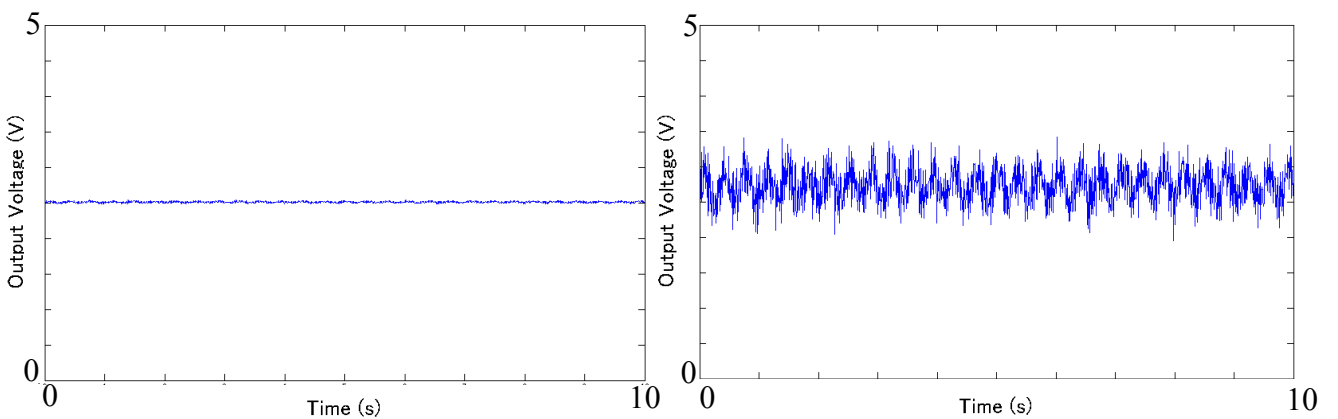


**FIGURE 23 - ROBOT ARM WAS MOVING WITH NOISE CANCELLING ON THE BIOELECTRICAL SENSOR(RIGHT IS ZOOMED UP)**

## 2.7 Discussion

The effectiveness of some of medical applications can be highly dependent on the frequency at which the patient uses the equipment. One of the main obstacles in the spread of these technologies is the difficulty of placing electrodes and performing measurements during daily life because of the requirements for skin preparation and the electromechanical contact problems associated with conventional electrodes. From a usability perspective, our electrodes are easier to use than any commercially available electrodes. Noise and parameter benchmark experiments suggest our system provides the high reliability required by professionals and end-users while also being the first time capacitive coupling based electrode measuring bioelectrical signals on non ideal conditions. As shown, skin preparation is unnecessary and our electrodes can even measure bioelectrical signals in covered body areas where electromechanical contact is impossible. This high usability has the potential to increase reliability. If electrodes are easier to use, the probability of human error is reduced. This higher usability makes our electrodes a significant step toward the popularisation of wearable sensors and computers during daily life.

The experimental results presented support our electrode impedance optimisation method and our optimal model in terms of its noise and frequency utility. The optimisation results showed that the noise levels were 4-6  $\mu\text{V}/\text{Hz}^{1/2}$  lower than those reported by other studies. The frequency response results were very close to the theoretical values; however, the observed difference suggested that the resulting input impedance in the actual electrode is slightly lower than the target value. This was not a problem for the applications described in this paper; however, some commercial and medical situations require very high levels of reliability or industrial standard definitions, so a full understanding of the electrode impedance may be required. An enhanced model that includes resistive and capacitive elements using additional board components and board design features, and different materials, may be introduced in future works.

## 2.8 Conclusion

In this chapter we designed a novel sensor circuit model based on the consideration of the electronic components imperfections and the user skin-sensor interface, which also accounted for the internal thermoelectrical noise sources and input bias current. The model contains the basic hybrid measurement principle derived from both resistive contact sensors and capacitive coupling sensors. On top of this we developed a bias current feedback circuit that eliminates current leakage and the increasing output voltage offset caused by it. Finally we expanded the circuit model into a dual input system for dual input environmental noise cancelling. Benchmark experiments showed that the parameters were as predicted by our models and that internal and external noise sources were processed as required by design.

# 3 Bioelectrical signal measurement using developed hybrid electrode

## 3.1 Introduction

In the previous part we focused on modelling and measurement of the basic capabilities and parameters of the developed electrodes. In this part we collected the ECG, lower limb and upper limb EMG, EOG and EEG bioelectrical data using our electrodes, which we compared with commercial traditional wet electrodes (Vitrode type D, Nihon Kouden) using both statistical methods and by observing characteristic points in the wave forms. Traditional wet electrodes were used due to the lack of commercial bioelectrical sensors capable of capacitive coupling for bioelectrical sensing. However, by showing that our sensors are capable of readings comparable to traditional wet electrodes we can prove the effectiveness of our sensors.

Data measurement hardware is the same as introduced in Chapter 2.5. Pearson's correlation coefficient  $\rho$  for the data collected from the hybrid electrode and wet electrodes was calculated as follows:

$$\rho = \frac{\sum_{i=0}^n X_i Y_i - \frac{\sum_{i=0}^n X_i \sum_{i=0}^n Y_i}{n}}{\sqrt{\left(\sum_{i=0}^n X_i^2 - \frac{(\sum_{i=0}^n X_i)^2}{n}\right) \left(\sum_{i=0}^n Y_i^2 - \frac{(\sum_{i=0}^n Y_i)^2}{n}\right)}} \quad (13)$$

where  $n$  is the number of samples,  $X_i$  is a normalised sample from our hybrid electrode and  $Y_i$  is a normalised sample from the Vitrode F electrode.

### 3.2 Bioelectrical signal measurement, evaluation methods and results

#### 3.2.1 Electrocardiogram measurement

In this experiment we verify if our electrode is capable of recording ECG signals with fidelity by verifying if the component waves of a standard ECG signal are present or not and by checking if the ECG signal is consistent over a long period of time. In this experiment two electrodes following standard ECG electrode placement methods as shown in Figure 24. The subject was wearing a cotton shirt with average thickness of 1 mm and the electrodes were placed above the shirt and 3 mm thick vinyl tape. Data was recorded for 20 seconds while the participant stayed seat comfortably on a chair and is shown in Figure 25.

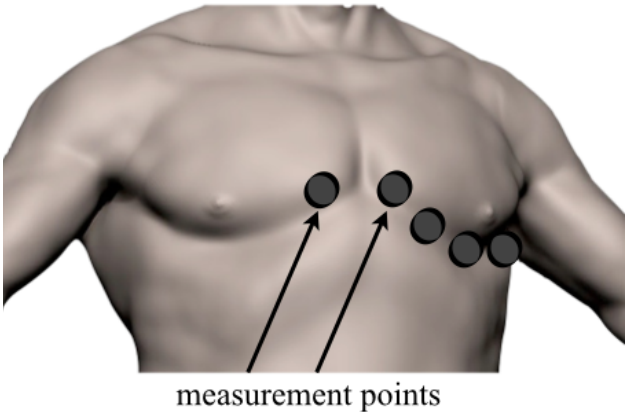


FIGURE 24 - ELECTRODE PLACEMENT FOR ECG MEASUREMENT

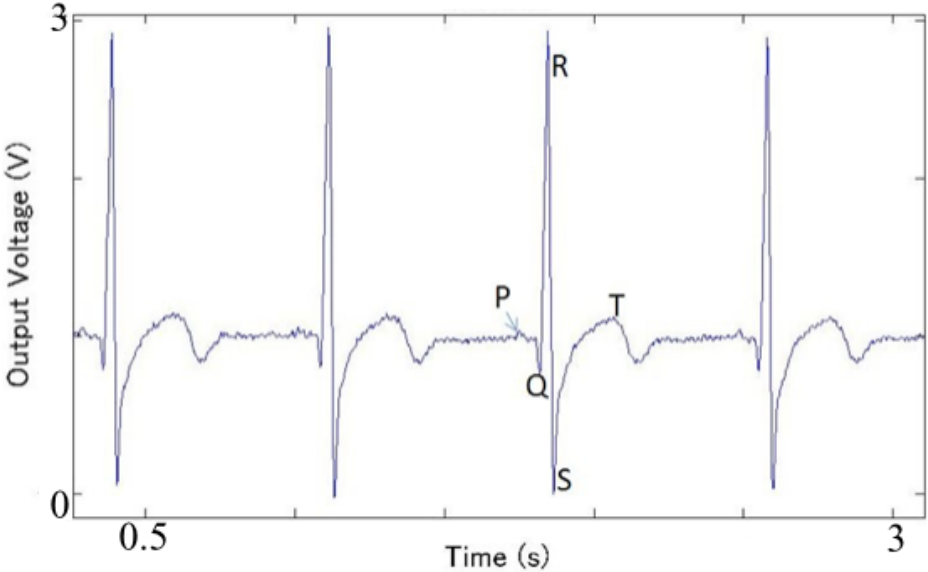


FIGURE 25 - MEASURED ECG DATA IN WHICH WE CAN VERIFY THE EXISTENCE OF ALL COMPONENT WAVE FORMS

### 3.2.2 Upper body electromyogram measurement

Several upper body EMG measurements were made under different loads and motion types.

In the first experiment we investigate the correlation between the myoelectrical signals such as the EMG data collected from a pair of hybrid electrodes with the EMG data collected simultaneously for a pair of conventional Vitrode disposable wet electrodes. Therefore we investigate the correlation of the data collected by both types of electrodes and verify the nature of the data collected by the developed capacitive coupling electrodes. Two developed hybrid electrodes are placed over the right biceps of the experiment participant. Between the right biceps skin and the electrode metallic plate a piece of cotton with thickness of 1 mm is placed in order to simulate clothing. The sensor in capacitive mode had a 3 mm thick vinyl tape glued on top of the sensing lead to guarantee isolation. Below the clothing, 2 Vitrode type D electrodes are placed as close as possible from the hybrid electrodes. Electrode placing position for upper limb EMG is shown in Figure 26 and 27. The experiment is performed by contracting the right biceps after 5s, keeping it in position for 10s and then relaxing for another 5s. The total measurement time is of 20s. Data is shown in Figure 28.

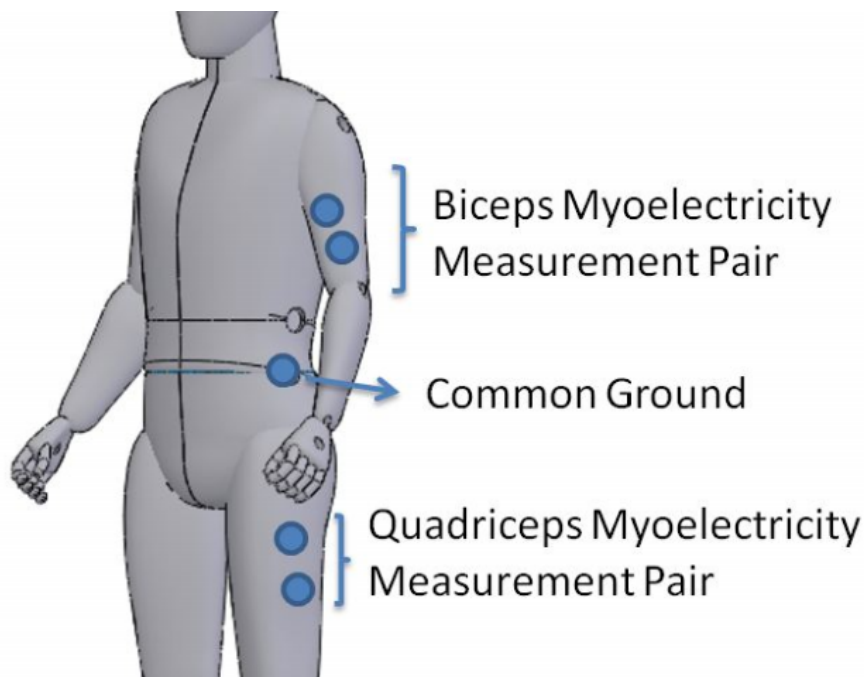
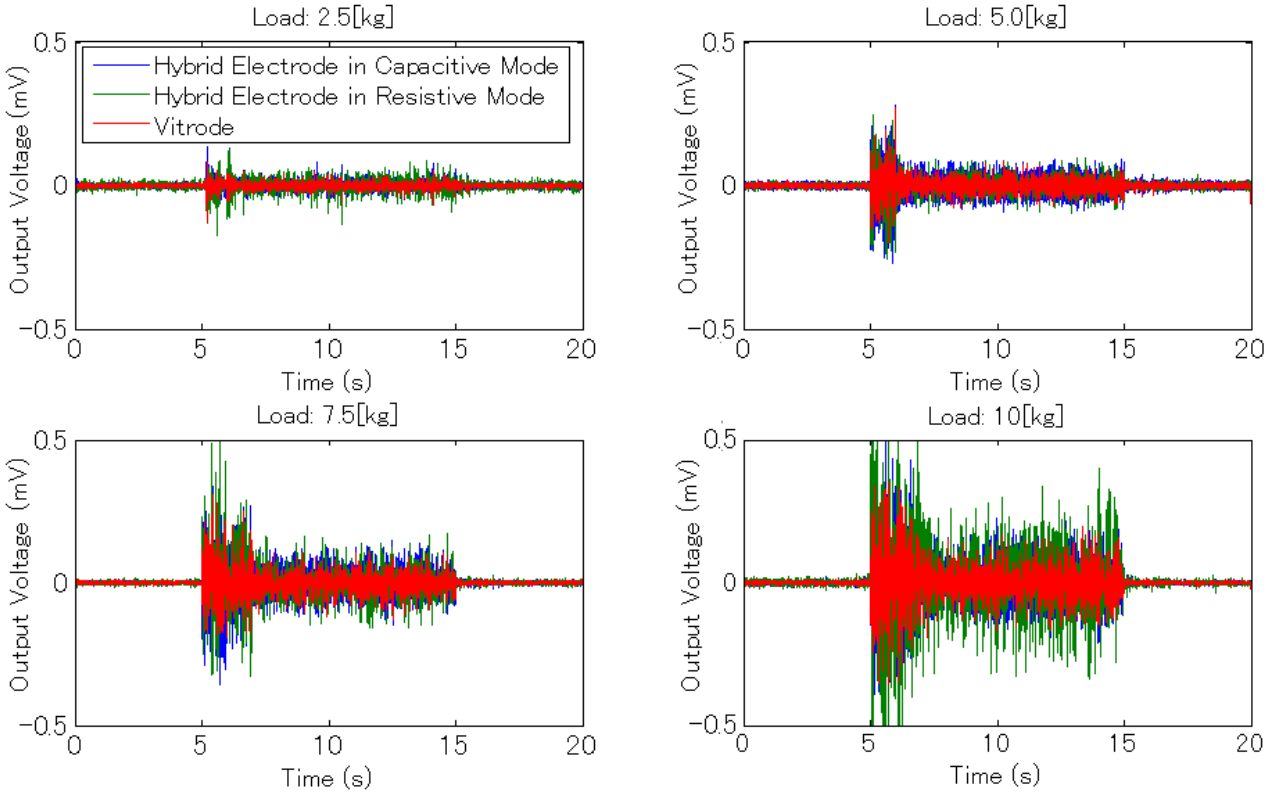


FIGURE 26 - POSITIONING OF THE SENSOR FOR EMG MEASUREMENTS



**FIGURE 27 - ELECTRODE POSITIONING OF THE SIMULTANEOUS DYNAMIC EMG MEASUREMENT WITH WET ELECTRODES AND HYBRID ELECTRODES IN CAPACITIVE MODE**



**FIGURE 28 - SIMULTANEOUS DYNAMIC EMG MEASUREMENT WITH WET ELECTRODES AND HYBRID ELECTRODES IN CAPACITIVE MODE**

In the second experiment we set to verify whether the developed hybrid electrode is capable of collecting EMG data from a muscle at different loads and is adequate to be used as an interface sensor for exoskeletons and assistive devices. The experiment setting is very similar to the previous experiment. However in this case the participant keeps his biceps under continuous stress for 10 seconds. Data is measured for loads of 2kg, 4kg, 6kg, 8kg and 10kg. Data is also measured when there is no load and the results are shown in Figure 29. Similar to the previous experiment, a pair of hybrid electrodes is placed above right biceps with a piece of cotton cloth with average thickness of 1 mm between the electrode and the skin to simulate clothing. The sensor in capacitive mode had a 3 mm thick vinyl tape glued on top of the sensing lead to guarantee isolation.

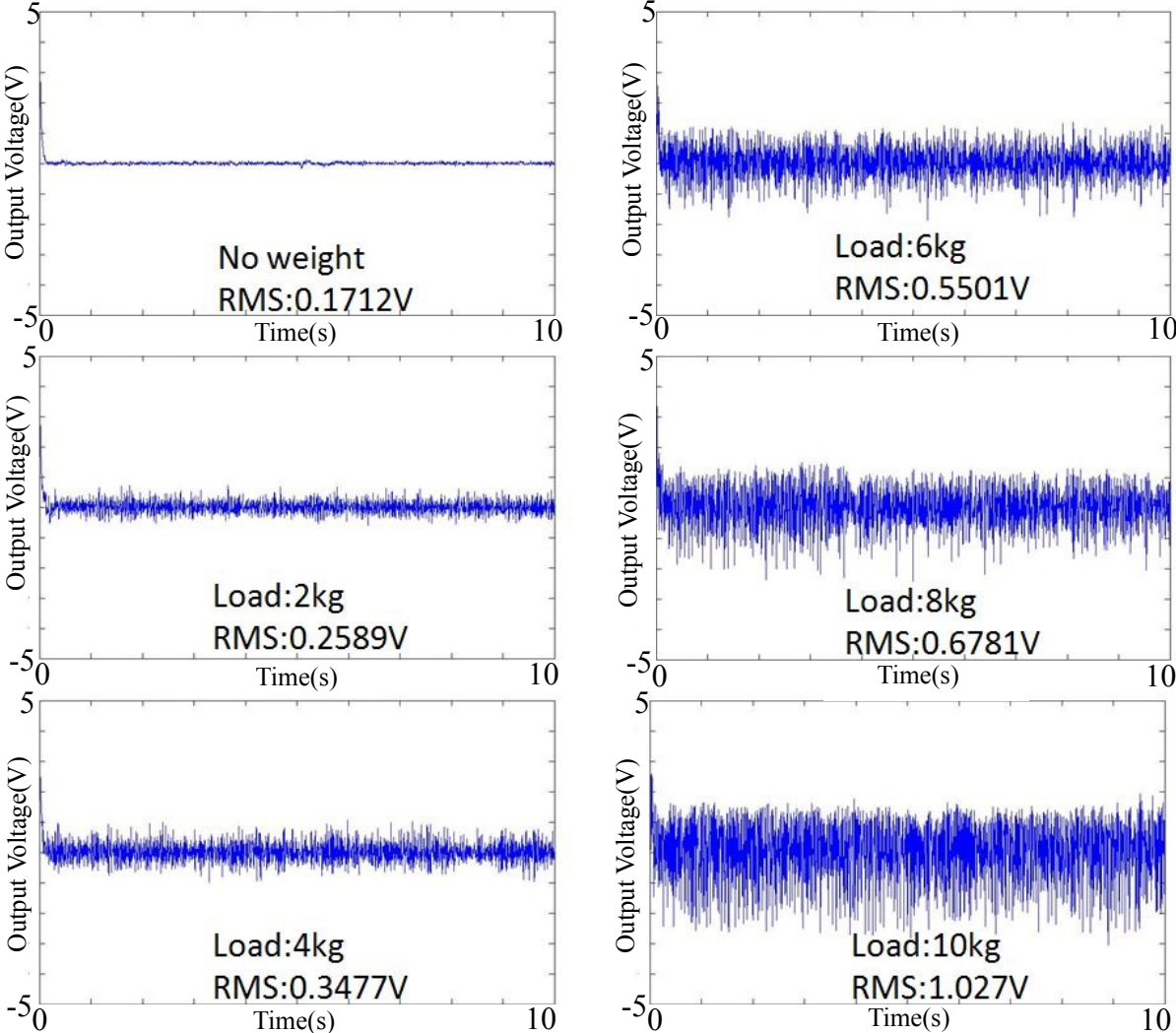


**FIGURE 29 - CAPACITIVELY COUPLED EMG MEASUREMENT UNDER MULTIPLE LOADS**

In the third and final experiment, in order to verify the operation of our developed electrodes near electrical appliances, a simple robot arm control experiment was also performed. While leaving the arm at rest, the robotic arm(Jaco by Kinova, Canada) also stayed at a resting position. By lifting the arm into a 45 degree position, the EMG signals from the biceps switch on the robotic arm, also rotating it 45 degrees. Each movement was repeated two times for 10 seconds. The participant's arm was in contact with the robotic arm through the entire experiment. Results are shown in Figure 30.

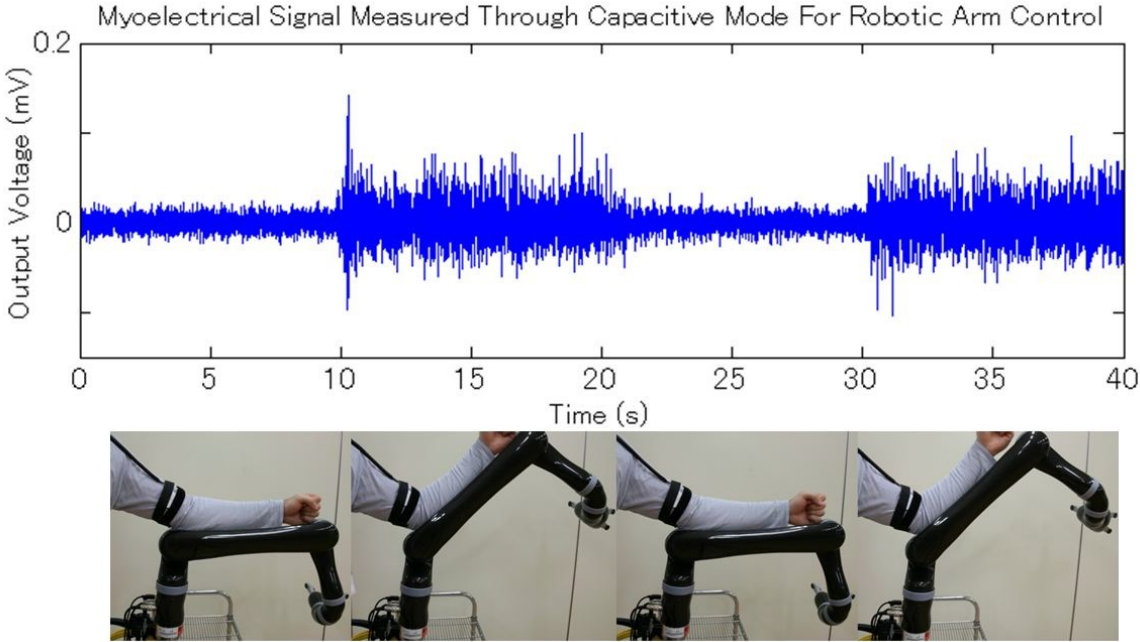


**FIGURE 30 - ROBOT CONTROL USING CAPACITIVELY COUPLED EMG**

### 3.2.3 Lower body electromyogram measurement

Measurement of EMG signals while walking is a fundamental procedure in rehabilitation treatments. In this study we evaluate the performance of our enhanced hybrid electrodes by measuring EMG signals from the quadriceps while walking on a treadmill.

In this experiment the participant walked at a constant speed of 1.2 m/s on a treadmill for a period of 20 seconds. The enhanced hybrid electrodes were attached to the quadriceps of the participant as shown in Figure 27. Simultaneous measurements on both resistive and capacitive mode were performed. Electrodes in capacitive mode were separated from the skin through a 2.2 mm jeans pants. Results are shown in Figure 31.

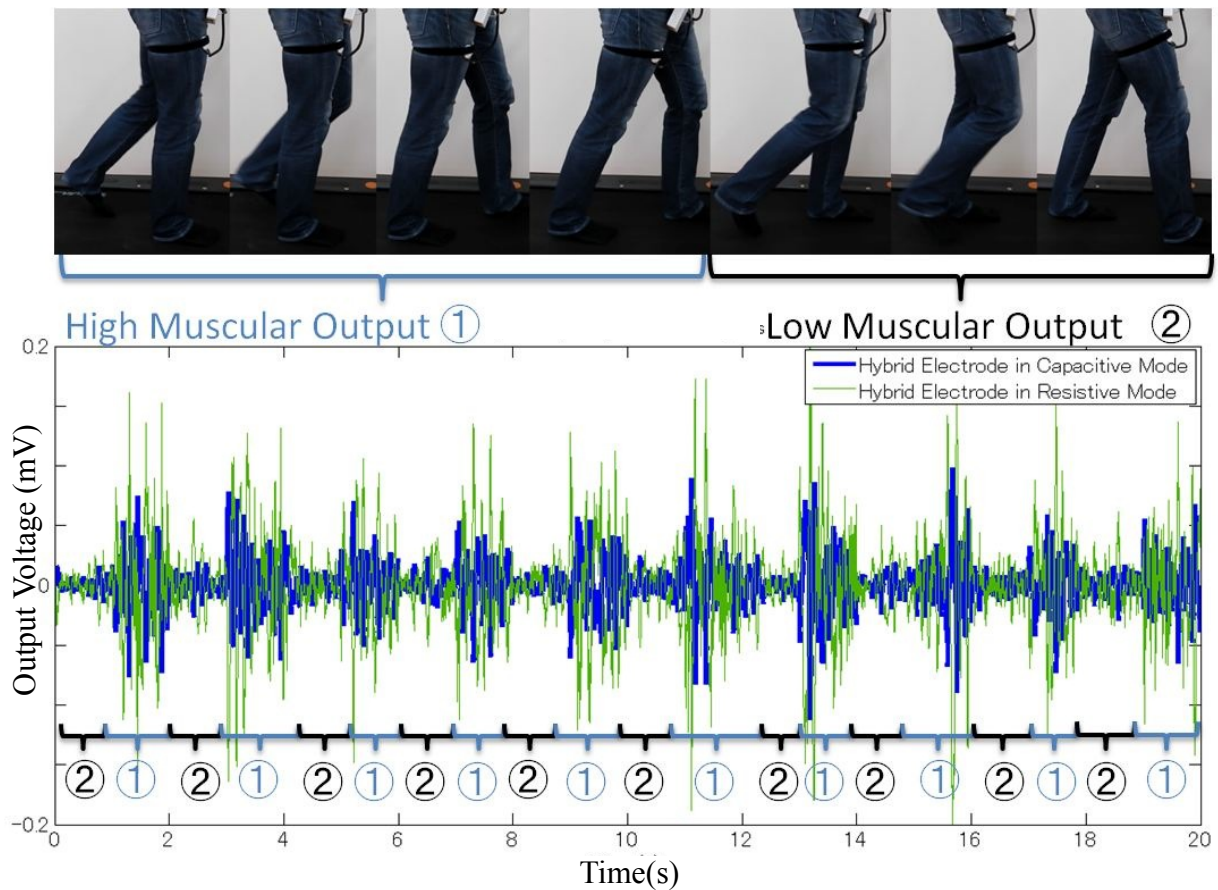
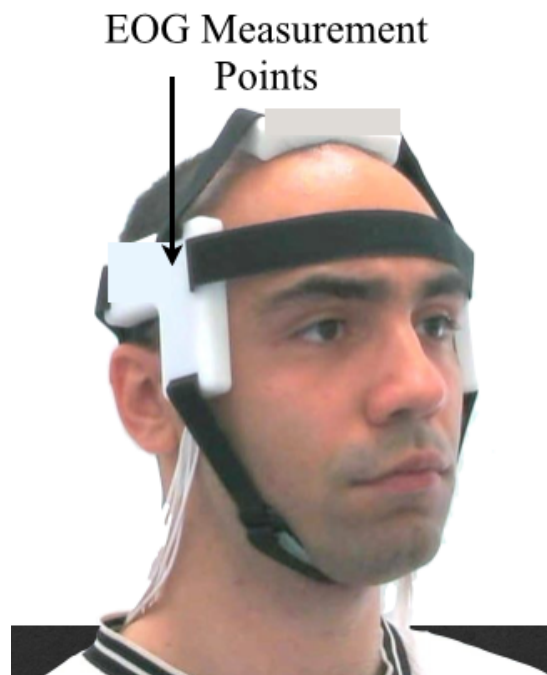


FIGURE 31 - CAPACITIVE COUPLED EMG FROM THE QUADRICEPS MEASURED DURING WALKING

### 3.2.4 Electrooculogram measurement

Eyeball and eyelid movement recordings were made using the developed hybrid electrodes in the resistive contact and capacitive coupling modes. The resistive contact and capacitive coupling mode recordings were made in a similar manner to the experiment described in previous experiments. Simultaneous recordings with Vitrode F were made for comparative purposes. The Vitrode F electrode pair was positioned as close as possible to our developed electrodes, where the center of each Vitrode electrode was 30 mm from the center of the nearest developed electrode. The Vitrode F electrodes were attached to skin areas that had been cleaned with alcohol to remove any sweat and skin oils, in accordance with the manufacturer's instructions. No skin preparation was required for our hybrid electrode in the resistive or capacitive modes. However, the electrode was isolated from the skin using a 3mm thick vinyl tape layer during the capacitive mode experiments. Electrodes were placed as shown in Figure 32. Blinking results are shown in Figure 33 and eyeball movement results are shown in Figure 34.



**FIGURE 32 - POSITIONING OF THE SENSORS FOR EOG MEASUREMENTS**

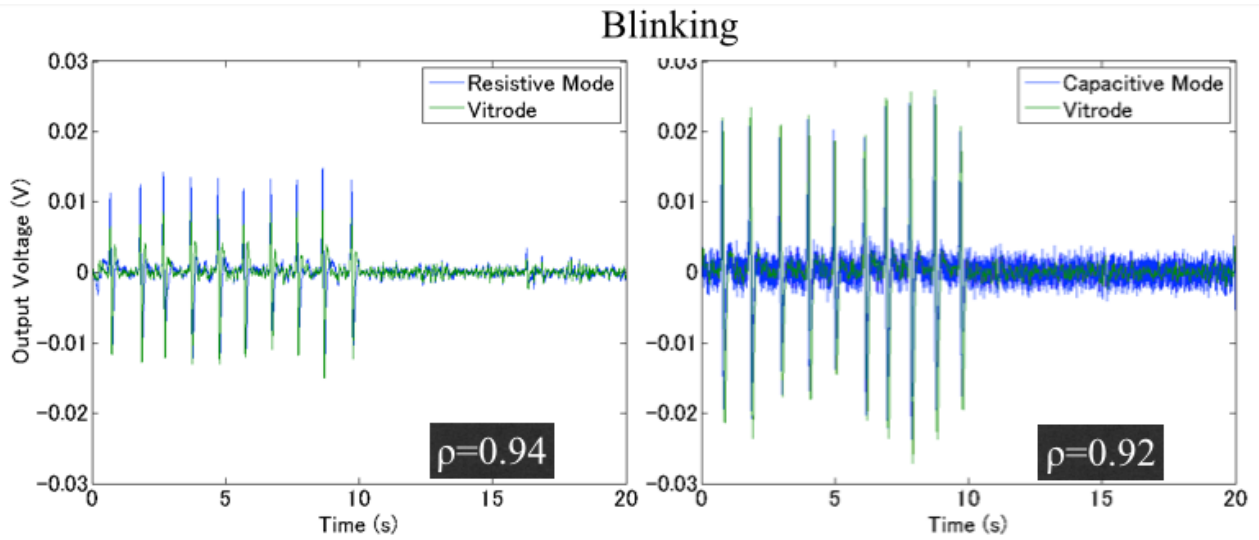


**FIGURE 33 - BLINKING RESULTS AND CORRELATION FACTOR WITH TRADITIONAL ELECTRODES**

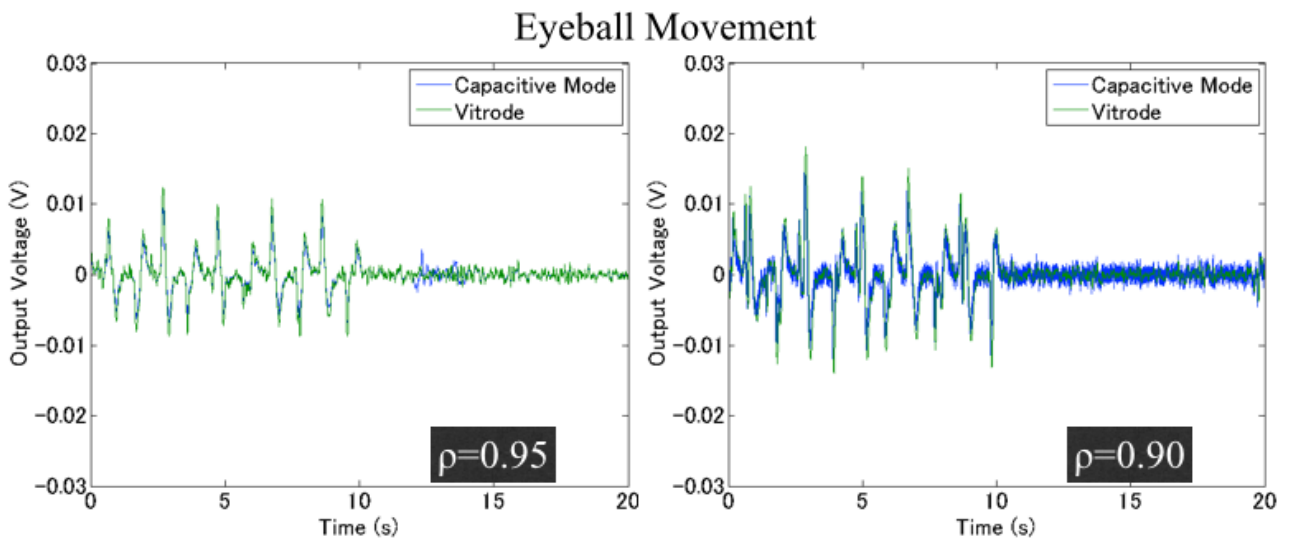


**FIGURE 34 - EOG(EYEBALL MUSCULAR ACTIVITY) MEASUREMENTS AND CORRELATION FACTOR WITH TRADITIONAL ELECTRODES**

### 3.2.5 Electroencephalogram measurement

The 10-20 Hz band bioelectrical signal recording capacity of our hybrid electrodes was tested by performing alpha and beta band EEG recording experiments. The three types of electrodes were placed over the skin. A pair of Type L electrodes was positioned, using the headset shown in Fig. 5, near the forehead and near points F3 and F4 in the International 10-20 Electrode Placement System[45]. The correlation coefficient for the data obtained using the hybrid electrode and the Vitrode was calculated using equation (13). Electrodes were placed as shown in Figure 35. Results are shown in Figure 36.

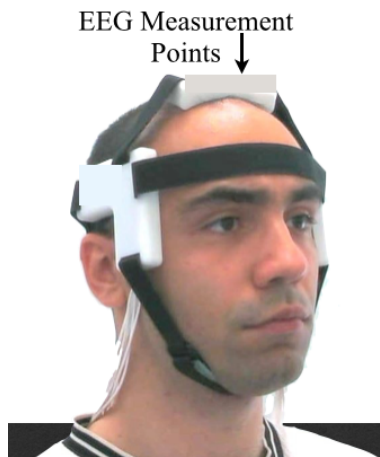


FIGURE 35 - POSITIONING OF THE SENSORS FOR EEG MEASUREMENTS

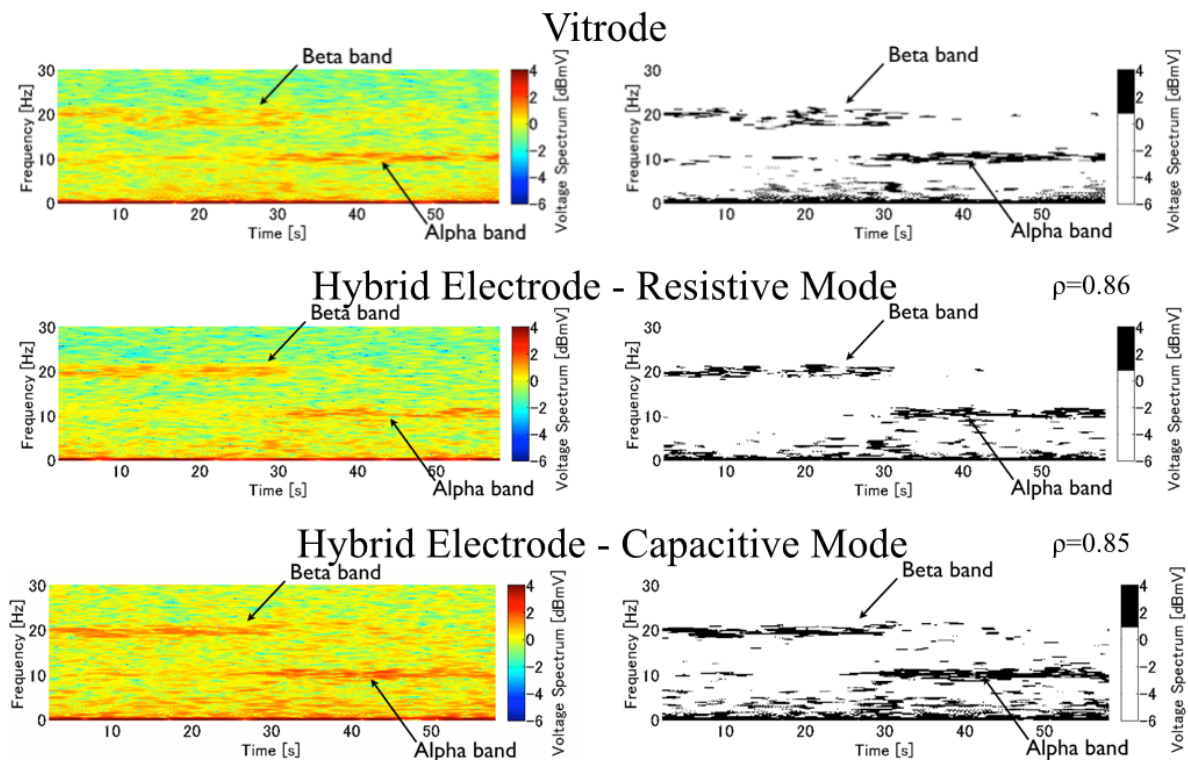


FIGURE 35 - EEG MEASUREMENT RESULTS WITH CORRELATION COEFFICIENTS

### **3.3 Bioelectrical signal measurement analysis**

#### **3.3.1 Electrocardiogram measurement**

Recorded data is shown in Figure 28. From the results we can see that our electrode was capable of recording ECG signals consistently over a period of time of 20 seconds. Also by plotting the data from the first three seconds in Figure 29, we are able to verify that the electrode recorded all the major component waves (P,Q,R,S,T,U waveforms) of the standard ECG waveform.

#### **3.3.2 Upper body electromyogram measurement**

In the first experiment, the recorded experimental data is shown in Figure 30. From the results we can see that the EMG data collected from the Vitrode pair of electrodes overlap most of the data collected by the hybrid electrodes. The calculated correlation coefficient for this dataset was of 0.93, showing that the developed capacitive electrodes are capable of collecting the signals originated from myoelectrical activity and that both the hybrid electrode and vitrode disposable wet electrodes are capable to collect very similar EMG signals.

In the second experiment, acquired results are shown in Figure 31. The root mean square (RMS) value for each case is calculated and displayed inside its corresponding graph. The results show that the developed hybrid electrode is capable of recording signals with variable intensities and from the RMS values, we verify that the heavier the load the stronger is the signal.

In the third the recorded experimental data for the robot arm control experiment is shown in Figure 32. The arm weight was enough to stimulate the biceps and create a signal strong enough to be used as in a simple trigger algorithm. Moreover, the presence of an electrical motor near the electrodes did not interfere with its functionality.

#### **3.3.3 Lower body electromyogram measurement**

The recorded experimental data for the treadmill walking experiment is shown in Figure 33. The results showed that the quadriceps is in constant work during the walking process but upon contact of the leg with the floor, the temporary weight supporting action of the muscle is the biggest. From the results we also can observe that the myoelectrical data collected by the

enhanced hybrid electrode in both resistive and capacitive mode is mostly overlapping, with a calculated correlation coefficient of 0.76. No visible motion artifacts were observed in the experiment data.

### **3.3.4 Electrooculogram measurement**

During eyelid movement recordings, the participant blinked at a frequency of 1 Hz, according to a metronome. The datasets obtained are shown in Figure 34. The calculated correlation coefficient for the data collected from our electrodes in the resistive contact mode and Vitrode F was 0.94, while the correlation coefficient for data collected from our electrodes in the capacitive coupling mode and Vitrode F was 0.92.

During eyeball movement recordings, the participant moved his eyeballs up and down at a frequency of 0.5 Hz, according to a metronome. The datasets obtained are shown in Figure 35. The calculated correlation coefficient for the data collected from our electrodes in the resistive contact mode and Vitrode F was 0.95, while the correlation coefficient for the data collected from our electrodes in the capacitive coupling mode and the Vitrode F was 0.90.

### **3.3.5 Electroencephalogram measurement**

EEG signals were measured while the participant kept their eyes open for 30 s when beta waves were predominant, and they were then closed for another 30 s when the alpha waves were predominant. Figure 13 shows the spectrograms of the recorded data and a binary version that only shows signals  $>1$  dBmV, for all three types of measurements. The spectrograms clearly show that our electrodes measured strong beta bands during the first 30 s and strong alpha bands during the last 30 s of the experiment. The calculated correlation coefficient for the data collected from our electrodes in the resistive contact mode and Vitrode F was 0.90, while the correlation coefficient for the data collected from our electrodes in the capacitive coupling mode and Vitrode F was 0.84. The results show that our hybrid electrodes delivered a performance that was comparable to that of conventional electrodes when sensing EEG signals.

## **3.4 Discussion**

One of the key aspects of this paper, the implementation of a dual signal lead system with a differential preamplifier unit built in the electrode, is better design choice than applying an analog or digital Low Pass Filter during signal conditioning because it removes a significant

amount of noise before the electrical signal enters our system, avoiding problems caused by the limits on operational amplifiers power supply. Both lower and upper limb EMG recordings did not show any major disturbances from nearby robotic arm and electrical treadmill. During experiment the first experiment in the EMG measurement experiment set, there are two reasons for the correlation coefficient between the data collected by the wet electrodes and the data collected by the developed hybrid electrodes to be 0.93 instead of 1. One reason is that EMG recorded by the hybrid electrodes at varying loads because the hybrid electrode and its correspondent wet electrode were not placed in the exact same place. Between the center of the hybrid electrode and the center of the wet electrode there was a distance of 3 cm. Previous research have shown that 3 cm is a distance big enough to produce create distortions between the data collect at two points. The second reason is in the fact that the measured physical phenomena between both types of sensors is slightly different. Wet electrodes are directly measurement the electrical current on the skin, where as hybrid electrodes are measuring the electrical field produced by those currents.

Similarly, the observed correlation coefficients for the EOG experiments presented in the last section were all above 0.90. However, the correlation coefficients in the EEG experiments in were between 0.84 and 0.90. The EEG readings had lower correlation coefficients because they were 10 to 100 times weaker than the EOG signals. Weaker signals had a larger effect on the random noise shown, which reduced the correlation between the two different readings. Another factor was the distance between the electrodes. Previous studies have shown that a 30-mm distance between the centers of the two electrodes during simultaneous recordings was sufficient to produce different signals and a lower correlation.

### **3.5 Conclusion**

In these experiments we verified through both characteristic waveforms as well as statistical analysis that our electrode maintained a low noise level that was comparable to the noise level maintained by traditionally wet electrodes during ECG, EMG, EOG and EEG measurements while also being providing the higher wearability and usability expected from non contact electrodes.

# **4 Wearable high resolution high speed hybrid resistive-capacitive bioelectrical sensing system**

## **4.1 Realising the full potential hybrid resistive capacitive measurement system**

Developing wearable systems that are built around the advantage of having high wearability and usability provided by capacitive coupling, but that are still strong against disadvantages such as higher environmental electrostatic noise sensitivity is the final step in taking full advantage of the hybrid resistive-capacitive bioelectrical measurement methods. In particular, self-contained wearable system capable of multichannel, high spatial and temporal resolution recordings using parallel analog and digital processing techniques could improve the signal and information quality recorded from the developed sensor while also demonstrates its usefulness and open the path for further improvements and applications, in particular for EEG measurements where high wearability, low noise, high spatial and temporal resolution are desirable qualities.

The use of brain machine interfaces for monitoring the changes in the brain activity of patients under rehabilitation treatments has been proven effective in the field of neuro-rehabilitation[46]. By constantly monitoring the brain activity of patients in rehabilitation, recordings of the stimulated areas of the brain during the total treatment period can be obtained, as opposed by sporadic data sets obtained through Magnetic Resonance Imaging (MRI). Analysing this data could help in the development of new more efficient training techniques, reducing the treatment time and improving the treatment results.

For both implementation of brain computer interfaces for disabled patients and rehabilitation training evaluation, it's required to develop a brain activity monitoring device that can be used during daily life. Such device would have to meet the following requirements:

(1)Portability: Patients already have to use beds and chairs cluttered with other medical equipment. It's mandatory that all the devices in the life support system, including brain machine interfaces to have the smallest footprint as possible. In addition to that, rehabilitation patients must be able to freely move while wearing the device.

(2)Reliability: The device must have high temporal and spatial data resolutions and high signal-noise ratios, in order to allow the implementation of efficient applications and construction of robust data sets.

(3)Wearability: The device also must easily be worn in order to reduce physical and psychological stress on the patient and reduce the error due to sensor misplacement. The

device must also be easily taken off for personal hygiene, personal comfort or maintenance purposes.

(4)Flexibility: to be able to adapt to the user needs. Rehabilitation patients may need only to monitor the motor cortex while patients may want to monitor the entire brain.

Numerous brain activity monitoring techniques exist. Functional Magnetic Resonance Imaging (fMRI), Positron Emission Topography (PET) and Magnetoencephalography (MEG) are high-precision techniques used in big hospitals and research centers. fMRI and PET, while capable of recording activity at less than a millimeter precision, those two techniques are dependent on blood flow variation[47]. Because of that, depending of the application they may not be responsive enough. Furthermore, all those three techniques require large scale equipment, have high initial and maintenance costs, highly specialized personal and the brain monitoring recordings must be executed under heavily controlled environments, making those techniques not adequate for constant brain monitoring.

On the other hand, small scale, low cost techniques such as functional Near-Infrared Spectroscopy (fNIRS) and EEG are widely adopted. Similarly to fMRI, fNIRS is also based on measuring variations in the blood flow and levels of oxygenation. While fNIRS data may help locating active areas of the brain with precision, previous researches have shown that it also contains delays and may not be suitable for real-time brain machine interfaces[48]. EEG, therefore, is the only brain monitoring technique that can potentially satisfy all the requirements listed in the previous section at satisfactory levels.

Currently there are several EEG recording devices commercially available[49][50][51]. However devices such as the EPOC (Emotiv Systems, Australia) headset lack flexibility and reliability, while devices such as the G.Tec headset (Guger Technologies, Austria) lack wearability and portability. Thus, an EEG monitoring system that satisfies all the requirements listed in the previous section does not exist yet.

In this research, we propose a design and build an EEG monitoring platform for rehabilitation and life support for disabled patients, that is wearable, user-friendly flexible and is capable of high-resolution data measurements.

In order to achieve this purpose we, first, develop an EEG sensor that can record EEG signal under a variety of circumstances, including lack of direct of contact with the scalp, and are easy enough to wear so that it can be used during daily life while still keeping signal/noise ratio high enough to be used for both rehabilitation and life support applications. Secondly, we develop a headgear using simple link mechanisms and elastic arrays in order to quickly and easily accommodate 119 electrodes on the users head. We also develop a embedded system to record the data and a computer software to record, analyse and display the data in real time. As for the next step, we perform device operation checks through a series of common EEG experiments to verify if our system perform capable to collect standard brain waves as well as other already available EEG recording devices.

## 4.2 Fully integrated electroencephalogram measurement system

### 4.2.1 Small package hybrid electrodes

Using the hybrid electrode design theory from Chapter 2, we developed hybrid electrodes in a small package all the conditions necessary to perform non-contact EEG recording through capacitive coupling and active EEG recordings. The electrode was designed by selecting an operational amplifier that at the same time had a input impedance of  $1\text{ T}\Omega$  and  $9\text{ nV/Hz}^{1/2}$  and low noise characteristics and by protecting the input with standard shielding techniques. The developed electrodes are pictured in Figure 36.

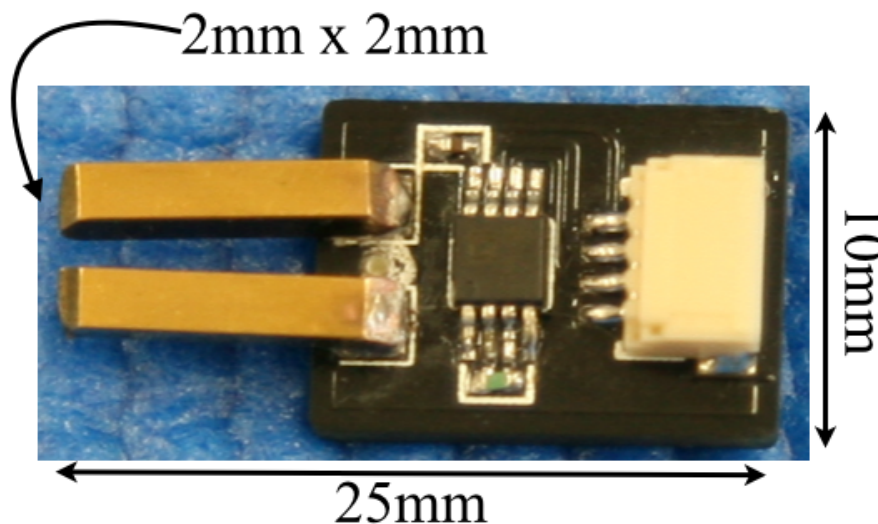


FIGURE 36 - DEVELOPED SMALL PACKAGE HYBRID ELECTRODES

### 4.2.2 Headgear mechanism

Commercial EEG monitoring devices can be divided in to 3 categories:

High wearability low flexibility devices: The Epoc headset is a major example. Epoc is capable of collecting data from 16 electrodes. However, the position and maximum number of electrodes is fixed eliminating any possibility of user customization. The low resolution may also not be enough for driving a multiple input computer based BMI system.

Mid wearability, mid flexibility devices: The G-tec head set is a major example. of this category of devices. Headsets in this category usually have between 48~96 electrodes.

However while the headset itself is wearable, the amplifiers and filter boxes are standalone devices connected to a PC. Furthermore, most headsets in this category require wet electrodes and need to be assembled every time measurements take place showing higher flexibility but lower usability than the headset such as the Epoc.

Low wearability, high flexibility: Custom electrode array attached directed to the scalp are a major example of this category of devices. In this category of headsets, users can freely place as many electrodes as they want, offering maximum flexibility in measurement. However, due to the fact the electrodes on those devices are usually attached to the scalp using the adhesive gel in the electrodes, when the user sweats or move the scalp too much, the electrodes lose contact and fall from the system. For this reason the maximum amount of time a measurement can take place is limited. Also, for the same reason, the patient must remove all hair from the head demonstrating very low usability.

The standard 10-20 electrode placement method is very old and only allows only up to 20 electrodes. It also only allows one reference electrode on a predetermined place. Depending on the experiment, such as Mu-rhythm monitoring, being able to select different or multiple reference electrodes is necessary. For those reasons, we developed a custom EEG electrode placement method. The scalp is divided in 7 areas, each are representing 1 microcontroller and all the electrodes attached to it. Each area can accommodate 16 EEG electrodes and 1 reference electrode. All the areas can share one or more reference electrodes by using an appropriate cable. Also, using software, it is possible to ignore the reference electrode input in each area and even create new reference electrodes, although in this case the number of channels is reduced. Our custom Electrode Placement Method is shown Figure 37.

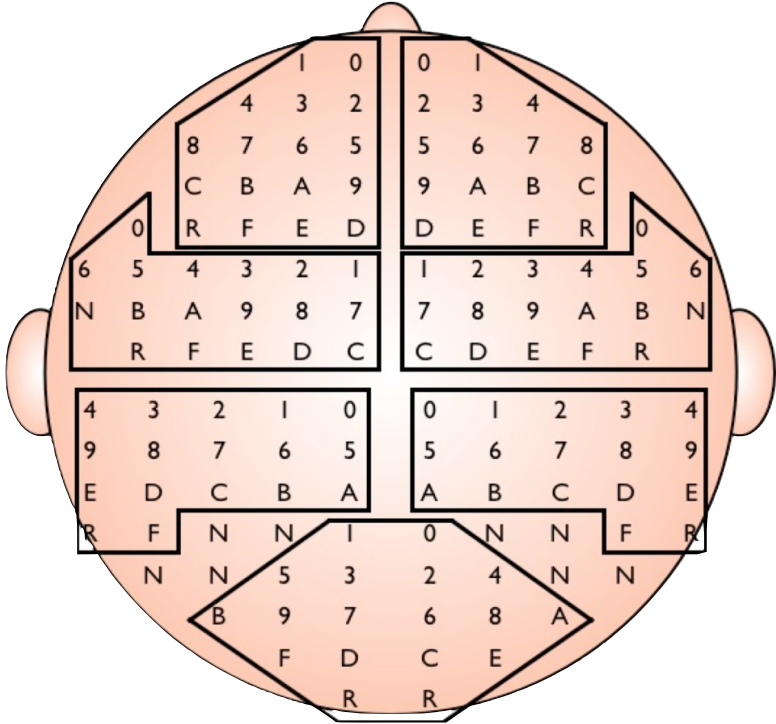


**FIGURE 37 - CUSTOM ELECTRODE PLACEMENT METHOD**

Our headgear mechanism is composed of a link mechanism, pictured in Figure 38 and a array made of elastic bands.

The link mechanism was designed based on the Statistical data offered by the Japanese National Institute of Advanced Industrial Science and Technology(AIST)[52]. The link mechanism has two main functions:

1. To keep the headgear in shape when it is not been worn. Because the electrodes are not taken removed from the headgear in order to save time when wearing it, if the is no mechanism to keep the shape of the headgear constant when nobody is wearing it, it would be very easy for large amount of cables to entangle. That could damage the electrode grid and the cable structure.
2. To provide a frame for the manufacturing of the elastic grid. Each link in the mechanism contains several holes which are used to fix the grid. The holes are equally distanced and allocated in order to create a grid capable accommodating up to 134(although only 119 were used in this research) electrodes.

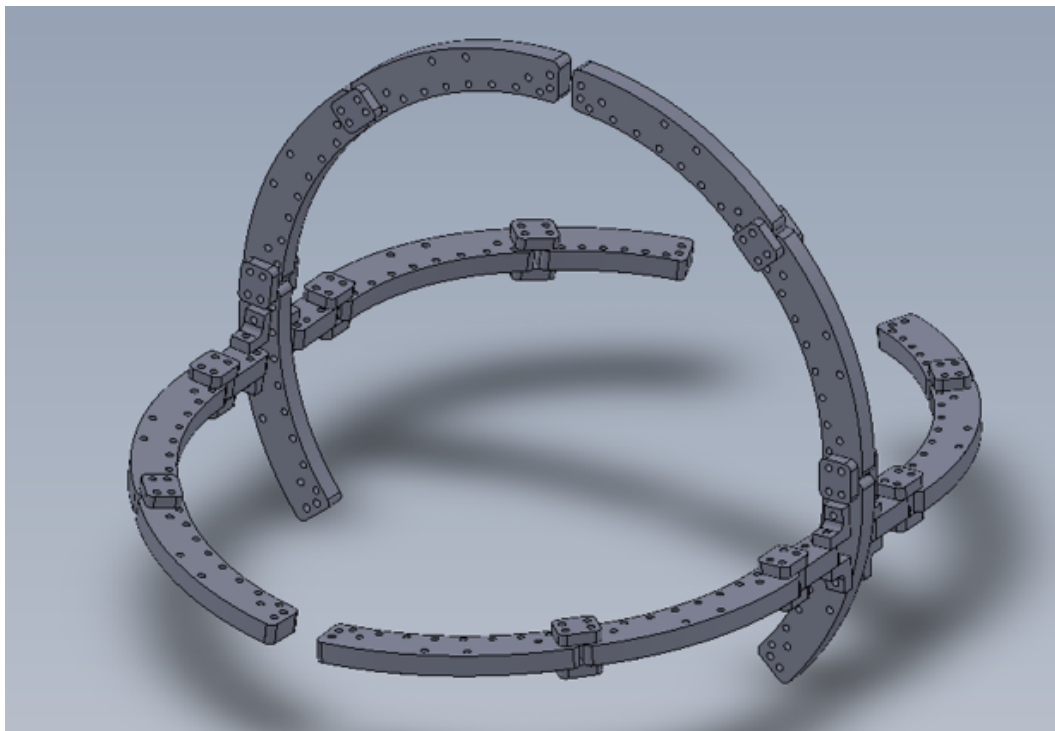


**FIGURE 38 - HEADGEAR FRAME**

The electrode grid is made of elastic band. Similarly to the link mechanism it has two primary functions:

1. To keep the headgear shape as close as possible to the users head shape by exerting constant pressure towards the center of the head. The headgear when not worn is smaller than the average human skull. When the headgear is worn, it stretches all its structures. fitting on the users head. The elastic grid pressure, keeps all the electrodes in constant contact with the scalp. If the users head is too small to stretch the elastic grid enough to produce a satisfactory pressure or if the users head is too big for the headgear to even fit, the user can just fasten

2. To mechanically link all electrodes together and keep them on the headgear using holes allocated in the electrode cases.

The electrode grid is configured as shown in Figure 39 and 40.

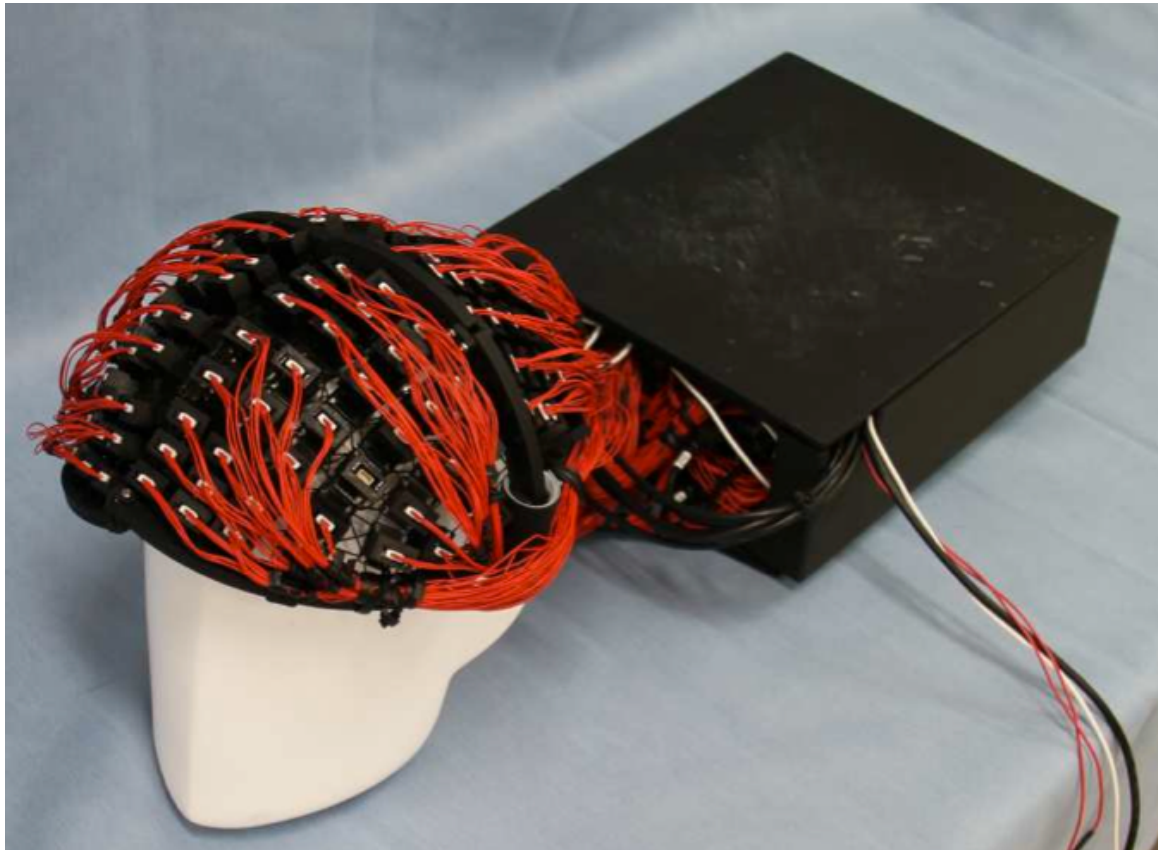


**FIGURE 39 - ELECTRODE GRID CONFIGURED**



**FIGURE 40 - COMPLETE WEARABLE ELECTRODE GRID WITH USER**

### 4.2.3 Built in electronics

In order to collect EEG data from 119 electrodes and transfer the data to a PC for recording and analysis an embedded system was designed.

Our embedded system is composed of 7 ARM Cortex M3 custom controller boards running in parallel. Each board can communicate independently with a host pc either using USB or Bluetooth communication protocols. In case of standard usage, where all the boards are connected the same host computer, all the boards are first connected to a 10 port USB HUB, converting seven USB cables into a single one. When using only one or two boards, Bluetooth connection can be used for data communication. With more devices, delay is observed and data is lost reducing the reliability of the system. Data can be collected from each board at the samplings rate of 125Hz, 250Hz, 500Hz and 1kHz.

Each board is composed of a 16 instrumentation amplifiers that calculate the difference of signal between each channel and the reference potential. The output of each instrumentation amplifier pass through a band pass filter(lower limit:0.1Hz, upper limit 1500 Hz) for signal conditioning. Finally the each conditioned data channel is sampled by a 16 bit external AD converter at 44100 Hz. All the 16 AD converters are connected to the ARM processor through a SPI network. The developed embedded system diagram is shown in Figure 41.

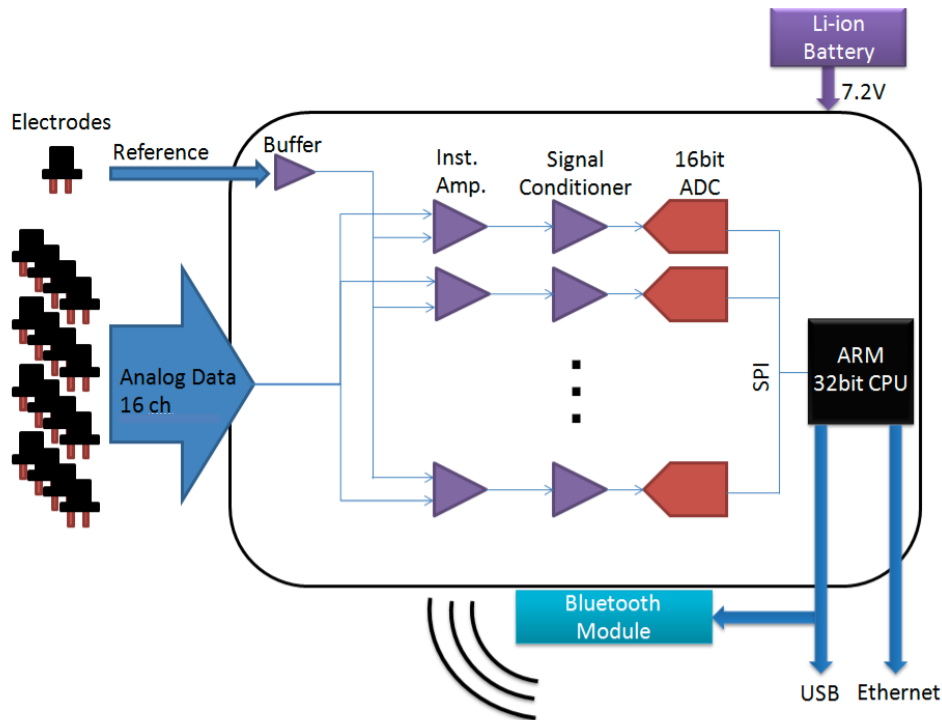
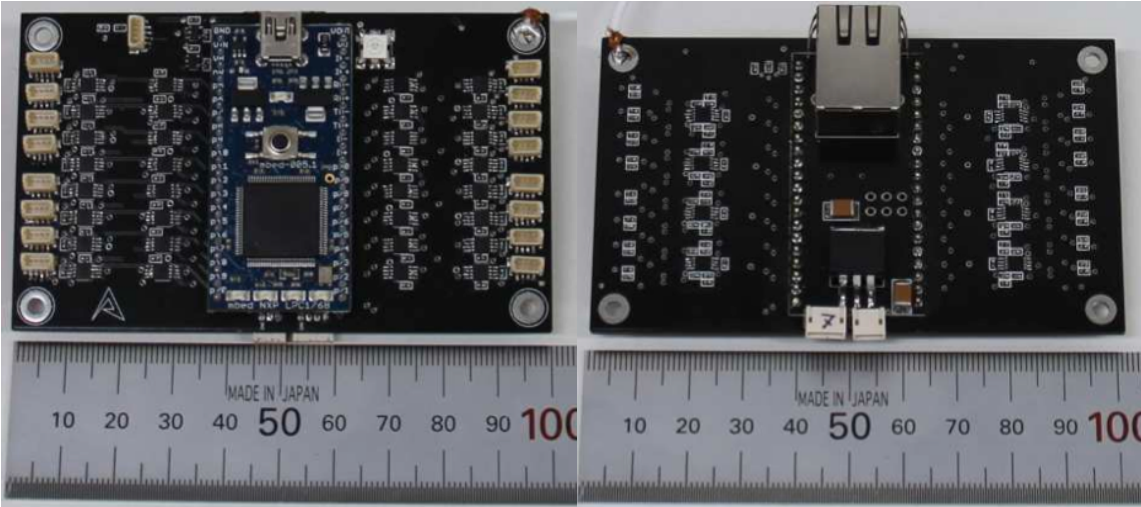


FIGURE 41. ADC BOARD DIAGRAM

This design is highly modular and, in the future, it can be recycled when design specialised headsets and applications, offering high reliability and flexibility on a device developer level. The controller board also contains a Ethernet port and is capable of running a web server for remote data accessing. The designed controller board is pictured at Figure 42 The controller box containing 7 controller boards is shown in Figure 43. All modules are connected through USB 3.0 to a dual core Intel Atom Based mother-board with a CUDA capable Nvidia Ion 2 chipset. This motherboard was extracted from a ASUS EEE PC 1215N netbook computer.



**FIGURE 42 - DEVELOPED ADC BOARD**

### 4.3 Parallel bioelectrical signal processing using wearable graphical processing unit

Most EEG monitoring devices either don't give the user access to the raw EEG data, making it impossible to directly check if the electrodes are functioning correctly the or require the use of complex and sometime slow software such as MATLAB. Such user interface problems make it very difficult for using those devices during daily life, especially if the user does not have technical background.

In this research we developed a software system to collect, save and analyse data in real time from our developed device that relies on a intuitive and straightforward graphical user interface(GUI).

Starting a measurement is done by simply connecting the USB cord in to the built in digital processing board, starting the software and pressing the "Start Communications" context menu button.

Selecting the areas and controllers used can be done on a graphical settings menu. In the same menu it's also possible to select sampling frequency and file buffer sizes. Adequate buffer sizes are important on PCs with low RAM or running 32bit operational systems, since a large amount of uncompressed analog data is collected per unit of time which could lead to buffer overflows and mini-dumps. Custom reference electrodes are also selected in this screen. Data is plot in real time, both in time domain and frequency domain as well as on 2D and 3D maps, as shown in Figure 43.

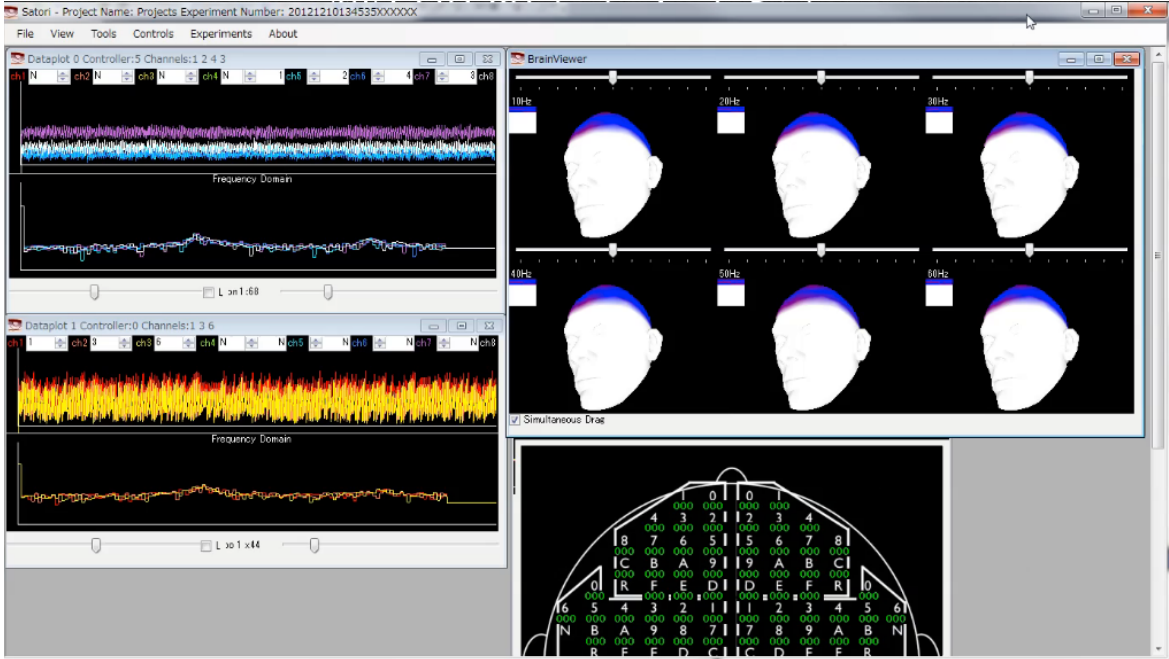


FIGURE 43 - DEVELOPED GUI

In order to perform digital signal processing and spectral analysis in real time for all EEG data channels, we propose the use General Purpose Graphical Processing Unit (GPGPU) available on modern computers and distribute the load between the CPU and hundreds of GPU cores. In order to do so, we chose to use CUDA (Nvidia Corporation) since it is, the fastest API available at the time of this research.

The digital signal processing algorithm used in our research is described in the flowchart in Figure 44.

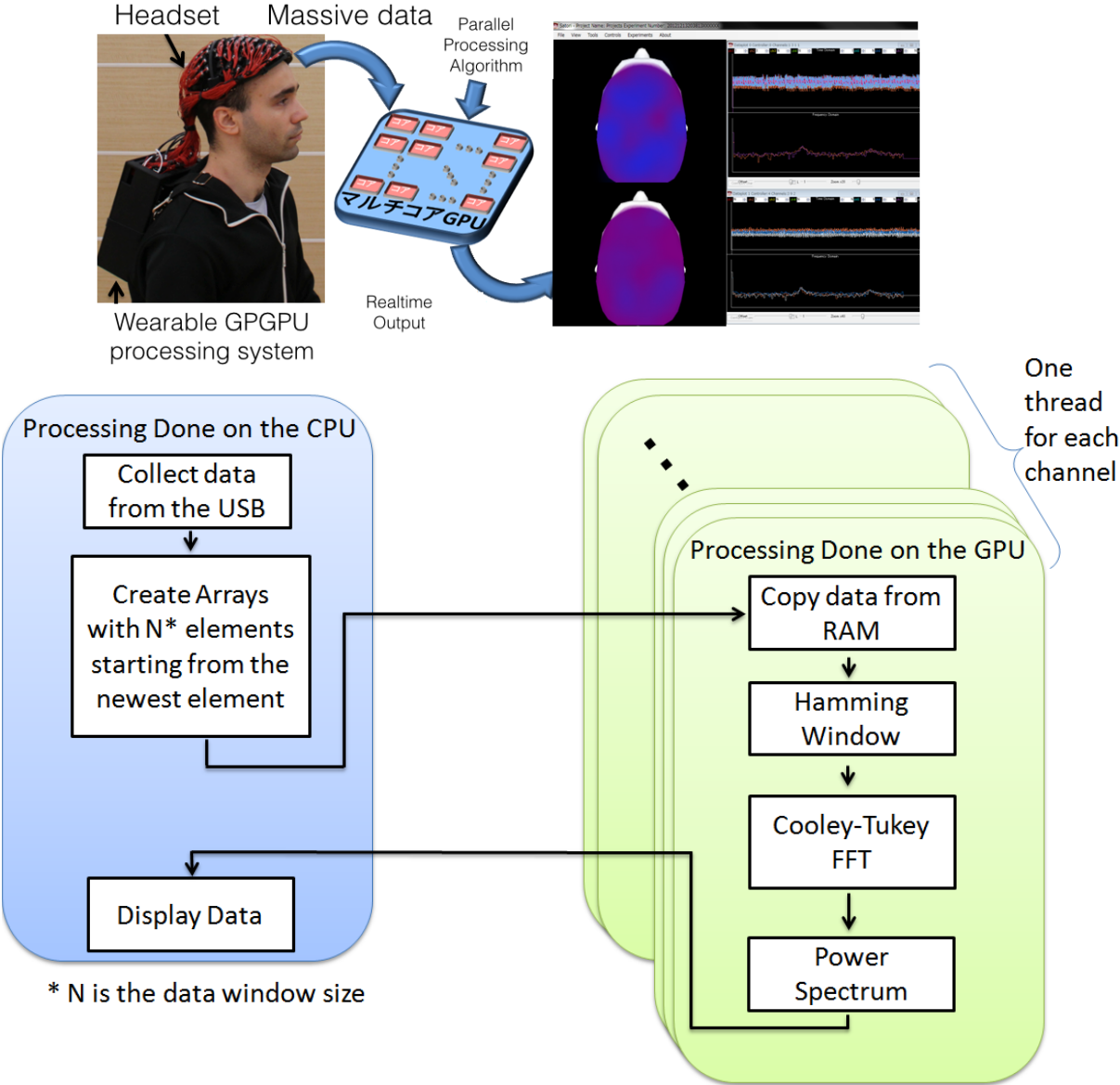


FIGURE 44 - DEVELOPED WEARABLE CUDA EEG DATA PROCESSING ALGORITHM

After each data channel is read from the USB port and saved in the RAM and HDD, an array of the size of a sampling window is created with this data and previous data is arranged in chronological order. Each array is send to the GPU and with the CUDA instruction set. Our custom instructions set contains a basic, a Hamming Window function, which is used if the according to the user settings, and a FFT based on Cooley-Tukey FFT algorithm and a function for calculating the power spectrum after the FFT is over. When all the processing is done, the GPU copies the result array from the VRAM to the RAM. Each channel runs on its own independent thread in parallel with all the other channels.

When a window of 1024 data points is set it takes the CPU 400ms to execute the process described above. Considering that even the slowest sampling rate our system can do is 125 samplings per seconds(8ms for , there would be only less than 1 ms for the processor to do everything including, but not limited to retrieving the data from the USB port, save the data and spectral analysis in to the hard disk and displaying data on the screen. In future works, when our device is used for BMI and complex pattern matching and machine learning algorithms, we won't be able to achieve real time performance by loading all the work on the CPU.

On the other hand, by using CUDA, hamming window, FFT and power spectrum calculations for all 112 under 1 ms. Not only a a large part of the workload is removed from the CPU, but by knowing that the GPU takes less than 1 ms to perform the calculations shows that there is still untapped processing power. In future works, this processing power should be used to develop EEG monitoring applications for BMI systems, while still keeping the software responsive and running in real time.

## **4.4 EEG measurement experiments**

### **4.4.1 Basic EEG measurement benchmark using the developed wearable EEG monitoring system and small size hybrid electrodes**

A standard experiment monitoring EEG signals was performed for in order to verify the recorded signals of a single sensor..

The experiment consists in measuring brain activity changes above the motor cortex that are due to hand and finger motions. When the participants' intention of movement is small, such as when the subject is at rest, it's possible to record strong signal on the 10 Hz  $\mu$ -rhythm frequency range, in the area above the motor cortex of the human brain. On the other hand, when the participant is moving one hand,  $\mu$ -rhythm gets weaker above the motor cortex opposite to the hand[53]. In this experiment we perform EEG recordings by placing the participants on a dark and silent room with the eyes closed. The subject stayed motionless for 30 seconds and then moved the right hand on a finger tapping movement, for another 30 seconds. This cycle was repeated 2 times for each experiment for a total experiment time of 120 seconds.

In order to evaluate the impact of the use of the GPU, the experiments was performed with and without using the CUDA features described in the previous sections. The experiments were performed with 2 participants, each experiment was performed 3 times.

For the second experiment, the developed system was also capable to record the data on both participants and the results matching previous researches. For both participants, when the participant is performing the finger tapping motion, the electrode C located on group 1 (Figure 39) of the system, above the left motor cortex, recorded alpha band signals weaker than the when the participant was at rest. Figure 45 shows the sample spectrogram for the target sensor with a visible  $\mu$ -band, showing that even on a multichannel system the developed sensors can still work as designed.

When experiments were executed with the CUDA features described in the previous section, the system was able to record data from all 112 channels at 1 kHz and perform FFTs for all channels after each sampling without delay or data loss. On the other hand, without using the CUDA features, thus allocating all the stress entirely on the CPU, the system took 400 ms to finish the FFTs for all channels and was unable to keep up with the 1 kHz sampling rate.

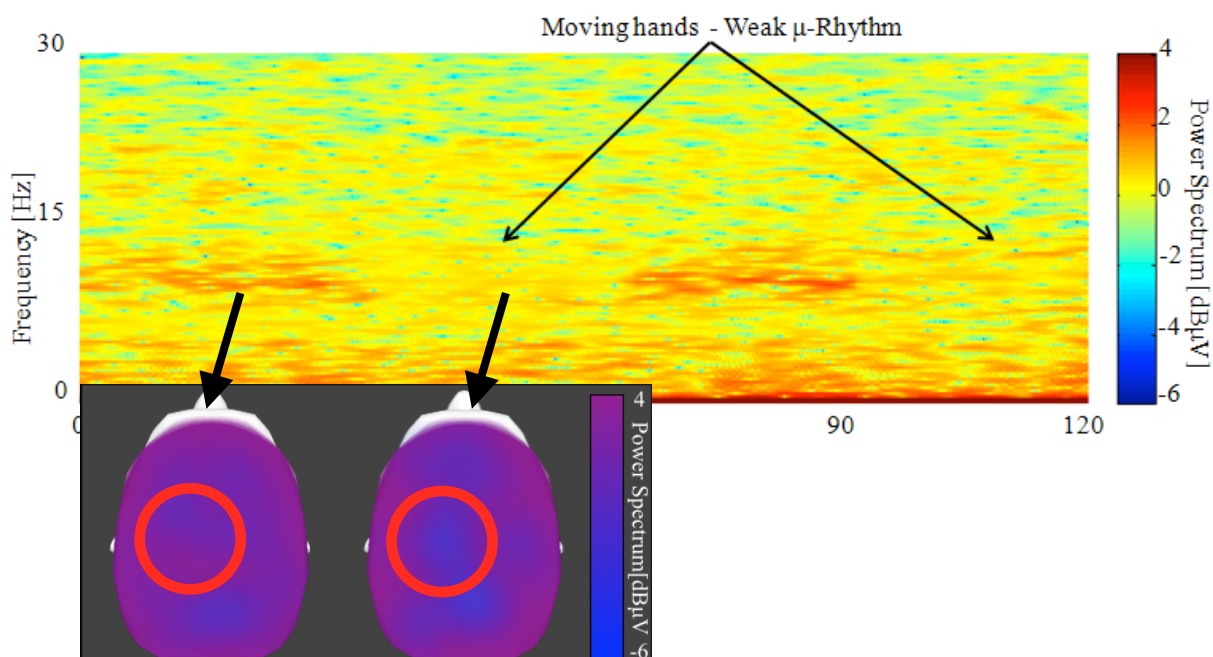


**FIGURE 45 - M-BAND MEASUREMENTS AS EEG RESPONSE TO MOTOR STIMULUS**

#### **4.4.2 Full scalp beta wave EEG measurement**

During intense mental activity, beta waves (15~25Hz) are known to appear in scalp area above the frontal lobe of the human brain[54]. In this experiment we attempt to evaluate the EEG measurement capabilities of our sensor on multichannel wearable setup by measuring beta waves during arithmetical calculations.

As shown in Figure 46 and 47, in this experiment 6 participants perform this test by deciding whether the mathematical equation on the display is correct or not. Strong signals in the beta band are expected to be detected by the electrodes in the region above the highlighted region shown in Figure when the participants are concentrating. Each participant is asked to go through 10 sets of problems, each set consisting of cycles of 30 seconds of problem solving and 30 seconds of relaxation. A robotic arm carrying a bottle of tea illustrating a possible application of our system in daily life support programmed so that if more than 8 sensors record beta wave signals stronger than 1dBmV, as shown in Figure 48, it will move and bring the tea bottle to the participant. During the problem solving. A sample of the mapping every 30 second for one participant is shown in Figure.

As shown on Table 1, the accuracy for all participants was above 75% confirming that all participants were concentrating and relaxing at the appropriated times during the test. Also all participants activated the robot over 7 out of the 10 trials. Considering those participants were untrained in this mental task, these results show that our hybrid electrodes not only can correctly measure EEG signals in a high resolution set up, but this set up allows users to with no experience to perform as well as users with experience using other types of lower resolution wearable EEG devices.

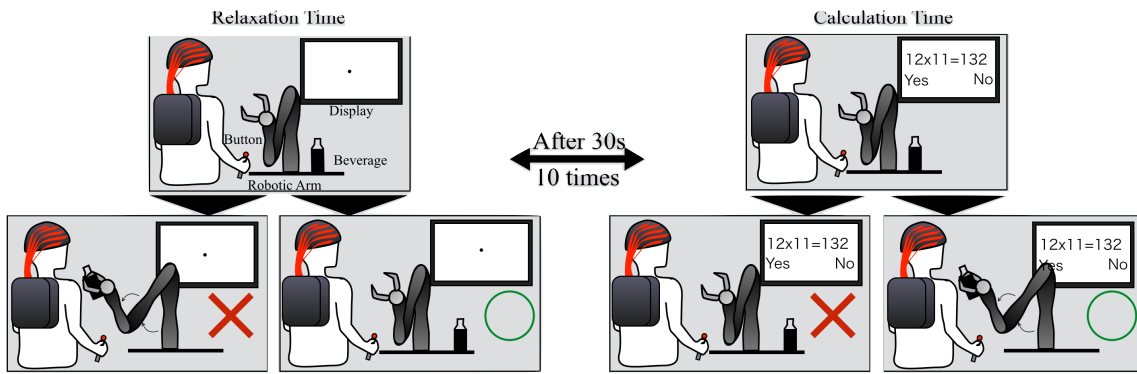


**FIGURE 46 - TASK DESIGN FOR BETA WAVE MEASUREMENT**

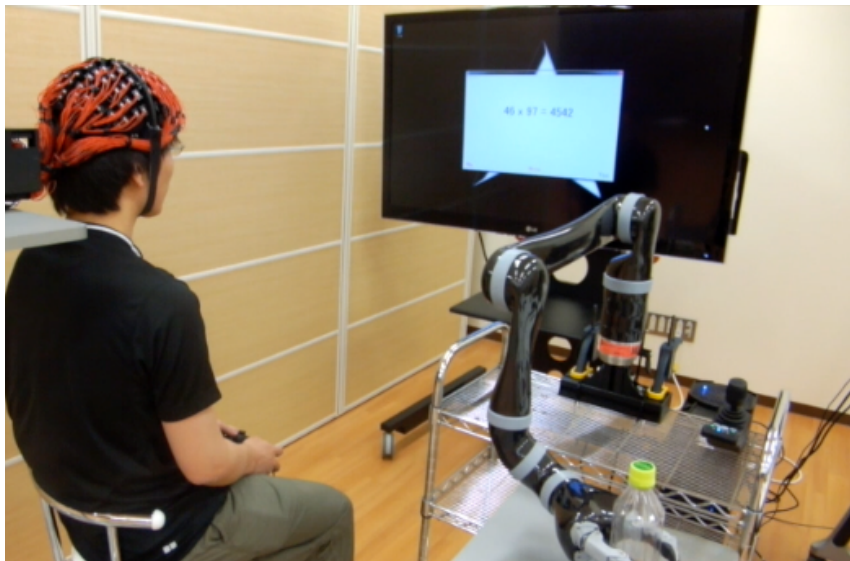


**FIGURE 47 - DURING THE BETA WAVE MEASUREMENT EXPERIMENT**

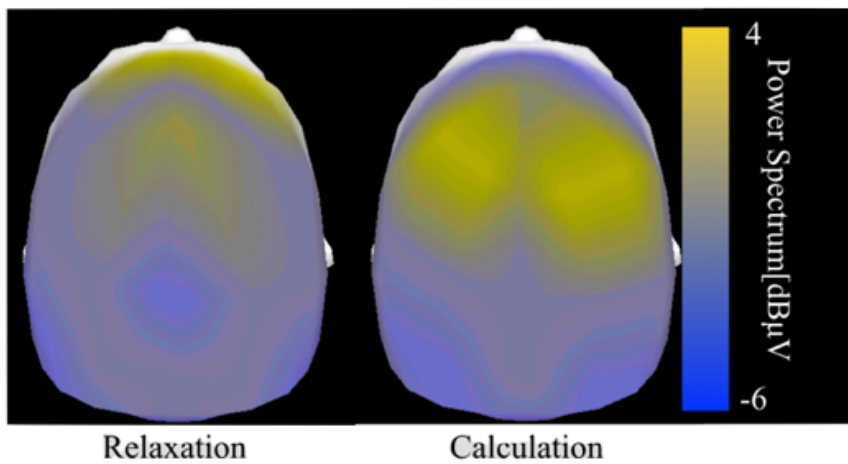


**FIGURE 48 - SAMPLE DATA SHOWING BETA WAVE DURING RELAXATION AND CALCULATION**

**TABLE 1 - Beta wave measurement rates for each participant during relaxation and calculation**

Participant	Failed Measurements More than 8 channels recorded beta waves during relaxation	Successful Measurement More than 8 channels recorded beta waves during calculation	Success Rate
A	2	9	85%
B	2	9	85%
C	1	8	85%
D	2	7	75%
E	3	7	70%
F	1	8	85%

## 4.5 Discussion

The experiments have shown that our electrodes were capable of recording both  $\mu$ -rhythm and beta waves without the need for skin preparation and that the results from our system are matched known brain activity phenomena. Our noise frequency analysis shows that our hybrid electrodes have a noise level below  $3 \mu\text{V}/\text{Hz}^{1/2}$ , performing at similar levels to commercially available electrodes. Both experiments suggest our system provides the high reliability required by professionals and end-users.

With our hybrid electrodes removed the need of skin preparation, the wearability of the system was further increased by using a novel mechanism the allows the placement of over a hundred EEG electrodes over the users scalp simultaneously, thus reducing the time for wearing our 119 electrode system to up to 5 minutes, similar to the time required for 1-16 electrode systems[55]. Quick and easy electrode placement is fundamental for daily life usage, as it gives the user time to perform other activities while also it does not require specialised staff or training for correctly wearing the system. Furthermore, the lack of conductive gel and the problems associated with it such as signal degradation over time are

completely avoided rendering battery capacity the only limiting factor for long continuous monitoring sessions. Using hybrid capacitive-resistive electrodes provided a high usability required by end users while also increasing the reliability of the system without reducing the spatial resolution of the sensor network.

The experiments have shown that our GPU based signal processing algorithm is powerful enough to perform FFTs for each channel after each sampling is finished, at 1 kHz sampling rate. While sampling at 1 kHz is a common practice, performing FFTs for each sampling at this rate is excessive considering the relatively low frequency EEG bioelectrical signals oscillate. However in this study, by showing that our system can perform heavy calculations at very fast rates, we show that our system perform in real time under heavy load by using algorithms optimised for parallel processing. On a realistic application scenario we can reduce the FFT execution and use the GPU processing power for other tasks capable of parallelisation, such as neural networks[56][57]. Offloading signal processing to the GPU using CUDA not only allowed us to perform frequency analysis at real time but also freed the CPU for writing data to the hard-disk as well as displaying a fully interactive GUI with a 3D map of the EEG signals over the scalp. The high speed data processing allowed us to support a high spatial and temporal resolution which increase the reliability of the signal while leaving the CPU free for user interaction contributing in increasing the usability of the system. Furthermore, using a mobile GPU allowed us to have all these advantages in a wearable package, achieving a system with high portability and removed the need to have an external host PC, creating an all-in-one integrated system.

The data transfer between the electrodes and the GPU equipped motherboard was performed by seven 16-channel modules. This modular design allows users to add or remove at will. Taking advantage of this design professional users can perform experiments and development using high-density sensor networks, whereas when supplying the EEG monitoring system for the end user they can easily reduce hardware and optimise the system for the target application while still maintaining system consistence, thus reducing costs but offering a high application flexibility. In this study our system was a proof-of-concept prototype, thus also containing not optimised off-the-shelf parts, such as the motherboard containing the GPU. With the popularisation of GPGPU capable System on Chip devices such as the Tegra 3 (Nvidia Corporation, USA) processor, further miniaturisation and increase in power efficiency can be achieved in the near future.

EEG signals are used extensively on sleep disorder diagnosis and treatment, assistive device control and neurorehabilitation. The effectiveness of some of these applications can be dependent on the frequency at which the patient uses EEG monitoring systems and is able to provide feedback to oneself as well as to the medical staff. While testing our new integrated system on a clinical environment is required, our tests with healthy participants suggest that the techniques in this study are a step forward in to increasing the impact of EEG technologies have in the medical field. Furthermore, the techniques introduced in this study can be extended towards other fields of wearable computing, robotics and medicine.

## 4.6 Conclusion

In this study we developed a novel integrated EEG monitoring system combining capacitive bioelectrical measurement and parallel computing technologies. A portable high-resolution EEG monitoring headgear composed of 112 sensing electrodes and 7 reference custom hybrid capacitive-resistive electrodes was developed. In order to record and analyse the massive amount of data from the headgear, a CUDA based wearable processing system was developed providing real-time signal analysis.

We confirmed the efficiency of the system both as a self-contained high-resolution device made to minimise the noise on the developed hybrid electrodes, but also takes full advantage of the enhanced wearability that our hybrid electrodes provide. Furthermore, in this chapter we developed the world first wearable GPGPU platform, optimised it so that even mobile GPUs can provide responsiveness that rivals desktop CPUs, and as mobile GPUs get more powerful in the future, our platform allow us to build more complete self-contained systems by using algorithms that can take advantage of the high parallelisation that GPGPU programming provides.

# 5 Discussion

## 5.1 Academic and practical advantages of the hybrid bioelectrical measurement model, noise cancelling methods and parallel processing methods

In this study we developed a system that satisfies all the requirements listed in the Chapter 1 of this paper in a much greater level than any previously developed capacitive coupling bioelectrical sensor.

In Chapter 2 we developed a novel type of hybrid electrode that, on Chapter 3, based on the desired user application can collect ECG, EMG, EOG and EEG data using either capacitive or resistive coupling. Our sensor is the first capacitive bioelectrical sensor that can collect all major, commonly used types of bioelectrical signals. The way the electrode operates can easily be set by the user by just changing how the electrode makes contact with the user's skin, thus minimising dependency of the bioelectrical information on the skin-electrode interface. Furthermore, on Chapter 4, we considered our sensing model on a system level and how it we could maintain it's performance. Doing so led us to into the development of the world first wearable GPGPU based parallel self-contained processing system and EEG measurement results that bring the performance expected from desktop type devices to fully wearable devices.

Our proposed model enables the design of flexible bioelectrical monitoring devices that can easily be customised according to the user or application need and, at the same time, user-friendly devices due to lack of need for skin preparation and conductive gels. Previous researches only considered the most basic skin-electrode capacitor model and because of that were limited to very specific situations. However in our research we fused resistive measurement, capacitive measurement, internal noise counter-measures and external noise cancelling techniques into one single model and a compact set of equations, this know how can be applied into the design of a variety of bioelectrical sensors that go beyond the scope of this study, such as flexible sensors or non wearable sensors, such as the one shown in Figure 49. In the development of further applications that contain potentially noise components, such as use of those sensors with wearable laser LEDs or exoskeletons equipped with electrical actuators, our proposed model can be expanded and electrode design parameters can be updated at will in order to satisfy new noise cancelling or internal noise requirements.

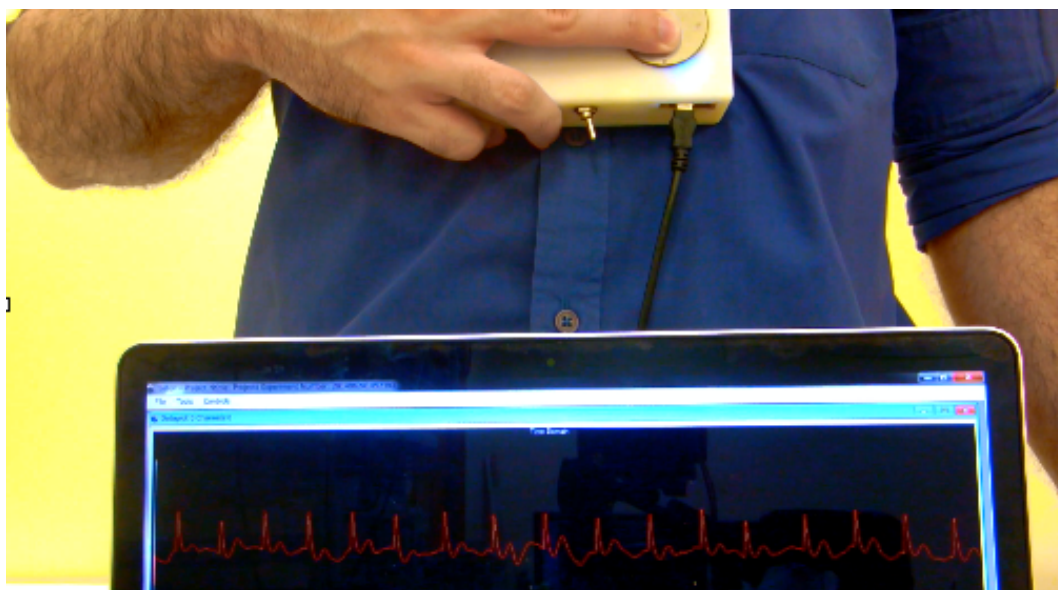


**FIGURE 49 - EXAMPLE OF EXPANDING THE WEARABLE INTERNAL AND EXTERNAL NOISE CANCELLING TECHNIQUES IN TO NON WEARABLE/HANDHELD BIOELECTRICAL MEASUREMENT DEVICES**

## **5.2 An engineering approach to prevention and treatment of major health issues**

As in this research we developed a sensing model that is considerably more complex than a traditionally used resistive contact electrode, new precision standards as well as data interpretation and device usage protocols may be required for clinical use of medical devices that employ our sensors for regulated medical applications. In order to do so, clinical studies on the application of our sensors on specific health disorders will be the focus of future research as the focus of this paper is purely on the physical properties of the developed method.

Due to the higher usability and wearability provided by our hybrid bioelectrical measurement method, we expect a bigger mainstream appeal compared to the traditional methods available in the market today. With that assumption in mind, the possibility of recording the various types of bioelectrical data from patients multiple times a day, or even continuously, open the possibilities for a new generation of treatment and prevention methods based on massive bioelectrical activity databases. However, design and development of large scale network systems for collecting this massive data, alongside extensive long term clinical trials with both healthy individuals as well as patients is necessary in order for our developed sensors to be recognised as reliable tools for the prevention and treatment of cardio, muscular and neural disorders. Until proper regulation is complete, however, sports and entertainment applications using our technologies can be introduced in the market as the advancements from the research and development for non medical applications can be later transferred for medical applications.

### **5.3 Further applications and expansions for the techniques developed in this research**

In this research we focused on minimising internal sensor sources, cancelling external sources and designing systems that do not interfere with the hybrid sensor basic capabilities while also taking full advantage of it's properties. As a result, we developed very sensitive sensor built upon a modular, powerful and flexible data processing platform.

While the focus of this research is on the development of wearable hybrid resistive-capacitive sensors, the input current feedback control, dual input noise cancelling and wearable GPGPU parallel concepts can be generalised and applied to a variety of other sensors in wearable and non wearable applications. As shown in Figure 50, future hardware development related research will focus in particular on application systems consisting of multiple types of bioelectrical signals simultaneously alongside non bioelectrical data and man-machine interactivity.

## 6 Conclusion

In this research we focused on bringing the signal robustness expected from traditionally used contact type resistive electrodes and to the potentially more comfortable and practical non contact type capacitive electrodes by reducing the dependency of the bioelectrical information on the contact state between the sensor and the user's skin. We approached this problem from both a internal and external level perspective as well as from system level perspective and developed a hybrid sensor capable of both resistive and capacitive ECG, EMG, EOG and EEG bioelectrical signal measurements in realistic conditions.

In this research, in order to realise the above, we performed the followed three steps:

(1) We performed a internal level analysis of the proposed sensing method by creating a novel electric circuit model based on both resistive and capacitive measurement principles as well as all the associated internal noise factors, namely internal thermoelectrical noise and current drift. Based on the new model we designed our sensor using a optimal minimal impedance and input current feedback circuit for minimal thermoelectrical noise, minimal current drift and quick saturating noise recovery while still being sensitive enough for all the target bioelectrical signals.

(2) Using the same model we also performed a sensor external level analysis by focusing on external noise sources, namely external electromagnetic noises and motion artifacts. Using this information, we developed a dual differential input noise cancelling method built in on each sensor. Using a secondary electrode circuit based on (1) but calibrated exclusively for external noise.

(3) We developed a sensor module satisfying the conditions of the developed models introduced in (1) and (2). Through experiments we verified superior frequency response parameters, noise characteristic, noise cancelling effectiveness compared to previous reported capacitive coupling electrodes. We also verified resistive and capacitive ECG, EOG and EEG measurements using our sensor with the same level of precision as traditional resistive coupling electrodes. Furthermore we verified for the first time, both resistive and capacitive robust EMG signals from both upper body and lower body limbs, an achievement that has yet to be reported by any other capacitive sensors research team.

(4) In order to minimise external electromagnetic noise sources as well as take full advantage of the contact state independency property of the developed hybrid resistive capacitive sensor, we developed a novel wearable high spatial and temporal resolution EEG self contained system. We developed a 112 channel compatible sensor mounting mechanism and realtime GPGPU based parallel signal processing and hardware. Using this world first GPGPU parallel processing wearable system we verified consistent and low noise EEG signals over the scalp of several untrained participants after quickly being able to wearing the entire system.

# 7 Future works

Designing a novel bioelectrical sensor by focusing simultaneously on both internal and external noise sources as well as a system level improvements that not only reduce noise but also take full advantage of the sensor practical properties, we were capable to measure all major types of bioelectrical signals at a higher precision than any other previously developed and reported type of capacitive bioelectric sensor or system. Being capable of simultaneously measure any bioelectrical signal using either the resistive or capacitive method allows the user to record bioelectrical signals regardless of the contact situation, such as clothes, dirty or body hair, between the sensor and skin, thus greatly improving user freedom during use. We hope to contributing bringing bioelectrical measurement based disease prevention, treatments and life support methods that rely on ECG, EMG, EOG or EEG signals. Furthermore, as shown in Figure 50 we hope to expand the developed noise cancelling and parallel processing methods into other types of biosignals as well as relevant environment signals. This extra information will not only help in the design of better self-contained wearable systems but in the measurement of better bioelectrical signals, and thus better medical applications.

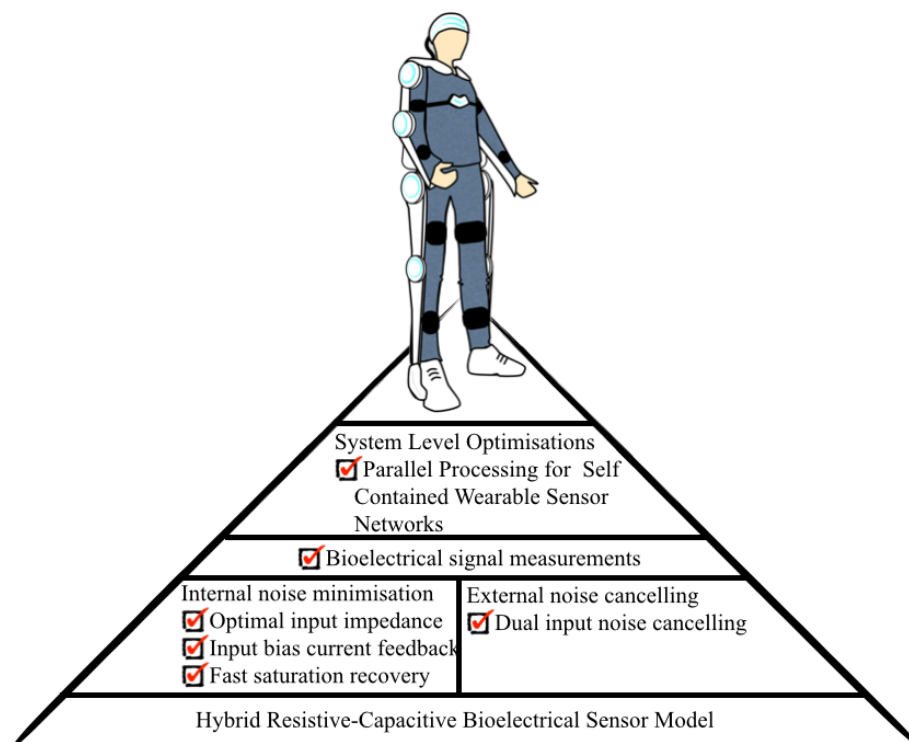


**FIGURE 50 - EXPANDING THE DEVELOPED NOISE CANCELLING AND PARALLEL PROCESSING METHODS INTO OTHER TYPES OF BIOSIGNALS AS WELL AS APPLICATION DEVELOPMENT FOR TREATMENT AND PREVENTION OF CARDIO, MUSCULAR AND NEURAL DISORDERS.**

# Acknowledgements

First and foremost, I would like to express my sincere gratitude to my advisor Prof. Yoshiyuki Sankai for the continuous support of my short 6 year academic career, for his patience, motivation, enthusiasm, hilarious jokes and immense knowledge. Prof. Sankai has been one of my main sources of inspiration, both as a scientist and business man, since I was a high-school student. An invaluable role model whose personality and accomplishments, including Cyberdyne Inc. as a whole, I will always help me shape my future as well as the future of my own ventures.

Besides my advisor, I would like to thank the my supervisors as well as my thesis examination committee: Prof. Noriyuki Hori, Prof. Hideaki Kuzuoka, Prof. Kenji Suzuki and Prof. Yasushi Nakauchi for their encouragement and critical feedback during the several presentations done through both the Masters and Ph.D. courses.

My sincere thanks also goes to Prof. Hiroaki Kawamoto for spend countless hours with insightful discussions, journal and conference paper reviewing and experiment participation.

I thank my fellow laboratory colleagues in the Cybernics Laboratory Medical Team: Atsushi Saito, Shota Ekuni, Kouichi Murata, Hiroaki Koshio, Shouri Kanou, Yasunari Asakura for the stimulating weekly discussions and for all the fun we have had during the course and extra class activities. Laboratory secretaries Chikako Suzuki and Reiko Kangori have my gratitude for the countless laughs, delicious food and critical paperwork processing. And finally a special thanks to senior lab member Dr. Shiori Oshima for invaluable advice and for being one of my biggest sources of inspiration as a professional.

I would like to thank the Ministry of Education, Culture, Sports, Science and Technology of Japan(MEXT) for financing my studies in Japan from 2005 until 2013. Thanks to the wonderful work from MEXT, I got a unique life changing chance that otherwise would not be possible. I simply cannot measure how many opportunities MEXT funded Foreign Student programs opened for me, and the least I can say is that I will not let all this support be wasted. I also would like to thank the Japan Society(JSPS) for the accepting me as Fellow Researcher (DC2) in 2014. Not only being selected for a highly competitive grant was a unique, rich and exiting experience, but research and business opportunities make me proud of being a JSPS Fellow Researcher.

Last but not least, I would like to thank my parents Igor Ianov and Maria Madalena Bernardo, as without the basic survival skills I was taught, I don't think I would be writing this document right now.

# Bibliography

- [1] M.L. Fantini, M. Michaud, N. Gosselin, G. Lavigne and J. Montplaisir: "Periodic leg movements in REM sleep behavior disorder and related autonomic and EEG activation", *Neurology*, Vol. 59, No. 12, 1889-1894 (2002)
- [2] R.M. Coleman, C.P. Pollak and E.D. Weitzman: "Periodic movements in sleep (nocturnal myoclonus): Relation to sleep disorders", *Annals of Neurology*, Vol.8, No.4, pp.416-421 (1980)
- [3] R.J.K. Jacob, "The use of eye movements in human-computer interaction techniques: what you look at is what you get", *ACM Transactions on Information Systems (TOIS) - Special issue on computer human interaction*, Vol.9, No.2, pp.152-169 (1991)
- [4] J.K. Chapin, K.A. Moxon, R.S. Markowitz, M.A.L. Nicolelis: "Real-time control of a robot arm using simultaneously recorded neurons in the motor cortex", *Nature Neuroscience*, Vol. 2, pp.664-670 (1999)
- [5] K.K. Ang, C. Guan, K.S.G. Chua, B.T. Ang, C. Kuah, C. Wang, K.S. Phua, Z.Y. Chin, H. Zhang: "Clinical study of neurorehabilitation in stroke using EEG-based motor imagery brain-computer interface with robotic feedback," *2010 Annual International Conference of the IEEE Engineering in Medicine and Biology Society*, pp.5549-5552, (2010)
- [6] J.D. Allison, K.J. Meader, D.W. Loring, R.E. Figueroa, J.C. Wright: "Functional MRI cerebral activation and deactivation during finger movement", *Neurology*, Vol.54, pp.135-142 (2000)
- [7] J.R. Wolpaw, N. Birbaumer, W.J. Heetderks, D.J. McFarland, P.H. Peckham, G. Schalk, E. Donchin, L.A. Quatrano, C.J. Robinson, T.M. Vaughan, "Brain-computer interface technology: a review of the first international meeting," *IEEE Transactions on Rehabilitation Engineering*, Vol.8, No.2, pp.164-173 (2000)
- [8] T.J. Sullivan, S.R. Deiss, T.P. Jung and G. Cauwenberghs: "A brain-machine interface using dry-contact, low-noise EEG sensors", *Proc. IEEE Int. Symp. Circuits and Systems*, pp. 1986-1989 (2008)
- [9] G. Gargiulo, R. A. Calvo, P. Bifulco, M. Cesarelli, C. Jin, A. Mohamed, A.V. Schaik: "A new EEG recording system for passive dry electrodes", *Clinical Neurophysiology*, Vol. 121, No. 5, pp.686-693 (2010)
- [10] A. Lopez and P. C. Richardson: "Capacitive electrocardiographic and bioelectric electrodes", *IEEE Transactions on Biomedical Engineering*, Vol.16, pp.299-300 (1969)
- [11] C.J. Harland, T.D. Clark and R.J. Prance: "Electric potential probes -new directions in the remote sensing of the human body", *Measurement Science and Technology*, Vol.2, pp.163-169 (2002)

- [12] Y.M. Chi, G. Cauwenberghs: "Micropower non-contact EEG electrode with active common-mode noise suppression and input capacitance cancellation," Engineering in Medicine and Biology Society, pp.4218-4221 (2009)
- [13] Y.M. Chi, T.P. Jung, G. Cauwenberghs: "Dry-Contact and Noncontact Biopotential Electrodes: Methodological Review", IEEE Reviews in Biomedical Engineering, Vol.3, pp. 106-119 (2010)
- [14] J. Harland, T.D. Clark and R.J.Prance:"Electrical potential probes - new directions in the remote sensing of the human body", Measurement Science and Technology, Vol.13, pp. 163-169 (2002)
- [15] M.J. Burke and D.T. Gleeson:"A micropower dry-electrode ECG preamplifier", IEEE Transactions on Biomedical Engineering, Vol.47, No.2, pp.155-162 (2000)
- [16] D.V. Moretti, F. Babiloni, F. Carducci, F. Cincotti, E. Remondini, P.M. Rossini, S. Salinari and C. Babiloni:"Computerized processing of EEG-EOG-EMG artifacts for multi-centric studies in EEG oscillations and event-related potentials", International Journal of Psychophysiology, Vol. 47, No.3, pp. 199-216 (2003)
- [17] J.C. Woestenburg, M.N. Verbaten and J.L. Slangen: "The removal of the eye-movement artifact from the EEG by regression analysis in the frequency domain", Biological Psychology, Vol.16, No.1-2, pp. 127-147 (1983)
- [18] W. Klimesch, B. Schack, M. Schabus, M. Doppelmayr, W. Gruber, P. Sauseng: "Phase-locked alpha and theta oscillations generate the P1?N1 complex and are related to memory performance", Cognitive Brain Research, Vol. 19, No.3, pp. 302-316 (2004)
- [20] G Rau, C Disselhorst-Klug: "Principles of high-spatial-resolution surface EMG (HSR-EMG): single motor unit detection and application in the diagnosis of neuromuscular disorders," Journal of Electromyography and Kinesiology ,Vol. 7, No. 4, pp. 233-239 (1997)
- [21] T. Hayashi, H. Kawamoto and Y. Sankai, "Control Method of RobotSuit HAL working as Operator's Muscle using Biological and Dynamical Information", Proc. of IEEE/RSJ International Conference on Intelligent Robots and Systems (IROS 2005), pp.3455-3460, 2005
- [22] H. Kawamoto and Y. Sankai, "Power assist method based on Phase Sequence and muscle force condition for HAL", Advanced Robotics, vol.19, no.7, pp.717-734, 2005
- [23] K. Suzuki, G. Mito, H. Kawamoto, Y. Hasegawa and Y. Sankai, "Intention-Based Walking Support for Paraplegia Patients with RobotSuit HAL, Advanced Robotics", Vol.21, No.12, pp.1441-1469, 2007
- [24] Saridis, George N.; Gootee, Thomas P.; , "EMG Pattern Analysis and Classification for a Prosthetic Arm," Biomedical Engineering, IEEE Transactions on , vol.BME-29, no.6, pp. 403-412, June 1982

- [25] Au, S.K.; Bonato, P.; Herr, H.; , "An EMG-position controlled system for an active ankle-foot prosthesis: an initial experimental study," *Rehabilitation Robotics*, 2005. ICORR 2005. 9th International Conference on , vol., no., pp. 375- 379, 28 June-1 July, 2005
- [26] X. Zhang, X. Chen, W. Wang, J. Yang, V. Lantz, and K. Wang, "Hand gesture recognition and virtual game control based on 3D accelerometer and EMG sensors," *Proceedings of the 14th international conference on Intelligent user interfaces (IUI '09)*, pp. 401-406, 2009
- [27] G.M.Lyons, P. Sharma, M. Baker, S. O'Malley, A. Shanahan, "A computer game-based EMG biofeedback system for muscle rehabilitation," *Engineering in Medicine and Biology Society, Proceedings of the 25th Annual International Conference of the IEEE* , vol.2, pp. 1625-1628, Sept. 2003
- [28] J.R. Wolpaw, N. Birbaumer, W.J. Heetderks, D.J. McFarland, P.H. Peckham, G. Schalk, E. Donchin, L.A. Quatrano, C.J. Robinson, T.M. Vaughan, "Brain-computer interface technology: a review of the first international meeting," *IEEE Transactions on Rehabilitation Engineering*, Vol.8, No.2, pp.164-173, 2000
- [29] T.J. Sullivan, S.R. Deiss, T.P. Jung and G. Cauwenberghs: "A brain-machine interface using dry-contact, low-noise EEG sensors", *Proc. IEEE Int. Symp. Circuits and Systems*, pp. 1986-1989, 2008
- [30] G. Gargiulo, R. A. Calvo, P. Bifulco, M. Cesarelli, C. Jin, A. Mohamed, A.V. Schaik: "A new EEG recording system for passive dry electrodes", *Clinical Neurophysiology*, Vol. 121, No. 5, pp.686-693, 2010
- [31] C.J. Harland, T.D. Clark and R.J. Prance: "Electric potential probes-new directions in the remote sensing of the human body", *Measurement Science and Technology*, Vol.2, pp. 163-169, 2002
- [32] Y.M. Chi, G. Cauwenberghs: "Micropower non-contact EEG electrode with active common-mode noise suppression and input capacitance cancellation," *Engineering in Medicine and Biology Society*, pp.4218-4221, 2009
- [33] Y.M. Chi, T.P. Jung, G. Cauwenberghs: "Dry-Contact and Noncontact Biopotential Electrodes: Methodological Review", *IEEE Reviews in Biomedical Engineering*, Vol.3, pp. 106-119, 2010
- [34] J. Harland, T.D. Clark and R.J. Prance: "Electrical potential probes - new directions in the remote sensing of the human body", *Measurement Science and Technology*, Vol.13, pp. 163-169, 2002
- [35] A. Lopez and P. C. Richardson: "Capacitive electrocardiographic and bioelectric electrodes", *IEEE Transactions on Biomedical Engineering*, Vol.16, pp.299-300, 1969

- [36] A. I. Ianov, H. Kawamoto, Y. Sankai, "Development of Hybrid Resistive-Capacitive Electrodes for Electroencephalogram and Electrooculogram", *IEEJ Transactions of Sensors and Micromachines*, Vol. 133, No. 3, 2012
- [37] R. E. Gander, B. S. Hutchins, "Power Spectral density of the surface myoelectric signal of the biceps brachii as a function of static load," *Electromyography and clinical neurophysiology*, Vol. 25, pp. 469-478, 1985
- [38] M.L. Fantini, M. Michaud, N. Gosselin, G. Lavigne and J. Montplaisir: "Periodic leg movements in REM sleep behavior disorder and related autonomic and EEG activation", *Neurology*, Vol. 59, No. 12, 1889-1894, 2002
- [39] J.K. Chapin, K.A. Moxon, R.S. Markowitz, M.A.L. Nicolelis: "Real-time control of a robot arm using simultaneously recorded neurons in the motor cortex", *Nature Neuroscience*, Vol. 2, pp.664-670, 1999
- [40] K.K. Ang, C. Guan, K.S.G. Chua, B.T. Ang, C. Kuah, C. Wang, K.S. Phua, Z.Y. Chin, H. Zhang: "Clinical study of neurorehabilitation in stroke using EEG-based motor imagery brain-computer interface with robotic feedback," 2010 Annual International Conference of the IEEE Engineering in Medicine and Biology Society, pp.5549-5552, 2010
- [41] C.T. Lin, L.W. Ko, M.H. Chang, J.R. Duann, J.Y. Chen, T.P. Su, T.P. Jung, "Review of Wireless and Wearable Electroencephalogram Systems and Brain-Computer Interfaces ? A Mini-Review." *Gerontology*, Vol. 56, pp. 112-119, 2010
- [42] G. Schalk, D.J. McFarland, T. Hinterberger, N. Birbaumer, J.R. Wolpaw, "BCI2000: a general-purpose brain-computer interface (BCI) system," *Biomedical Engineering, IEEE Transactions on*, vol.51, no.6, pp.1034-1043, June 2004
- [43] J.R. Wolpaw, N. Birbaumer, W.J. Heetderks, D.J. McFarland, P.H. Peckham, G. Schalk, E. Donchin, L.A. Quatrano, C.J. Robinson, T.M. Vaughan, "Brain-computer interface technology: a review of the first international meeting," *IEEE Transactions on Rehabilitation Engineering*, Vol.8, No.2, pp.164-173, 2000
- [44] A. I. Ianov, H. Kawamoto, Y. Sankai, "Development of a Capacitive Coupling Electrode for Bioelectrical Signal Measurements and Assistive Device Use", *Proceedings of the 2012 ICME International Conference on Complex Engineering*, pp. 593-598, July, 2012
- [45] A. I. Ianov, H. Kawamoto, Y. Sankai, "Development of Hybrid Resistive-Capacitive Electrodes for Electroencephalogram and Electrooculogram", *IEEJ Transactions of Sensors and Micromachines*, Vol. 133, No. 3, 2012(Accepted for publication, in press)
- [46] J.A. Wilson, J.C. Williams, " Massively Parallel Signal Processing using the Graphics Processing Unit for Real-Time Brain-Computer Interface Feature Extraction", *Front Neuroengineering*, Vol. 2, Article 11, 2009

- [47] A. Nukada, Y. Ogata, T. Endo, S. Matsuoka, "Bandwidth intensive 3-D FFT kernel for GPUs using CUDA," High Performance Computing, Networking, Storage and Analysis, 2008. SC 2008. International Conference for , pp.1-11, 15-21 Nov. 2008
- [48] AIST, "RIO-DB: Available Database", <http://riodb.ibase.aist.go.jp/dhbodydb/index.php.ja>, March 6th, 2012 [September 14th, 2012]
- [49] A. Craig, P. McIsaac, Y. Tran, L. Kirkup, A. Searle, "Alpha wave reactivity following eye closure: a potential method of remote hands free control for the disabled," Technology and Disability, Vol. 10, No. 3, pp. 187-194, January 1999
- [50] A. Craig, Y. Tran, P. McIsaac, P. Moses, L. Kirkup, A. Searle. "The effectiveness of activating electrical devices using alpha wave synchronisation contingent with eye closure," Applied Ergonomics, Vol. 31, No. 4, pp. 377-382, August 2000
- [51] A. R. Luft, S. McCombe-Waller, J. Whittall, L. W. Forrester, R. Macko, J. D. Sorkin, J. B. Schulz, A. P. Goldberg, D. F. Hanley, "Repetitive Bilateral Arm Training and Motor Cortex Activation in Chronic Stroke", JAMA., Vol. 292(15):1853-1861, 2004
- [52] T. Balla, A. Schreiber, B. Feige, M. Wagner, C. H. Lücking and R. K. Feig, "The Role of Higher-Order Motor Areas in Voluntary Movement as Revealed by High-Resolution EEG and fMRI," NeuroImage, Vol. 10(6), pp. 682-694, 1999
- [53] Y.M. Chi, T.P. Jung, G. Cauwenberghs: "Dry-Contact and Noncontact Biopotential Electrodes: Methodological Review", IEEE Reviews in Biomedical Engineering, Vol.3, pp. 106-119 , 2010
- [54] H. Jang, A. Park, K. Jung, "Neural Network Implementation Using CUDA and OpenMP," Computing: Techniques and Applications, 2008. DICTA '08. Digital Image, pp. 155-161, 1-3 Dec. 2008

# Related Papers

## Journal Papers

[1] A. I. Ianov, H. Kawamoto, Y. Sankai, “Development of Hybrid Resistive-Capacitive Electrodes for Electroencephalogram and Electrooculogram”, IEEJ Transactions of Sensors and Micromachines, Vol. 133, No. 3, pp.57-65, 2012

## Proceedings

[1] A. I. Ianov, H. Kawamoto, Y. Sankai, “Wearable Parallel Processing Based High-Resolution High-Speed Electroencephalogram Monitoring Integrated System”, Proceedings of the International Symposium on System Integration (SI International 2012), pp. 186-191, 2012

[2] A. I. Ianov, H. Kawamoto, Y. Sankai, “Development of a Capacitive Coupling Electrode for Bioelectrical Signal Measurements and Assistive Device Use”, Proceedings of the 2012 ICME International Conference on Complex Engineering, pp. 593-598, 2012

[3] A. Saito, A. Ianov, Y. Sankai, “Measurement of Brain Activity Using Optical and Electrical Method”, Proceedings of the 2009 IEEE International Conference on Robotics and Biomimetics (ROBIO 2009), pp. 1555-1560, 2009

## Other publications

[1]A. Saito, A. Ianov and Y. Sankai, "Measurement of Brain Activity Using Optical and Electrical Method" ,Biologically Inspired Robotics, Chapter 10, ISBN:978-1-4398548-8-4, 2011

## Presentations

[1]A. I. Ianov, H. Kawamoto, Y. Sankai, “Wearable Parallel Processing Based High-Resolution High-Speed Electroencephalogram Monitoring Integrated System”, 2012 IEEE/SICE International Symposium on System Integration(SII2012), Fukuoka, Japan, December 16-18, 2012

[2]A. I. Ianov, H. Kawamoto, Y. Sankai, “Development of a Capacitive Coupling Electrode for Bioelectrical Signal Measurements and Assistive Device Use”, 2012 ICME International Conference on Complex Medical Engineering, Kobe, Japan, July 1-4, 2012

[3] A. Saito, A. Ianov, Y. Sankai, "Measurement of Brain Activity Using Optical and Electrical Method", 2009 IEEE International Conference on Robotics and Biomimetics (ROBIO 2009), Guilin, China, December 19-23, 2009

## **Awards**

[1] A. I. Ianov, H. Kawamoto, Y. Sankai, SII2012 Best Paper Award(SI), 2012 IEEE/SICE International Symposium on System Integration, "Wearable Parallel Processing Based High-Resolution High-Speed Electroencephalogram Monitoring Integrated System", Centennial Hall Kyushu University School of Medicine, Fukuoka, Japan, 2012/12/17

[2] A. I. Ianov, H. Kawamoto, Y. Sankai, Best Student Paper Award, 2012 ICME International Conference on Complex Medical Engineering, "Development of a Capacitive Coupling Electrode for Bioelectrical Signal Measurements and Assistive Device Use", Ana Crowne Plaza, Kobe, Japan, 2012/07/03

[3] イアノフ アレクサンデル イゴレヴィチ(Alexsandr Ianov), 電気学会学術奨励賞, "容量性カップリングに基づく非接触電極の開発", 2010/03/25